TOP NODE STATIC BOTTOM HOLE PRESSURE CALCULATION OF SINGLE PHASE WET GAS WELLS USING APPARENT MOLECULAR WEIGHT PROFILING

BY

Nasser Mubarak Saeed Al-Hajri

A Thesis Presented to the
DEANSHIP OF GRADUATE STUDIES

KING FAHD UNIVERSITY OF PETROLEUM & MINERALS

DHAHRAN, SAUDI ARABIA

In Partial Fulfillment of the
Requirements for the Degree of

MASTER OF SCIENCE

In

PETROLEUM ENGINEERING

January 2017

KING FAHD UNIVERSITY OF PETROLEUM & MINERALS

DHAHRAN- 31261, SAUDI ARABIA

DEANSHIP OF GRADUATE STUDIES

This thesis, written by **Nasser Mubarak Saeed Al-Hajri** under the direction his thesis advisor and approved by his thesis committee, has been presented and accepted by the Dean of Graduate Studies, in partial fulfillment of the requirements for the degree of **MASTER OF SCIENCE IN PETROLEUM ENGINEERING**

Dr. Sidqi A. Abu-Khamsin
(Advisor)

Dr. Abdullah S. Sultan
Department Chairman

Dr. Mohamed A. Mahmoud
(Member)

Dr. Salam A. Zummo
Dean of Graduate Studies

Dr. Dhafer A. Al-Shehri
(Member)

29/12/16
Date

This work is dedicated to my grandfather

ACKNOWLEDGMENTS

Praise be to Allah, the Cherisher and Sustainer of the worlds (Quran 1:2)

I would like to acknowledge the support of KFUPM community towards achieving this milestone. My sincerest gratitude to Dr. Sidqi Abu-Khamsin my thesis advisor for his guidance. Thesis committee Dr. Mohammed Mahmoud and Dr. Dhafer Al-Shehri are also acknowledge for their helpful contribution to complete my thesis work.

The support of my family is dearest to my heart. Their continuous words of encouragement have filled me with energy and pride.

TABLE OF CONTENTS

LIST OF TABLES

LIST OF FIGURES

ABSTRACT

Full Name : Nasser Mubarak Saeed Al-Hajri

Thesis Title : Top Node Static Bottom-Hole Pressure Calculation of Single Phase Wet Gas Wells Using Apparent Molecular Weight Profiling

Major Field : Petroleum Engineering

Date of Degree : January 2017

This thesis introduces a new calculation methodology to predict the static bottom-hole pressure for natural gas wells. The advantageous feature of this method compared to existing methods, is the utilization of the apparent molecular weight profiling concept. Based on the inputs of pressure and temperature gradient data, an iterative calculation scheme is applied to produce a well-specific molecular weight profile. Then, a modified form of the equation of state is used to perform the pressure calculations on the outputs of the apparent molecular weight profiling.

The new calculation method was applied on two calculation modes: calibration and time-lapse. In the calibration mode, the static bottom-hole pressure is predicted on the same gradient survey used to generate the apparent molecular weight profile. On the other hand, the time-lapse calculation mode use is to predict the static bottom-hole pressure after a period of time has elapsed from the gradient survey used to build the molecular weight profile. Both calculation modes were tested on 138 case studies from 8 different fields and 8 different reservoirs. Several combinations of pseudo-critical properties and z-factor correlations were tested to produce the best performing correlation combination.

The results of this work showed that the top node calculation method was accurate in predicting the static bottom-hole pressures. In addition, the top node method has outperformed four previous methods to predict the bottom-hole pressure, which were (Rawlins & Schellhardt, Cullender & Smith, Average Z & T, and Sukkar & Cornell). The use of the apparent molecular weight profiling has shown that there are changes in the gas molecular weight (and specific gravity) in wet gas wells that are not properly captured by well stream gas gravity. A complete error analysis and sensitivity studies are presented in this work.

ملخص الرسالة

الاسم الكامل: ناصر مبارك سعيد الهاجري

عنوان الرسالة: حساب الضغط الساكن لآبار الغاز السائل باستخدام العقدية العلوية وتنميط الوزن الجزيئي

التخصص: هندسة البترول

تاريخ الدرجة العلمية: ديسمبر 2016

تقدم هذه الرسالة طريقة حسابية جديدة لإيجاد الضغط الساكن لآبار الغاز الطبيعي. تتميز هذه الطريقة، عند مقارنتها بالطرق السابقة، باستخدامها لتنميط الوزن الجزيئي. لإتمام التنميط الجزيئي لبئر الغاز تستخدم هذه الطريقة قياسات الضغط والحرارة من أعماق متعددة في بئر الغاز ومن ثم يطبق مخطط تكرار حسابي على جميع الأعماق لإتمام بناء التنميط للوزن الجزيئي. بعد ذلك، يستخدم قانون الغازات المثالية بطريقة معدلة لحساب الضغط الساكن لبئر الغاز من العقد العلوية حتى عمق البئر.

استخدمت هذه الطريقة الحسابية على تقسيمين حسابيين مختلفين: طريقة المعايرة وطريقة تنبؤ الوقت الفاصل. في طريقة المعايرة، يحسب الضغط الساكن لبئر الغاز من نفس القياسات الضغطية والحرارية المستخدمة في تنميط الوزن الجزيئي. بينما في طريقة تنبؤ الوقت الفاصل، تجرى حسابات الضغط الساكن بعد مرور وقت فاصل بين الحسابات وبين قياسات الضغط والحرارة المستخدمة في التنميط الجزيئي. طبقت هذه الطريقة الحسابية، بقسميها المختلفين، على 138 بئر غاز من 8 حقول غاز مختلفة ومن 8 مكامن. استخدمت مجموعة علاقات حسابية لمعامل الانضغاط و الخصائص الشبه حرجة لاختبار أي مجموعة علاقات ستنتج أفضل النتائج.

نتائج هذا البحث العلمي أظهرت أن هذه الطريقة الحسابية قادرة على التنبؤ بالضغط الساكن بأخطاء صغيرة. أيضا، أظهرت هذه الدراسة أن نتائج الطريقة العقدية العلوية كانت أفضل من الطرق السابقة في التنبؤ بالضغط الساكن للآبار الغاز. من نتائج هذا البحث أن تنميط الوزن الجزيئي قدر على توثيق تغيرات في الوزن الجزيئي (والثقل النوعي) في آبار الغاز السائل والتي لم تكن موثقة بشكل جيد في الطرق الحسابية السابقة. تحتوي هذه الرسالة على تحليل كامل للأخطاء ودراسات الحساسية الرياضية.

CHAPTER 1

INTRODUCTION

1.1 Thesis Outline:

The first chapter of this thesis is an introductory chapter that provides an overview of the subject's main concepts. This chapter also outlines the research motive, expected outcomes, and objectives.

Chapter 2 is a literature survey section where several previous methods used to calculate the static bottomhole pressure is explained along with their simplifying assumptions.

In Chapter 3, the proposed calculation method is thoroughly explained with the calculation modes employed in this research. The chapter also, contains the correlations combinations used for computation in this work. The theoretical assumption of this method is stated in Chapter 3 as well.

Chapter 4 presents and discusses the calculation results of the top node method. The results are broken down for each calculation mode and correlation combination. Chapter 5 compares the results of the top node method with four other existing methods in the literature.

In Chapter 6, the error analysis is presented. Descriptive statistics of the error along with its distribution is discussed. The breakdown of error by reservoir and field is presented.

Chapter 7 studies the effect of ten parameters on the error performance of the proposed method. The results of the sensitivity studies are also discussed.

Finally, Chapter 8 presents the main conclusions of this work.

1.2 Subject Overview:

A reservoir's static bottom-hole pressures (SBHP) has wide applications in the oil and gas industry that include reserves estimation, reservoir characterization, pressure transient analysis, numerical reservoir simulations, and such. Other applications of SBHP measurements include well control where the desired mud weight to overbalance a well is designed based on the SBHP measurements.

SBHP is typically measured using down hole gauges that are run in a well using wireline or other conveyance methods. The well is shut-in for a period of time to allow for wellbore fluids stabilization. However, such measurements are often costly and could expose the asset owner to a variety of mechanical problem resulting from well intervention. Consequently, accurate calculation of the SBHP of a well could eliminate the associated costs and operational issues from well intervention for pressure measurements.

An overview of the main concepts applied in this work is introduced in the remainder of this overview.

Ideal Gas

The “Ideal Gas” is a hypothetical gas that has the following properties: the volume of the gas molecules is insignificant compared with the total volume of the gas, no attractive or repulsive forces exist among the molecules or between the molecules and the container walls, and all molecular collisions are perfectly elastic.

Boyle’s law and Charles’ law describe the relationship between the volume occupied by a gas and the pressure and temperature. Boyle’s states that for a given mass of gas at a constant temperature, the pressure-volume product is constant. Charles’ states that for a given mass of gas at a constant pressure, the volume/temperature ratio is constant.

The combination of the two laws is called the equation of state (EOS) for ideal gases:

$$PV = nRT \qquad \text{Eq. (1.1)}$$

Where:

P: Pressure, psia

V: Volume, ft^3

n: Number of moles

R: Universal Gas Constant, 10.732 $psia.ft^3/lb\ mole.\ °R$

T: Temperature, °R

Real Gas

The behavior of most real gases does not deviate drastically from the behavior predicted by Eq. (1.1). Accordingly, the EOS for real gases can be obtained by simply adding a correction factor (z) – known as the gas deviation factor – to the EOS for ideal gases. The equation becomes:

$$PV=ZnRT \qquad \text{Eq. (1.2)}$$

Where:

Z: Gas Deviation Factor, dimensionless

This dimensionless factor (z) accounts for the non-ideal behavior of the real gas. It depends on pressure, temperature and gas composition. The common methods to obtain the value of z are by laboratory experiment of the sampled gas or using existing mathematical correlations.

Properties of a Gas Mixture

- **Apparent Molecular Weight**

Since a gas mixture is composed of molecules of various sizes and different molecular weights, it doesn't have an explicit molecular weight. However, a gas mixture behaves as if it has a definite molecular weight. This molecular weight is known as the apparent molecular weight and is defined as:

$$\text{MMa} = \sum_i y_i M_i \qquad \text{Eq. (1.3)}$$

Where:

MM_a: Apparent Molecular Weight, lb/lb-mole

M_i: Molecular Weight of i^{th} gas component, lb/lb-mole

M_{air}: Molecular Weight of air=28.96, lb/lb-mole

y_i: Mole fraction of a particular component in the gas mixture

- **Density**

Since density is defined as the mass of gas per unit volume, an equation of state can be used to calculate the density of a gas at various temperatures and pressures:

$$\rho_g = \frac{m}{V} = \frac{PMM_a}{ZRT} \quad \text{Eq. (1.4)}$$

Similarly, the gas pressure gradient is calculated as follows:

$$\alpha_g = \frac{\rho_g}{144} = \frac{PMM_a}{144ZRT} \quad \text{Eq. (1.5)}$$

Where:

ρ_g: Gas Density, lbm/ft^3

m: Mass, lbm

α_g: Gas Wellbore Pressure Gradient

- **Specific Gravity**

The specific gravity of a gas is defined as the ratio of the density of the gas to the density of dry air, both measured at the same temperature and pressure:

$$\gamma_g = \frac{\rho_g}{\rho_{air}} \quad \text{Eq. (1.6)}$$

Or

$$\gamma_g = \frac{M_a}{M_{air}} = \frac{M_a}{28.97} \quad \text{Eq. (1.7)}$$

Where:

γ_g: Gas Specific Gravity

ρ_{air}: Dry Air Density, lbm/ft^3

Note that this equation is strictly true only if both the gas and air act like ideal gases.

Law of Corresponding States

The Law of Corresponding States show that all pure gases have the same z-factor at the same values of reduced pressure and reduced temperature. Reduced pressure and reduced temperature for pure compounds are defined as:

$$P_{pr} = \frac{P}{P_c} \qquad \text{Eq. (1.8)}$$

$$T_{pr} = \frac{T}{T_c} \qquad \text{Eq. (1.9)}$$

Where:

Pr: Reduced Pressure

Pc: Critical Pressure, psia

Tr: Reduced Temperature

Tc: Critical Temperature, R

Consequently, the pseudoreduced pressure and pseudoreduced temperature for gas mixtures are defined as:

$$P_{pr} = \frac{P}{Pp_c} \qquad \text{Eq. (1.10)}$$

$$T_{pr} = \frac{T}{Tp_c} \qquad \text{Eq. (1.11)}$$

Where:

Ppr: Pseudoreduced Pressure

Ppc: Pseudocritical Pressure, psia

Tpr: Pseudoreduced Temperature

Tpc: Pseudocritical Temperature, °R

A well-known chart is the one by Standing and Katz that shows the behavior of the z-factor for hydrocarbon gases with respect to reduced pressures and reduced temperatures.

Pseudocritical Gas Properties Calculation

There are methods for calculating the pseudocritical pressure and temperature of a hydrocarbon gas mixture which provide a means to correlate the physical properties of mixtures with the Law of Corresponding States. One of these methods is Sutton's Correlations for unknown gas composition. Using data from 264 gas samples, Sutton developed a correlation for estimating pseudocritical pressure and temperature as a function of gas specific gravity:

$$P_{pch} = 756.8 - 131.0\gamma_h - 3.6\gamma_h^2 \qquad \text{Eq. (1.12)}$$

$$T_{pch} = 169.2 + 349.5\gamma_h - 74.0\gamma_h^2 \qquad \text{Eq. (1.13)}$$

Where:

P_{pch}: Pseudocritical Pressure of Hydrocarbon Components, psia

T_{pch}: Pseudocritical Temperature of Hydrocarbon Components, °R

γ_h: Specific Gravity of Hydrocarbon Components

This correlation is applicable for $0.57<\gamma_h<1.68$ and for gases containing < 12 mol% of CO_2, < 3 mol% of nitrogen, and no H_2S. However, if the gas contains > 12 mol% of CO_2, > 3 mol% of nitrogen, or any H_2S, then the gas gravity should be re-calculated by:

$$\gamma_h = \frac{\gamma_w - 1.1767 y_{H2S} - 1.5196 y_{CO2} - 0.9672 y_{N2} - 0.6220 y_{H2O}}{1 - y_{H2S} - y_{CO2} - y_{N2} - y_{H2O}} \quad \text{Eq. (1.14)}$$

Where:

y_{H2S}: Mole Fraction of H_2S

y_{CO2}: Mole Fraction of CO_2

y_{N2}: Mole Fraction of N_2

y_{H2O}: Mole Fraction of H_2O

And then the pseudocritical properties are calculated by the following equations:

$$P_{pc} = (1 - y_{H2S} - y_{CO2} - y_{N2} - y_{H2O}) P_{pch} + 1{,}306 y_{H2S} + 1{,}071 y_{CO2} + 493.1 y_{N2} + 3{,}200.1 y_{H2O} \quad \text{Eq. (1.15)}$$

$$T_{pc} = (1 - y_{H2S} - y_{CO2} - y_{N2} - y_{H2O}) T_{pch} + 672.35 y_{H2S} + 547.58 y_{CO2} + 227.16 y_{N2} + 1{,}164.9 y_{H2O} \quad \text{Eq. (1.16)}$$

1.3 Research Motive & Expected Outcomes:

The motive of this research is to overcome the limitations of existing methods in the petroleum literature to calculate the static bottom-hole pressure for single phase, wet gas wells. Methods in the literature are intended for dry gas wells and most of these methods are made with simplifying assumption such as average pressure, average temperature, and average gas deviation (Z-factor). The proposed methods for dry gas wells are not suitable

for wet gas wells applications due to the variation in gas gravity with pressure and temperature changes in single phase gas wellbores that produces condensate. Variation of gas gravity affects the accuracy of pseudocritical pressures and temperatures, the corresponding reduced values, and gas deviation. The added value of this work will be the use of apparent molecular weight profiling developed from pressure and temperature gradient surveys. The apparent molecular weight profile will be used to capture gas gravity changes within the wellbore. Hence, the pressure calculations are performed based on representative values of pseudocritical and reduced pressures and temperatures. This will enable proper simulation of Z-factor changes inside the single phase wet gas wellbore.

The research also aims at introducing yet another method in the petroleum literature that deploys the principles of apparent molecular weight profiling to predict the bottom-hole pressure. The implementation of such methodology will entail considerable cost saving to oilfield operators and would not expose the operator to mechanical risks associated with wireline intervention.

1.4 Research Objectives:

The detailed research objectives of this thesis are as follows:

1- Develop a method of profiling apparent molecular weight changes for single phase wet gas wells. The developed method is to be equally applicable to dry gas wells.
2- Perform top node calculations of static bottomhole pressures of single phase wet gas wells on a representative data sample. The top node calculations are to be performed using different z-factor and pseudo-critical pressure and temperature correlations.
3- Compare the calculations results with actual field measurements.
4- Compare the calculations results with previous methods in the literature.

5- Perform sensitivity analysis of apparent molecular weight profiling and top node calculations and identify sources of error.

CHAPTER 2

LITERATURE SURVEY

2.1 Rawlins & Schellhardt (1936):

The method introduced an equation to calculate the static bottom hole pressure for dry gas using the following equation:

$$P_2 - P_1 = P_1(e^{0.0000347GX} - 1) \qquad \text{Eq. (2.1)}$$

Where:

P_2: Bottom hole static pressure, psia

P_1: Shut-in Wellhead Pressure, psia

G: Gas gravity

X: Depth of well, ft

2.2 Rzasa & Katz (1945):

The researchers presented three methods of calculating static bottom hole pressure for dry gas wells using surface shut-in measurements as follows:

Method 1

The general flow equation was reduced to:

$$\int_1^2 VdP + \Delta X = 0 \qquad \text{Eq. (2.2)}$$

Given that the static conditions have no velocity, work, friction loss, or other energies, combining Eq. (1.2) and Eq. (2.2) gives:

$$\int_1^2 \frac{ZNRT}{P} dP = X \qquad \text{Eq. (2.3)}$$

In this method, the gas composition must be known to determine the gas gravity, pseudocritical pressure, and pseudocritical temperature. Also, the shut-in pressure and temperature gradient are needed to perform the trial and error calculation of this method using the Eq. (2.4), which is the integration solution of Eq. (2.3):

$$P_2 - P_1 = P_1 \left(e^{\frac{X}{ZNRT}} - 1\right) \qquad \text{Eq. (2.4)}$$

Based on the temperature gradient of the well, incremental pressures are calculated by trial and error till the bottom hole depth is reached.

Method 2

This method uses Eq. (2.4) (?????) but with the assumption of constant temperature and Z-factor at an assumed average pressure. Calculation of bottom hole pressure is also based on trial and error. Method 2 requires knowledge of the shut-in wellhead pressure, gas gravity, and gas pseudocritical properties. Using Eq. (2.4), a bottom hole pressure is assumed as a first trial and an average wellbore pressure is computed. Then, reduced pressures and temperatures and corresponding Z-factor at the assumed average pressure are all calculated. These values are inputted into both sides of Eq. (2.4) to determine the accuracy of the trial. Further trials are made till the values converge.

Method 3

The third method uses Eq. (2.2) with the assumption that little difference is observed when assuming a constant pressure or an average value of V when the temperature and Z-factor are assumed constant. Hence, the static bottom hole pressure can be determined by trial and error using the following equation:

$$\Delta P \left(1 - 0.00937 \frac{XG}{T_a Z_a}\right) = 0.01874 P_1 \frac{XG}{T_a Z_a} \qquad \text{Eq. (2.5)}$$

Where:

T_a: The constant temperature at an assumed average pressure, °R

Z_a: The constant Z-factor at an assumed average pressure

P_1: Shut-in Wellhead Pressure, psia

Similar to method 2, trial and error calculation based on an assumed bottom hole pressure are made until a bottom hole pressure value satisfying both sides of Eq. (2.5) is reached.

2.3 Sukkar & Cornell (1954):

Sukkar & Cornell proposed a method to calculate the bottom hole pressure for dry gas wells derived from the general flow equations with a simplifying assumption of constant temperature. When the temperature is constant, Z-factor is a function of Pr only. The bottom hole pressure equation proposed by Sukkar & Cornell can be used to calculate static pressures as a special case of the gas flow equation (where Q = 0). The static bottom hole equation is:

$$\frac{Z\,(dP_r)}{P_r} = \frac{0.01877 \times G \times X}{T} \qquad \text{Eq. (2.6)}$$

2.4 Cullender & Smith (1956):

Cullender & Smith introduced an equation to calculate the subsurface pressure in static dry gas wells that was derived from the mechanical energy balance. The equation does not make assumptions related to either temperature or Z-factor as with the methods of Rzasa & Kats. The proposed equation to calculate the static well pressure is generated by integrating the following term:

$$\frac{GH}{53.33} = \int_{Pe}^{Pt} \frac{TZ}{P} d(P) \qquad \text{Eq. (2.7)}$$

Where:

G: Gas gravity

H Difference in elevation, ft

P_t: Formation pressure, psia

P_e: Shut-in wellhead pressure, psia

The trapezoidal and Simpson's rules were proposed by Cullender & Smith to carry out the numerical integration needed to calculate the static well pressure.

2.5 Aziz (1967):

Aziz applied the Newton-Raphson iteration scheme to the Cullender & Smith method. The goal of introducing this method to calculate the static bottom hole pressures is to minimize the number of iterations required to carry out the computations. The method can be solved with any numerical integration scheme.

The Cullender & Smith equation is re-arranged and a second-order iteration scheme for the equation is found as follows:

$$\emptyset'\left(P_s^{(n)}\right) = \frac{T_s Z_s^{(n)}}{P_s^{(n)}} \qquad \text{Eq. (2.8)}$$

Where:

$$P_s: \quad \frac{GH}{53.33} - \int_{Pe}^{Pt} \frac{TZ}{P} d(P)$$

2.6 Fang (1967):

Fang introduced equation Eq. 2.9 based on density variation to calculate the static pressure for dry gas wells:

$$\mathrm{P_j} = \mathrm{P_{j-1}} + \frac{\mathrm{g}}{\mathrm{g_c}} \rho(\mathrm{P}, \mathrm{T}) \Delta \mathrm{X} \qquad \text{Eq. (2.9)}$$

This method assumes a linear temperature profile in the well and requires knowledge of gas composition to compute the pressure. The density is calculated from the Redlinch-Kwong equation.

CHAPTER 3

METHODOLOGY

3.1 Overall Methodology Description

A well-specific apparent molecular weight profile is built. The profile is generated using a previous pressure and temperature gradient survey from the same well targeted by the calculation. Once the molecular weight profile of a well is built, the top node SBHP calculation can be performed on the gas well using the shut-in wellhead pressure and well depth. The top node calculations are performed using the same apparent molecular weight profile regardless of the elapsed duration of time if both the temperature profile used to build the apparent molecular weight profile and the composition of the wet gas entering the wellbore have not changed significantly.

There are two calculation modes performed in this research as follows:

1. **Calibration Models**

The calibration models utilized a baseline gradient pressure and temperature survey to build the apparent molecular weight profile. The top node calculations are carried out to predict the SBHP for the same gradient survey used to build the apparent molecular weight profile. The objective of the calibration models is to predict the downhole pressure for known temperature profile. The calibration model use exact temperature values measured from the well to build the apparent molecular weight profile. While, the time-lapse models use a

previous (baseline) temperature profile to generate the apparent molecular weight profile. Given the accuracy of the temperature profile used for the calibration model, it is expected that these models will produce a better error than the time-lapsed ones due to slight variation of the temperature profile with time. A total of 63 calibration models (for 63 gas wells) were built as part of this research.

2. **Time-lapse Prediction Models**

The time-lapse prediction models utilized a baseline gradient pressure and temperature survey to build the apparent molecular weight profile. The top node calculations are carried out to predict the SBHP for the well after a lapsed duration of time with a different shut-in wellhead pressure. A total of 75 calibration models (for 75 gas wells) were built as part of this research.

3.2 Apparent Molecular Weight Profiling

Baseline gradient pressure and temperature surveys are the cornerstone of the overall methodology to calculate static bottom hole pressure surveys from surface shut-in pressure data. Baseline gradient surveys are used to develop wells' specific apparent molecular weight profiles across segmented wellbore intervals.

The profiling of apparent molecular weight in this method uses measured pressure and temperature gradient surveys to calculate the apparent molecular weight corresponding to each segment in the wellbore. Figure 1 portrays a conceptual diagram of apparent molecular weight profiling.

Steps to compute the apparent molecular weight for each depth interval are outlined below:

1. Use an MMa_i value of 16.0 gram/mole as a starting value for the top segment.

2. Calculate the specific gas gravity using Eq. (1.7).

3. Calculate the pseudo-critical gas properties using an applicable correlation.

4. Compute the average pressure (P_{avg}), temperate (T_{avg}), and pressure gradient (αg_{avg}) for each depth interval from the baseline survey data.

5. Calculate the pseudo-reduced gas pressure and temperature using Eq. (1.10) and Eq. (1.11). The pseudo-reduced properties are to be obtained from the pseudo-critical properties of Step.3. The pressures and temperatures used to calculate the pseudo-reduced properties are obtained from Step.4

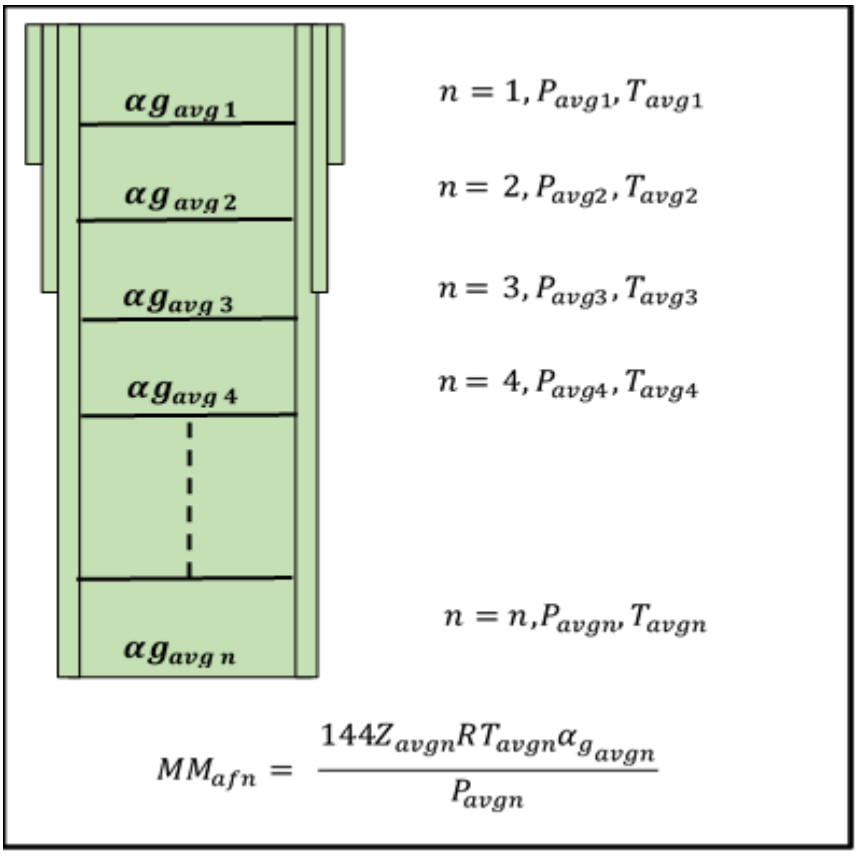

Figure 1: Apparent Molecular Weight Profiling Conceptual Diagram

6. Obtain the gas deviation factor (Z) using an applicable correlation

7. Calculate the MMa_f value using the following equation:

$$MM_{af} = \frac{144 Z_{avg} R T_{avg} \alpha_{g_{avg}}}{P_{avg}} \quad \text{Eq. (3.1)}$$

8. Compute the absolute value of the relative error between MMa_i (Step.1) and MMa_f (Step.7).

9. If absolute value of MM relative error is <= 0.001%, MMa has converged; move to the next depth interval. If not, add 0.001 to MMa_i value and repeat steps 2 through 9

The above procedure is applied on all available depth intervals in the baseline pressure and temperature survey. Corresponding apparent molecular weight values for each depth interval are used for segmented pressure gradient calculations in subsequent time-lapses to the baseline survey using the top node approach. Figure 2 shows the apparent molecular weight profiling method workflow.

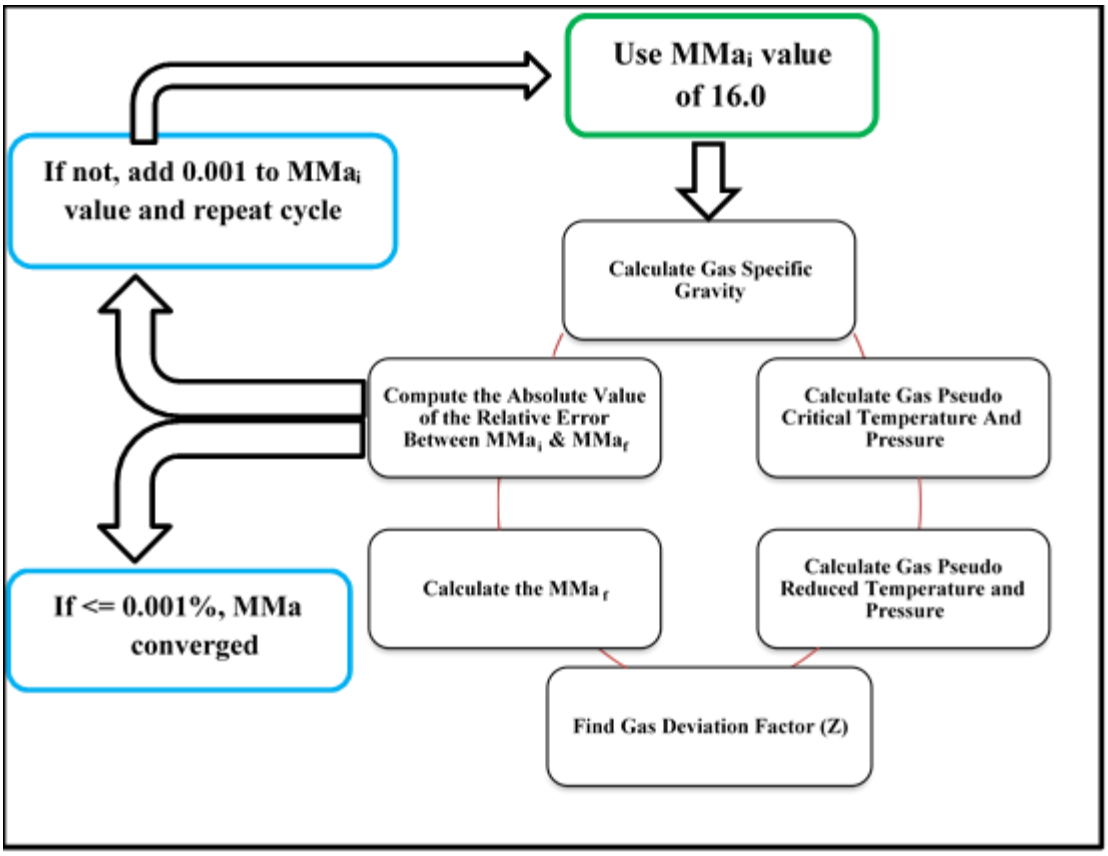

Figure 2: Apparent Molecular Weight Profiling Workflow

3.3 Top Node Calculation:

The top node approach uses arbitrary number of segments within the gas column in the wellbore. Generally, the more the wellbore is segmented the more accurate the results are. For each segment in the wellbore, the upper pressure and temperature values are referred to as top nodes parameters. The apparent molecular weight values generated from the profiling described in the previous section, are used as inputs for corresponding depth segments in the top node method. The working equation for this method is Eq (1.5). This equation is applied to each segment to calculate the segment average pressure gradient. This average pressure gradient is to compute the incremental gravitational pressure (i.e. ΔP

gravity). Then, the incremental gravitational pressure is added to the previous reference pressure (top node pressure) to obtain the pressure at the bottom of the segment. These segmental calculations are repeated till the bottom hole depth is reached. Figures-3 and 4 show conceptual diagrams of the top node method.

Each depth interval inside the wellbore has a top node and a bottom node. The top node is known when starting the calculation from the known shut-in wellhead pressure. The bottom node is calculated by adding the top node pressure to the gas gradient corresponding to each interval. These calculations continue for all wellbore depth intervals until the bottom hole depth is reached.

The steps to calculate the top node pressures are as follows:

1- Use an MMaf value corresponding to each depth interval as calculated in the apparent molecular weight profiling.
2- Calculate the specific gas gravity using Eq. (1.7).
3- Calculate the pseudo-critical gas properties using an applicable correlation.
4- Calculate the pseudo-reduced gas pressure and temperature at the top node pressure and temperature
5- Calculate the pseudo-reduced gas pressure and temperature using Eq. (1.10) and Eq. (1.11). The pseudo-reduced properties are to be obtained from the pseudo-critical properties of Step.3. The pressures and temperatures used to calculate the pseudo-reduced properties are obtained from Step.4
6- Obtain the gas deviation factor (Z) using an applicable correlation
7- Calculate the gas gradient corresponding to each depth interval using the following equation

$$\alpha_g = \frac{\rho_g}{144} = \frac{PMM_a}{144ZRT} \qquad \text{Eq. (1.5)}$$

A computer programing language will be used to carry out the calculations. This methodology will be applied on and compared with actual filed data. Error analysis with all possible sources of error will be performed to further enhance the method.

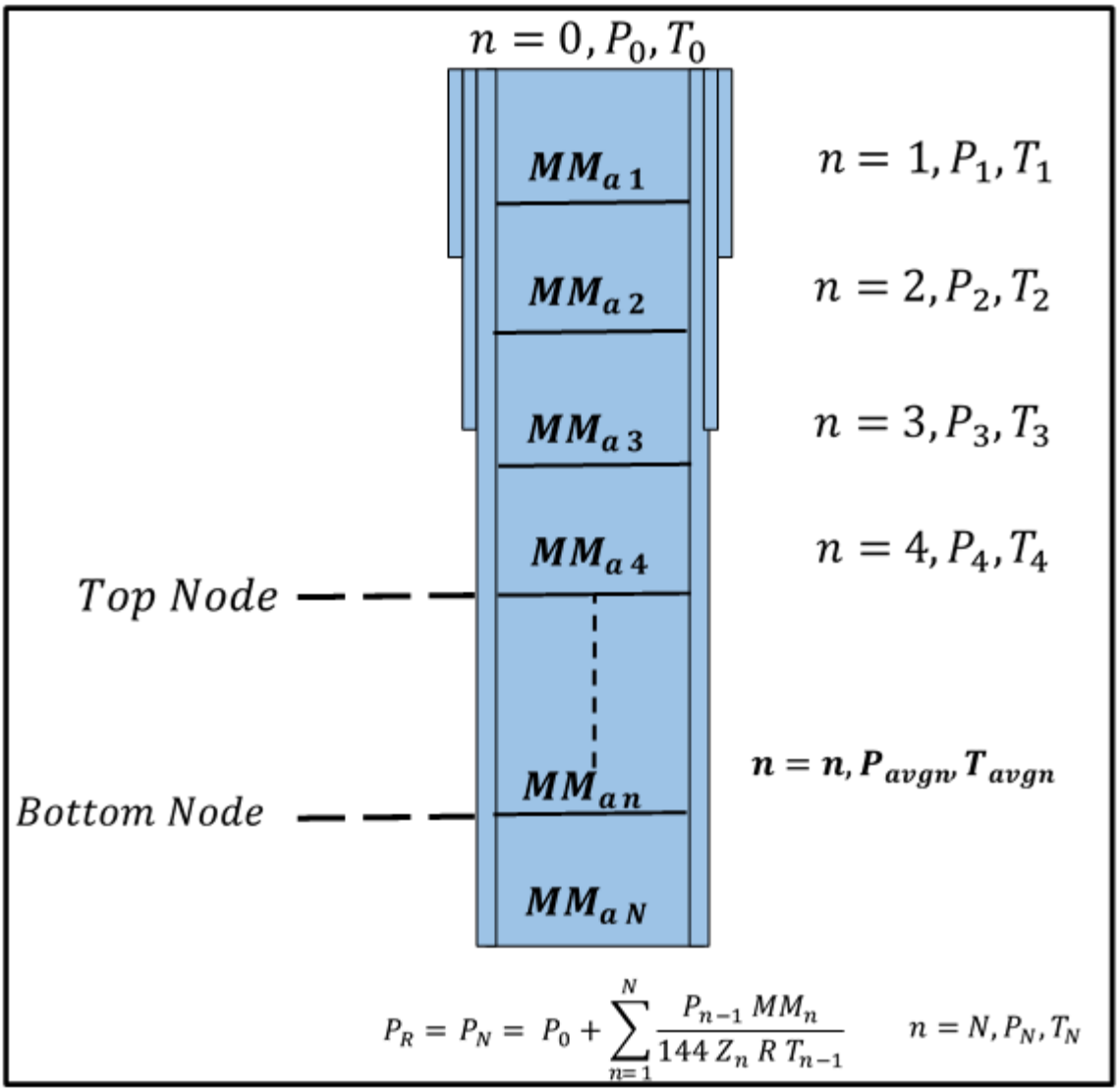

Figure 3: Top Node Calculations Conceptual Diagram

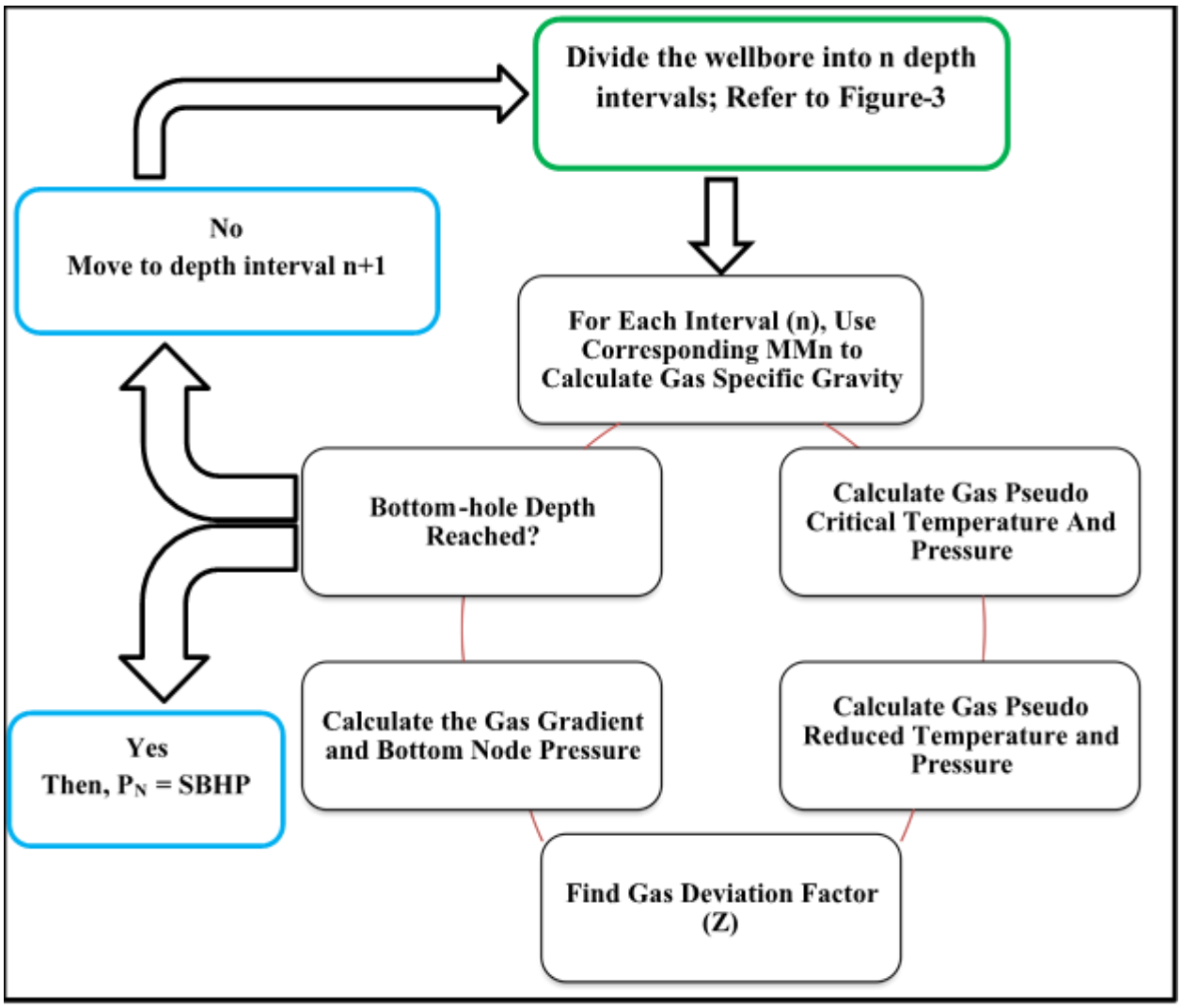

Figure 4: Top Node Calculations Workflow

3.4 Correlations Used for Apparent Molecular Weight Profiling and Top Node Calculations:

In this work, a combination of different z-factor and pseudo critical properties correlations were used to carry out the apparent molecular weight profiling and top node pressure computations. The objective of using multiple correlations are summarized in the following points:

1- The use of different correlations will allow enhanced error analysis through studying the effect of correlations in the overall error.

2- The prediction performance of each combination of z-factor and pseudo critical properties correlation will aid in selecting the recommended correlations for future implementation of the methodology proposed by this research.

The following three different z-factor correlations were tested:

1. Dranchuk and Abou-Kassem (DAK) Z-Factor Correlation

$$Z = 1 + \left(A_1 + \frac{A_2}{T_{pr}} + \frac{A_3}{T_{pr}^3} + \frac{A_4}{T_{pr}^4} + \frac{A_5}{T_{pr}^5}\right)\rho_{pr} + \left(A_6 + \frac{A_7}{T_{pr}} + \frac{A_8}{T_{pr}^2}\right)\rho_{pr}^2 -$$

$$A_9\left(\frac{A_7}{T_{pr}} + \frac{A_8}{T_{pr}^2}\right)\rho_{pr}^5 + A_{10}\left(1 + A_{11}\rho_{pr}^2\right)\left(\frac{\rho_{pr}^2}{T_{pr}^3}\right)EXP(-A_{11}\rho_{pr}^2) \qquad \text{Eq. (3.2)}$$

Where,

$$\rho_{pr} = 0.27 * \left(\frac{P_{pr}}{zT_{pr}}\right)$$

The constants in the DAK correlation are tabulated below:

A_1	A_2	A_3	A_4	A_5	A_6	A_7	A_8	A_9	A_{10}	A_{11}
0.3265	-1.07	-0.5339	0.01569	-0.05165	0.5475	-0.7361	0.1844	0.1056	0.6134	0.721

Table 1: DAK Correlation Constant Values

2. Brill and Beggs' Z-Factor Correlation

$$Z = A + \frac{1-A}{e^B} + CP_{pr}^D \qquad \text{Eq. (3.3)}$$

Where,

$$A = 1.39\sqrt{T_{pr} - 0.92} - 0.36T_{pr} - 0.101,$$

$$B = (0.62 - 0.23T_{pr})P_{pr} + \left[\frac{0.066}{T_{pr}-0.86} - 0.037\right]P_{pr}^2 + \frac{0.32}{10^{(T_{pr}-1)}}P_{pr}^6,$$

$$C = 0.132 - 0.32\ log_{10}T_{pr},$$

$$D = 10^{(0.3106-0.49T_{pr}+0.1824T_{pr}^2)}.$$

3. Mahmoud's Z-Factor Correlation

$$Z = (\ 0.702\ e^{-2.5T_{pr}})\ (P_{pr}^2) - (5.524\ e^{-2.5T_{pr}})\ (P_{pr}) + (0.044\ T_{pr}^2 - 0.164\ T_{pr} + 1.15) \qquad \text{Eq. (3.4)}$$

4. Standing's Pseudo-Critical pressure and temperature correlation for wet gases

$T_{Pc} = 187 + 330\ \gamma_g - 71.5\ \gamma_g^2$ °R Eq. (3.5)

$P_{Pc} = 706 - 51.7\ \gamma_g - 11.1\ \gamma_g^2$ psi Eq. (3.6)

5. Sutton's Pseudo-Critical pressure and temperature correlation

$$P_{pch} = 756.8 - 131.0\gamma_h - 3.6\gamma_h^2 \quad \text{Eq. (1.12)}$$

$$T_{pch} = 169.2 + 349.5\gamma_h - 74.0\gamma_h^2 \quad \text{Eq. (1.13)}$$

Where:

P_{pch}: Pseudocritical Pressure of Hydrocarbon Components, psia

T_{pch}: Pseudocritical Temperature of Hydrocarbon Components, R

γ_h: Specific Gravity of Hydrocarbon Components

Based on the above five correlations, six combinations of z-factor and pseudo critical properties were considered as follows:

1- DAK's z-factor and Standing's pseudo critical correlations
2- DAK's z-factor and Sutton's pseudo critical correlations
3- Brill and Beggs' and Standing's pseudo critical correlations
4- Brill and Beggs' and Sutton's pseudo critical correlations
5- Mahmoud's and Standing's pseudo critical correlations
6- Mahmoud's and Sutton's pseudo critical correlations

The detailed results and discussion of those six combinations are presented in Chapter-4.

3.5 Theoretical Premises:

The scope of this research is concentrated on wet gas wells. For the purposes of this research, the following characteristics of wet gases are introduced:

1- The wet gas in the wellbore column crosses the dew point line.
2- Crossing the dew point line entails liquid drop out within the wellbore, which could alter the gas molecular weight with changes in pressure and temperature across the well depth.
3- Liquid pressure gradients do not exist within the well hydrostatic column. Therefore, wells with pressure gradients above 0.20 psi/ft were excluded from applicability of the top node method in this work.

With the above characteristics in mind, the following theoretical premises constitute the presiding assumptions that govern the working equations behind the top node calculation method:

1. The top node method is independent of changes in reservoir properties

Inputs required to carry out the computations of the top node are: gradient pressure and temperature surveys, well depth, and shut-in wellhead pressure. The reservoir specific properties such as gas composition and associated Hydrogen Sulfide, Carbon Dioxide, and Nitrogen impurities are not factored into the calculations. This makes application of the top node SBHP method appropriate for all types of reservoirs and conditions.

To corroborate this theoretical premise, the top node SBHP calculations were carried out on a representative and large sample of data from different fields and across multiple reservoirs.

As will be seen in the results sections, the outputs of the computations were comparable in accuracy throughout the sampled data irrespective of reservoir or field properties and conditions.

2. Change in wellbore temperature profile is negligible with time

The top node method uses a baseline gradient survey to build a specific well apparent molecular weight profile. The well specific profile is used to carry out the top node calibration run, and subsequently predict the SBHP after an elapsed time using the shut-in wellhead pressure and depth of the well.

Accordingly, an assumption is made that the well's temperature profile in the baseline survey does not change during the time lapsed period to predict the SBHP. Any changes in the well temperature profile, especially in the shallower parts of the wellbore, are neglected during the time lapse calculations. Figures 5, 6, 7, and 8 show temperature profile changes overtime for several wells where the top node method was used to predict their time lapsed SBHP.

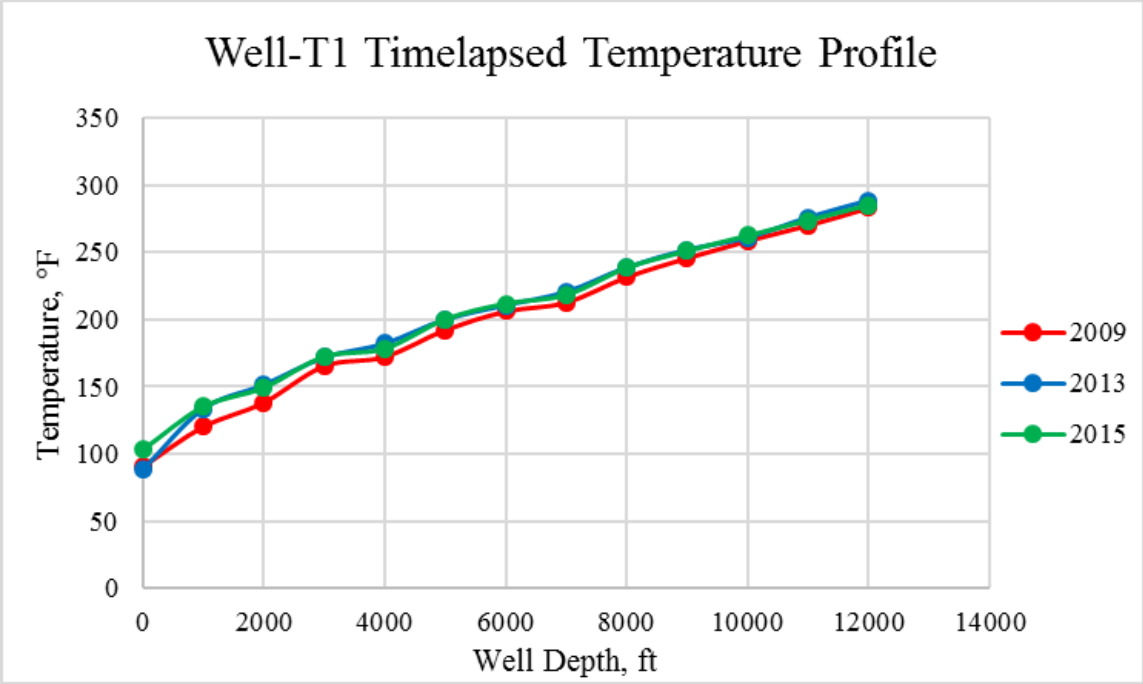

Figure 5: Well-T1 Time lapsed Temperature Profile

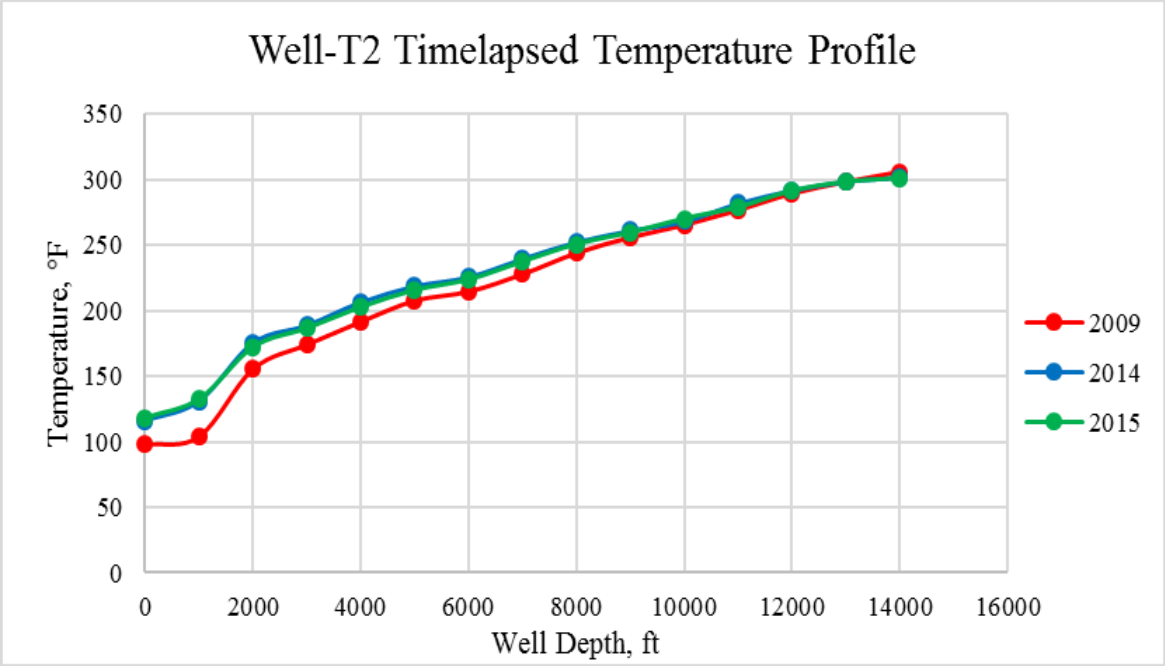

Figure 6: Well-T2 Time lapsed Temperature Profile

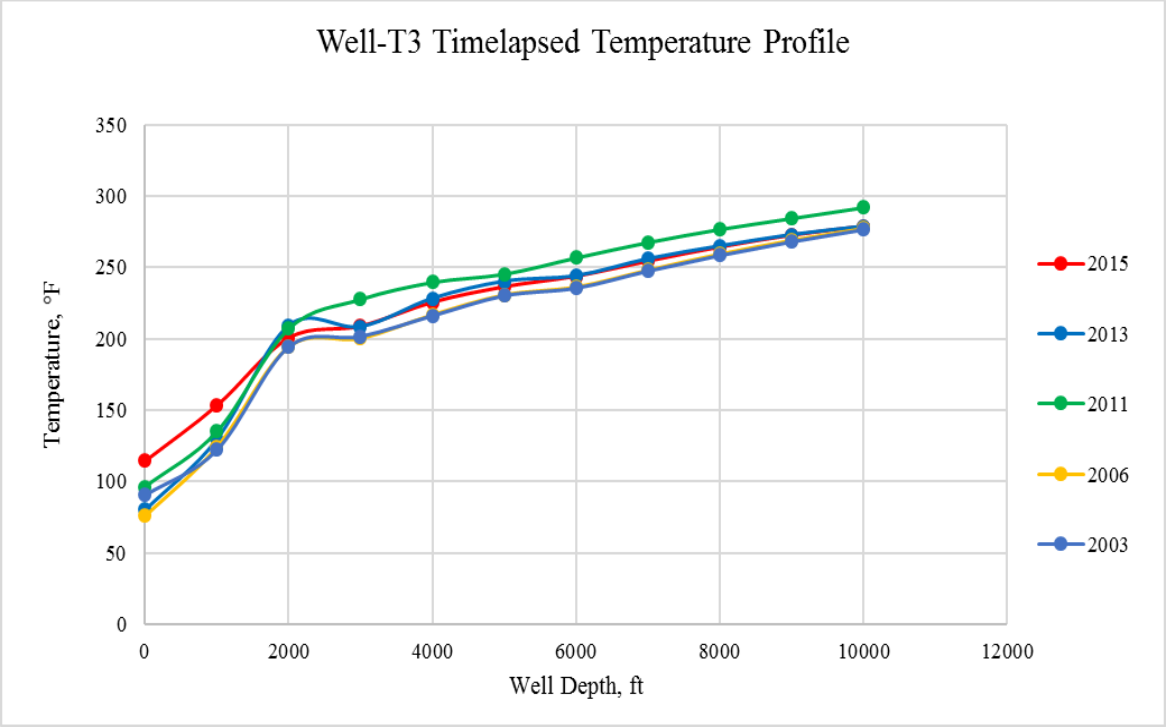

Figure 7: Well-T3 Time lapsed Temperature Profile

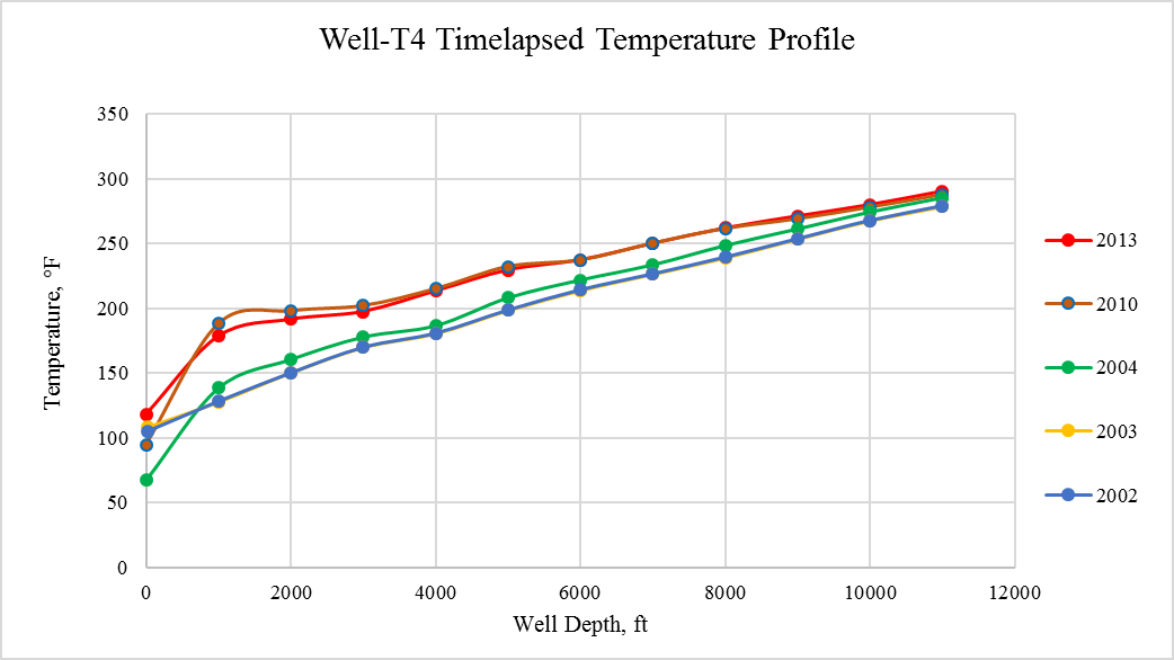

Figure 8: Well-T3 Time lapsed Temperature Profile

3. Changes in apparent molecular weight profile with time are neglected.

The top node calculations are based on Eq. (1.5) below. The mathematical re-expression of the equation of state will use the apparent molecular weight profile as the input for the top node calculations. Given that the temperature is assumed constant with time, the apparent molecular weight changes with time are neglected as well.

$$\alpha_g = \frac{\rho_g}{144} = \frac{\mathrm{PMM_a}}{144\mathrm{ZRT}} \qquad \text{Eq. (1.5)}$$

This theoretical premise is introduced for practicality consideration. When the apparent molecular weight profile - that is built from baseline gradient survey - is assumed constant with time, there will not be a need for another gradient survey.

4. Any liquid that forms and is entrained in the gas in the upper sections of the well will not re-vaporize during the shut-in period nor interfere with gradient profile.

For the purposes of this top node methodology, it is assumed that when the gas crosses the dew point line, the formed liquid will not interfere with the pressure profile, i.e. liquid gradient will not be present within the wellbore. Also, the dropped liquid should not re-vaporize at high pressures in the lower parts of the wellbore. Figure 9 below show the phase diagram of wet gases. We have added a blue dotted line to illustrate a possible path of wet gas through the wellbore.

To further validate this theoretical premise, acoustic meters can be installed on a wet gas well. The acoustic meter sends a sound wave downhole that gets reflected from the gas-liquid interface. The travel time of the acoustic waves will determine the presence of any liquid within the gas column.

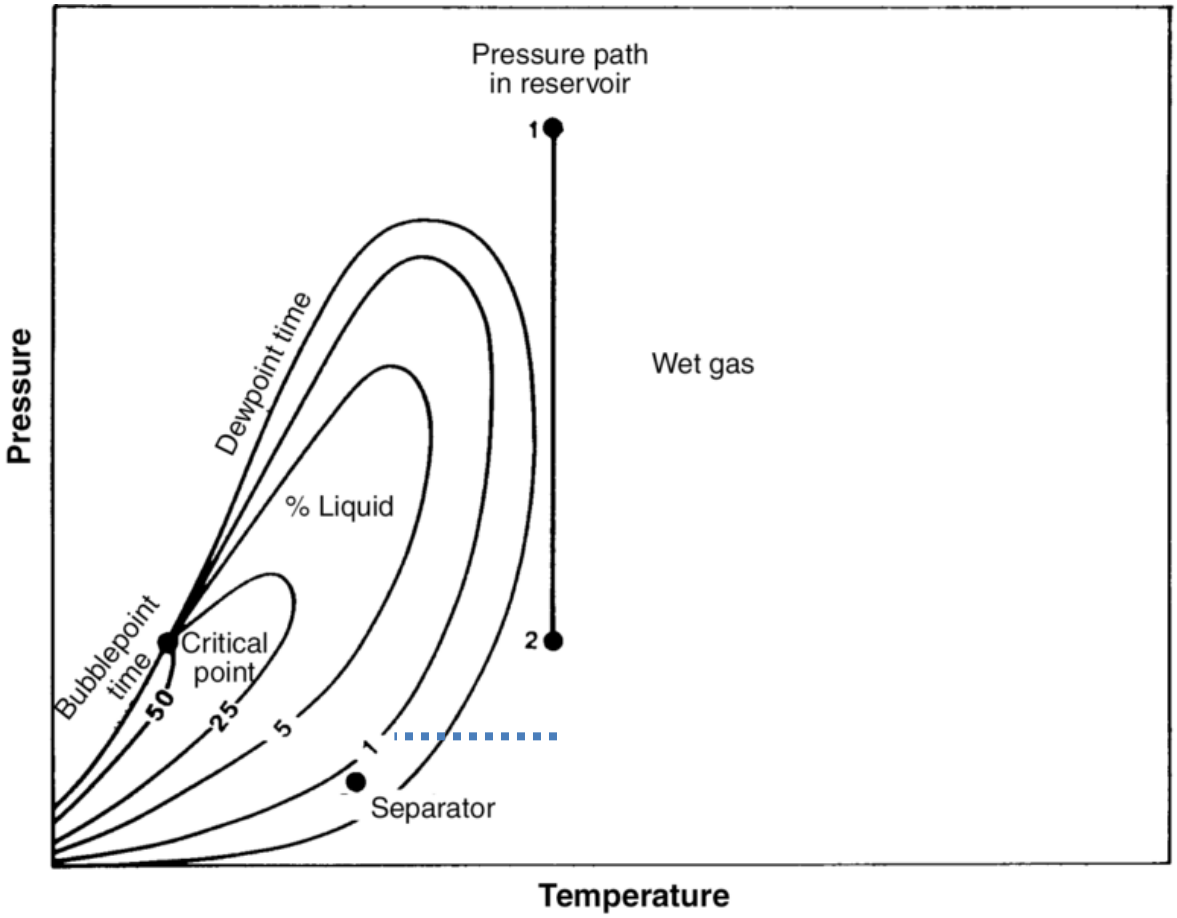

Figure 9: Phase Diagram for Wet Gases (Courtesy of McCain W.D, The Properties of Petroleum Fluids).

5. The top node SBHP calculation method is applicable to dry gases

Although the top node method has been designed to calculate the SBHP by capturing changes in gas column molecular weight using the apparent molecular weight profiling, the method is equally applicable to dry gas wells.

Given the definition of wet gases introduced at the beginning of this section, the main variable between wet and dry gas wells is the change in gas gravity. In dry gas wells, a single value of specific gravity will be present in all wellbore depths when the apparent molecular weight profiling is applied. This singular value of specific gravity can be used to compute the pseudo-critical and reduced pressures and temperatures as well as the z-factors

for all wellbore depths. Then, the top node calculations are applied on all wellbore intervals using the modified form of equation of state.

CHAPTER 4

TOP NODE BOTTOMHOLE PRESSURE CALCULATION

4.1 Data Representation:

A large and representative data sample was used to test the accuracy of the top node calculations to predict the bottomhole pressures using the apparent molecular weight profile. The data sample has the following characteristics:

1- Total number of case studies is 138.

2- Data were sampled from 8 different fields.

3- Data were sampled form 8 different reservoirs with varying properties.

Additionally, the data sample was quality controlled and assured to exclude inapplicable wells to the top node SBHP calculation method. Mainly, wells which have developed liquid columns within the wellbore were excluded from the top node calculation.

4.2 Calculation Results:

Top node calculations were preformed based on six combinations of z-factor and pseudo-critical pressures and temperature correlations, as stated in section **3.4** above. The complete results are found in Appendices A, B, C, D, E, and F. The tables below show the prediction performance for all 138 case studies of each combination of correlations in terms of absolute pressure difference in psi and absolute relative error. The results are categorized as follows:

1- Calibration Models Results (63 Models/Wells)

	DAK-Sutton, psi	DAK-Standing, psi	Brill & Beggs-Sutton, psi	Brill & Beggs-Standing, psi	Mahmoud-Sutton, psi	Mahmoud-Standing, psi
Avg.	**91.96**	**116.73**	**12.83**	**11.15**	**22.83**	**9.56**
Min.	**0.81**	**10.26**	**0.01**	**0.00**	**0.01**	**0.00**
Max.	**234.54**	**315.71**	**266.59**	**157.64**	**333.78**	**80.14**

Table 2: Calibration Prediction Performance in terms of Absolute Pressure Difference

	DAK-Sutton, %	DAK-Standing, %	Brill & Beggs-Sutton, %	Brill & Beggs-Standing, %	Mahmoud-Sutton, %	Mahmoud-Standing, %
Avg.	**2.51**	**3.08**	**0.32**	**0.29**	**0.46**	**0.26**
Min.	**0.02**	**0.14**	**0.00**	**0.00**	**0.00**	**0.00**
Max.	**5.96**	**8.69**	**5.21**	**3.08**	**4.22**	**2.58**

Table 3: Calibration Prediction Performance in terms of Absolute Relative Error

2- Time-lapse Prediction Models Results (75 Models/Wells)

	DAK-Sutton, psi	DAK-Standing, psi	Brill & Beggs-Sutton, psi	Brill & Beggs-Standing, psi	Mahmoud-Sutton, psi	Mahmoud-Standing, psi
Avg.	**116.11**	**137.14**	**79.59**	**78.78**	**95.91**	**86.37**
Min.	**3.85**	**4.00**	**0.43**	**0.20**	**0.21**	**0.23**
Max.	**346.24**	**334.99**	**226.15**	**217.78**	**294.73**	**250.54**

Table 4: Time-lapse Prediction Performance in terms of Absolute Pressure Difference

	DAK-Sutton, %	DAK-Standing, %	Brill & Beggs-Sutton, %	Brill & Beggs-Standing, %	Mahmoud-Sutton, %	Mahmoud-Standing, %
Avg.	**2.60**	**3.01**	**1.73**	**1.71**	**2.06**	**1.86**
Min.	**0.06**	**0.08**	**0.01**	**0.00**	**0.00**	**0.00**
Max.	**8.06**	**8.43**	**5.89**	**5.68**	**7.68**	**5.78**

Table 5: Time-lapse Prediction Performance in terms of Absolute Relative Error

4.3 Results Discussion:

The overall results of the top node calculation showed relatively comparable results with actual field measurements in both calculation categories: calibration and time-lapse. However, the error performance of the calibration models are better than those for the time-lapse. The reason behind the healthier error performance on the calibration models is that

they were built as training models for the time-lapse prediction models. Also, the calibration models capture the same pressure and temperature profile of the gradient survey used to perform the calculations without accounting for possible changes in gradient profile with time which has enhanced the prediction performance of the calibration models.

Since the objective of this research is to introduce a new calculation capability, only the results of the calibration models are presented in this research. The focus of results discussion and sensitivity studies is devoted to the best performing correlation combination of the time-lapse predication models.

The combination of Brill & Beggs z-factor correlation with Standing pseudo critical pressure and temperature properties was found to be the best performing combination amongst the six combinations in terms of absolute pressure difference and absolute relative error. These average values, produced by the Brill & Beggs-Standing combination, was found to be the lowest among all six combinations over the data sample used for this research. This combination produced an average absolute pressure difference between calculated SBHP and field measurements of 78.78 psi. This absolute pressure difference translates into an absolute relative error of 1.71%. It is worth noting that the Brill & Beggs-Sutton and the Mahmoud-Standing combinations produced similar error performances. The Brill & Beggs-Sutton combination produced an average absolute pressure difference of 79.59 psi (1.73% absolute relative error), while the Mahmoud-Standing combination produced an average absolute pressure difference of 86.37 psi (1.86% absolute relative error).

CHAPTER 5

COMPARISON WITH PREVIOUS METHODS

As stated in the research motive of section (1.3), the objective of this research is to introduce the apparent molecular weight profiling to perform the top node calculations. The ability to profile and capture changes in the apparent molecular weight (and consequently changes in specific gravity) in wet gas wells will improve the SBHP prediction. Conversely, using a singular value of specific gravity (typically well stream gravity) will not account for molecular weight and specific gravity changes. Hence, assuming the presence of one single specific gravity value for the wet natural gas well reduces the accuracy of the SBHP calculation.

This section will compare the prediction performance of the top node method with previous methods in the literature. The following four methods were selected:

1- Rawlins & Schellhardt method
2- Cullender & Smith method
3- Rzasa & Katz (Average Z & T) method
4- Sukkar & Cornell method

5.1 Input Data used for SBHP Comparison

To perform the SBHP calculations, all methods require the knowledge of the shut-in wellhead pressure and the well depth. However, the methods vary in other additional inputs

to complete the bottomhole pressure calculations. Table 13 lists all the required input to perform the SBHP calculations.

Method	Shut-in Wellhead Pressure	Well Depth	Specific Gravity	Pressure & Temperature Survey
Top Node	Yes	Yes	No	Yes
Rawlins & Schellhardt	Yes	Yes	Yes	No
Cullender & Smith,	Yes	Yes	Yes	Yes
Rzasa & Katz	Yes	Yes	Yes	Yes
Sukkar & Cornell	Yes	Yes	Yes	Yes

Table 6: Summary of Input Data Required for All Calculation Methods

All methods, except for the top node, require knowledge of the specific gas gravity (typically the well stream gravity). The gas gravity is calculated from gas composition obtained using laboratory work. A singular value of gas gravity is used which does not capture changes in gas gravity similar to the top node. Hence, the top node method has outperformed the other four methods in terms of prediction performance. Appendix-G shows the apparent molecular weight profiling that captures changes of molecular weight and specific gas gravity with depth for some of the wells used to carry out the comparison.

Another advantageous feature of the top node method, besides its superior prediction performance, is that it does not require the gas gravity as an input. For the four other methods, the well stream gas composition needs to be established using laboratory work which makes it impractical. Alternatively, the gas gravity can be populated or assumed constant to apply the four SBHP calculation method which will impact the prediction accuracy.

The other input that is not constant in all methods is the pressure and temperature surveys. Pressure and temperature surveys are required at least once during the life time of a well. From such surveys, a baseline molecular weight profile can be built to apply the top node

method, while the shut-in wellhead and bottom hole temperature measurements can be used to perform the SBHP calculations for the Cullender & Smith, Rzasa & Katz, and Sukkar & Cornell methods. The Rawlins & Schellhardt method is the only method that does not require pressure and temperature surveys.

5.2 Comparison Results:

A total of 12 case studies were used to compare between the top node calculation (using the Brill & Beggs-Standing combination) and the previous methods. The data sample used for the comparative analysis is characterized as follows:

1- Wells' data are from four different fields.
2- Two wells were compared using the calibration calculation mode.
3- Ten wells were compared using the time-lapse calculation mode.

The comparison results of the top node calculation with the four previous method are listed in Tables 6 to 10.

Well	Top Node Predicted Pressure, psi	Absolute Pressure Difference, psi	Absolute Relative Error, %
A	5969.70	**2.51**	**0.04**
B	5207.80	**0.22**	**0.00**
C	5307.65	**0.20**	**0.00**
D	5770.57	**4.83**	**0.08**
E	5159.88	**3.21**	**0.06**
F	3071.49	**7.98**	**0.26**
G	3159.16	**6.36**	**0.20**
H	4971.05	**0.95**	**0.02**
I	3835.98	**5.22**	**0.14**
J	7076.71	**51.94**	**0.73**
K	5214.68	**99.49**	**1.95**
L	5327.92	**54.39**	**1.03**

Table 7: Top Node Method Prediction Performance Results

Well	Rawlins & Schellhardt Predicted Pressure, psi	Absolute Pressure Difference, psi	Absolute Relative Error, %
A	5636.23	**330.96**	**5.55**
B	4865.37	**342.21**	**6.57**
C	5001.09	**306.36**	**5.77**
D	5321.62	**453.78**	**7.86**
E	6051.87	**895.20**	**17.36**
F	3128.03	**64.52**	**2.11**
G	3226.39	**73.59**	**2.33**
H	4762.17	**209.83**	**4.22**
I	3784.31	**56.89**	**1.48**
J	7924.60	**795.95**	**11.17**
K	5516.85	**401.66**	**7.85**
L	5717.28	**443.75**	**8.41**

Table 8: Rawlins & Schellhardt Method Prediction Performance Results

Well	Cullender & Smith Predicted Pressure, psi	Absolute Pressure Difference, psi	Absolute Relative Error, %
A	5496.36	**470.83**	**7.89**
B	4828.03	**379.55**	**7.29**
C	4914.35	**393.10**	**7.41**
D	5115.24	**660.16**	**11.43**
E	5784.39	**627.72**	**12.17**
F	3132.95	**69.44**	**2.27**
G	3245.01	**92.21**	**2.92**
H	4760.09	**211.91**	**4.26**
I	3819.33	**21.87**	**0.57**
J	7243.34	**114.69**	**1.61**
K	5294.34	**179.15**	**3.50**
L	5465.29	**191.76**	**3.64**

Table 9: Cullender & Smith Method Prediction Performance Results

Well	Average Z & T Predicted Pressure, psi	Absolute Pressure Difference, psi	Absolute Relative Error, %
A	5479.86	**487.33**	**8.17**
B	4813.36	**394.22**	**7.57**
C	4899.31	**408.14**	**7.69**
D	5096.77	**678.63**	**11.75**
E	5763.32	**606.65**	**11.76**
F	3116.37	**52.86**	**1.73**
G	3218.71	**65.91**	**2.09**
H	4750.57	**221.43**	**4.45**
I	3794.55	**46.65**	**1.21**
J	7223.44	**94.79**	**1.33**
K	5264.50	**149.31**	**2.92**
L	5436.53	**163.00**	**3.09**

Table 10: Rzasa & Katz Method Prediction Performance Results

Well	Sukkar & Cornell Predicted Pressure, psi	Absolute Pressure Difference, psi	Absolute Relative Error, %
A	5449.51	**517.68**	**8.68**
B	4776.39	**431.19**	**8.28**
C	4884.04	**423.41**	**7.98**
D	5078.20	**697.20**	**12.07**
E	5746.38	**589.71**	**11.44**
F	3129.56	**66.05**	**2.16**
G	3262.73	**109.93**	**3.49**
H	4746.27	**225.73**	**4.54**
I	3731.68	**109.52**	**2.85**
J	7194.18	**65.53**	**0.92**
K	5262.41	**147.22**	**2.88**
L	5462.24	**188.71**	**3.58**

Table 11: Sukkar & Cornell Method Prediction Performance Results

5.2 Results Discussion:

The comparison results revealed that the top node method has outperformed all four other methods to calculate the SBHP in terms of absolute pressure difference in psi and absolute relative error.

In this data sample, all twelve case studies (calibration and time-lapse) showed that the top node method provided a better prediction than the other four methods. The average errors of all four methods are summarized in the Table 11 (absolute pressure difference) and Table 12 (absolute relative error).

	Top Node, psi	Rawlins & Schellhardt, psi	Cullender & Smith, psi	Rzasa & Katz, psi	Sukkar & Cornell, psi
Avg.	**19.78**	**364.56**	**284.37**	**280.74**	**297.66**
Min.	**0.20**	**56.89**	**21.87**	**46.65**	**65.53**
Max.	**99.49**	**895.20**	**660.16**	**678.63**	**697.20**

Table 12: Overall Prediction Performance of All Methods in terms of Absolute Pressure Difference

	Top Node, %	Rawlins & Schellhardt, %	Cullender & Smith, %	Rzasa & Katz, %	Sukkar & Cornell, %
Avg.	**0.38**	**6.72**	**5.41**	**5.31**	**5.74**
Min.	**0.00**	**1.48**	**0.57**	**1.21**	**0.92**
Max.	**1.95**	**17.36**	**12.17**	**11.76**	**12.07**

Table 13: Overall Prediction Performance of All Methods in terms of Absolute Relative Error

It is worth noting that Wells E & D developed the highest error in all previous methods (Rawlins & Schellhardt, Cullender & Smith, Rzasa & Katz, and Sukkar & Cornell). This was found to be due to the deviation of the single value of gas gravity used for calculation compared with the gas gravities generated by molecular weight profiling.

CHAPTER 6

ERROR ANALYSIS

As stated in Chapter-4 (section **4.3**), the Brill & Beggs z-factor correlation combination with Standing pseudo critical pressure and temperature properties correlation will be the focus of the error analysis chapter. This combination was found to be the best performing correlation amongst the six combinations in terms of absolute pressure difference and absolute relative error.

6.1 45-Degree Line Analysis

The prediction performance results of the Brill & Beggs-Standing combination were analyzed using the famous statistical tool; 45-Degree Line. The actual downhole static bottomhole pressures of the case studies were plotted against top node method predictions. The plot shows a strong correlation between the predicted and actual value with a regression coefficient of 0.9906.

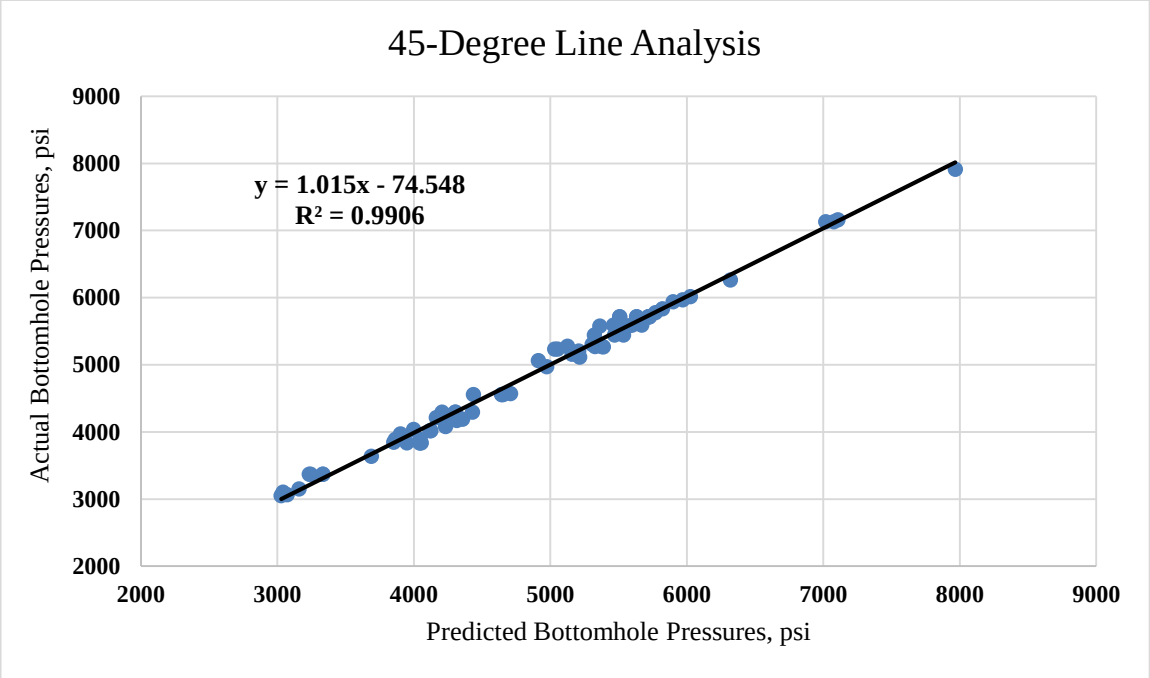

Figure 10: 45-Degree Line Plot

6.2 Error Descriptive Statistics

The descriptive statistics of the Brill & Beggs-Standing combination results to predict the SBHP using the top node is presented in the below two tables. Table 14 describes the absolute pressure difference in psi, while Table 15 describes the absolute relative error.

Absolute Pressure Difference Descriptive Statistics	
Mean, psi	**78.78**
Standard Error, psi	**7.60**
Median, psi	**68.61**
Standard Deviation, psi	**65.84**
Range, psi	**217.57**
Minimum, psi	**0.20**
Maximum, psi	**217.78**
Count	**75**

Table 14: Descriptive Statistics of the Best Performing Correlations in terms of Absolute Pressure Difference

Absolute Relative Error Descriptive Statistics	
Mean, %	**1.71**
Standard Error, %	**0.17**
Median, %	**1.44**
Standard Deviation, %	**1.50**
Range, %	**5.67**
Minimum, %	**0.0038**
Maximum, %	**5.68**
Count	**75**

Table 15: Descriptive Statistics of the Best Performing Correlations in terms of Absolute Relative Error

The following points describe the major observations from the above tables:

1- A maximum error of 217.78 psi (5.68 %) from true value attests to the excellent prediction performance of the proposed methodology.

2- An average absolute pressure difference of 78.78 psi (1.71 %) with a standard deviation of 7.60 psi (0.17 %) is obtained. Such a small standard deviation shows that the prediction results are very close to the average and widely applicable to the whole of the data sample.

6.3 Overall Error Distribution

The time-lapse predicting performance error distribution of the Brill & Beggs-Standing combination is analyzed using two histograms. The first histogram (Fig. 10) shows the overall error distribution in terms of absolute pressure difference in psi. While, the second histogram (Fig. 11) shows the overall distribution in terms of absolute relative error.

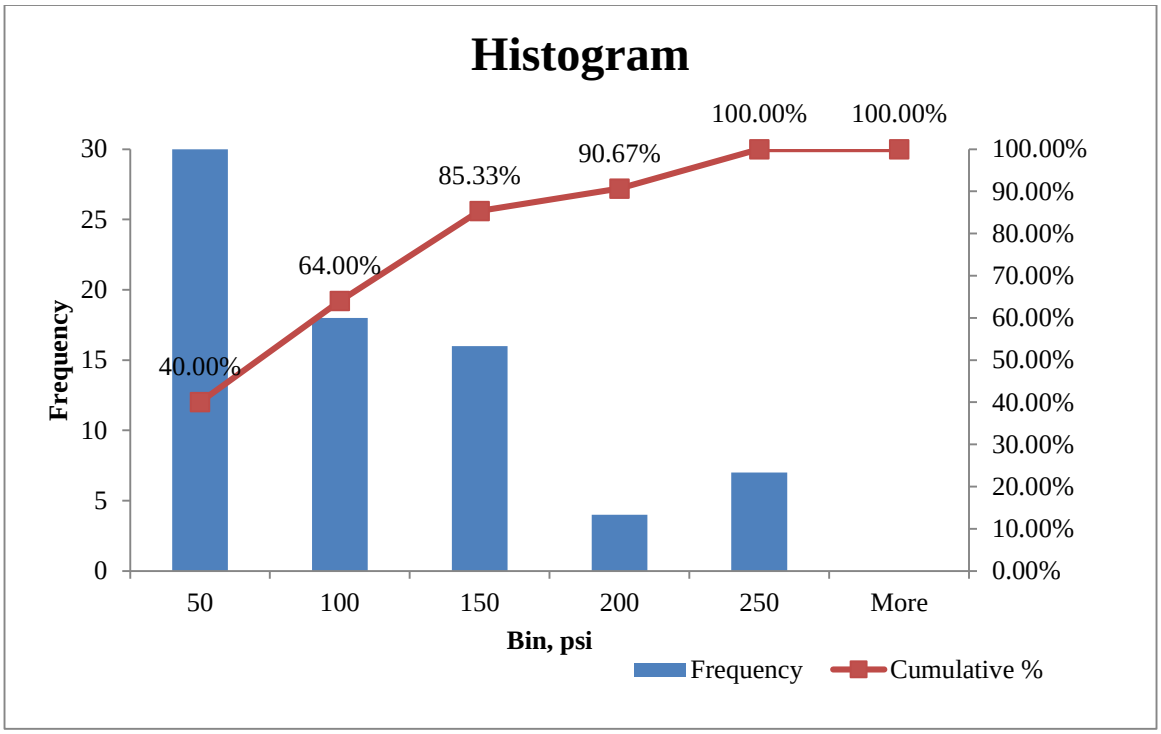

Figure 11: Overall Error Distribution Histogram - Absolute Pressure Difference

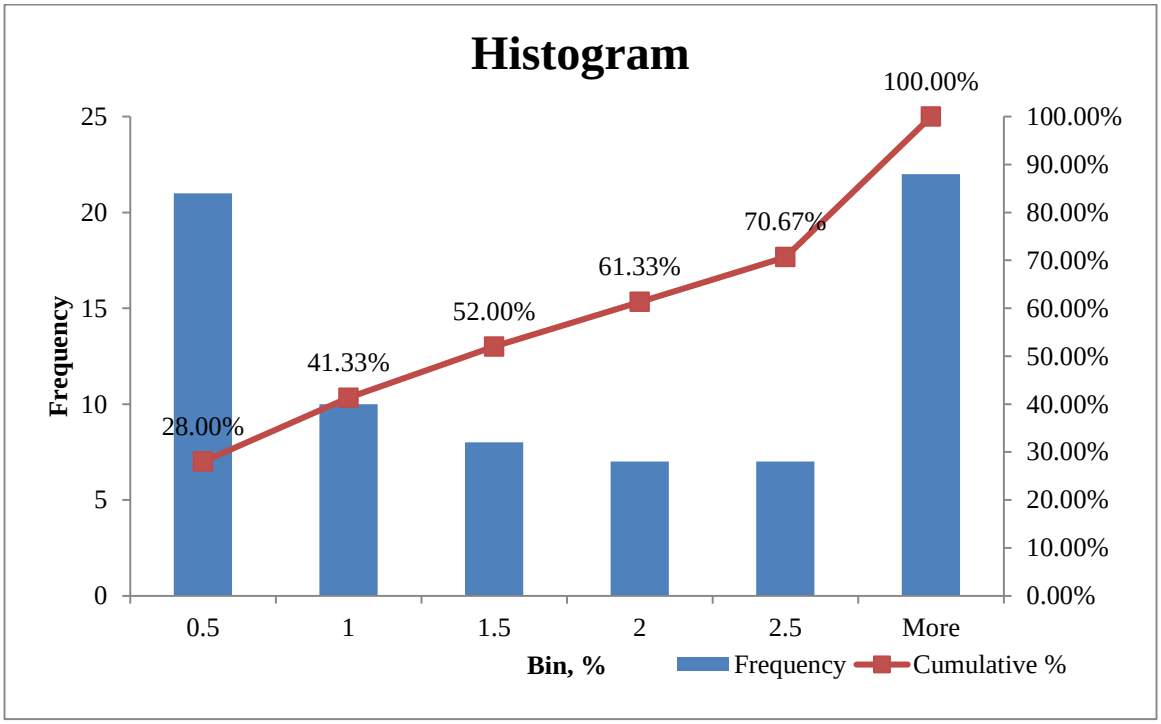

Figure 12: Overall Error Distribution Histogram - Absolute Relative Error

The points below summarize the major observations from the above histograms:

1- More than half of the data (64 %) produced an absolute pressure difference of 100 psi or less, while 90.67% of the data was below 200 psi.

2- More than half of the data (52 %) produced a relative error of 1.5% or lower while 70.67% of the data was below 2.5 % relative error.

6.4 Error Breakdown by Reservoir and Field

This section of the error analysis discusses the results of both the calibration and time-lapse predication models using the Brill & Beggs-Standing combination of correlations. The reason for the combined analysis of both calculation categories is to study the first theoretical premise which states independence of this method of reservoir and field properties.

Field	No. of Wells	Absolute Pressure Difference, psi	Reservoir	No. of Wells	Absolute Pressure Difference, psi
A	27	50.31	RA	1	1.32
B	10	3.98	RB	73	50.52
C	2	2.05	RC	5	32.27
D	4	29.22	RD	32	48.01
E	59	81.83	RE	12	46.04
F	5	13.02	RF	3	10.43
G	28	7.06	RG	11	57.11
H	3	0.69	RH	1	11.81

Table 16: Error Breakdown by Reservoir & Field in terms of Absolute Pressure Difference

Field	No. of Wells	Absolute Relative Error, %	Reservoir	No. of Wells	Absolute Relative Error, %
A	27	1.12	RA	1	0.02
B	10	0.07	RB	73	1.15
C	2	0.03	RC	5	0.63
D	4	0.39	RD	32	1.08
E	59	1.81	RE	12	1.05
F	5	0.29	RF	3	0.34
G	28	0.21	RG	11	1.01
H	3	0.01	RH	1	0.20

Table 17: Error Breakdown by Reservoir & Field in terms of Absolute Relative Error

It is important to note that the wells which were used to carry out the computations associated with this research may be located within the same reservoir in two different fields. For example, reservoir RB is a large reservoir located in Fields A, C, D, G, and H. On the other hand, one field (for example Field-E) has wells completed in multiple reservoir such as RA, RB, RD, RF, and RG.

With the above in mind, the random distribution of error across multiple fields and reservoirs shows clearly that the specific properties which constitute a field or a reservoir did not produce a noticeable error trend. Thus, it is concluded that reservoir or field properties do not affect the error of the top node SBHP calculation.

CHAPTER 7

SENSITIVITY ANALYSIS

This chapter will present the effect of ten parameters on the error performance of the Brill & Beggs-Standing combination of correlations. The objective of this chapter is to delineate possible distinct relationships between any parameter with the prediction error performance of the time-lapse models. In addition, the effect of non-hydrocarbon components and water vapor content on the top node are studied.

The ten parameters listed below will be studied in terms of absolute pressure difference in psi and absolute relative error in %.

1- Shut-in Wellhead Pressure
2- Shut-in Wellhead Temperature
3- Well Depth
4- Bottomhole Pressure
5- Bottomhole Temperature
6- Well Gradient
7- Average Well Z-Factor
8- Average Well Molecular Weight
9- Average Well Specific Gravity
10- Elapsed Time

The sections to follow will present the relationship between any of the parameters with the error along with the best-fit-equation that describes the relationship. The last section of this chapter will discuss the results of these sensitivity studies.

It is important to note that the objective of the sensitivity studies section is not to correlate parameters with calculation results. The prime objective of running the sensitivities is to determine whether or not a certain parameter produces a trend that can be used to incorporate correction factors to the overall methodology and, hence, further enhances its accuracy.

7.1 Effect of Shut-in Wellhead Pressure

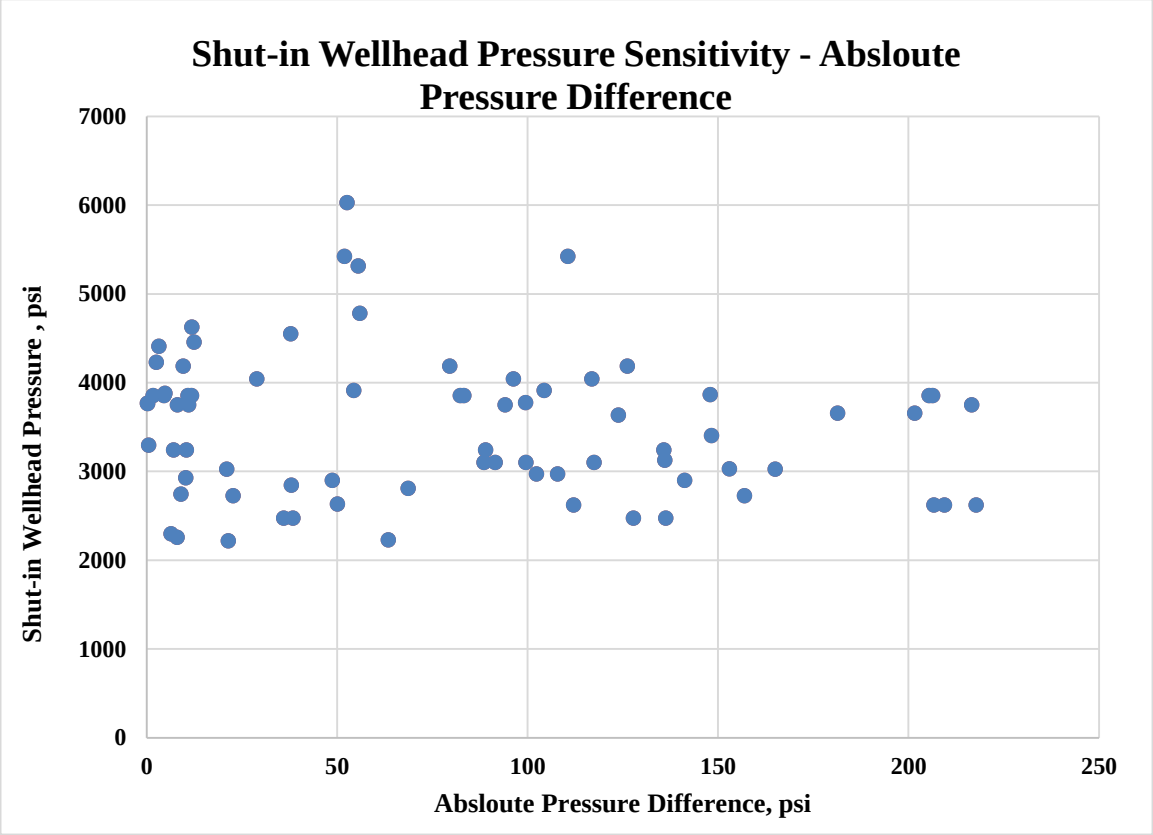

Figure 13: Shut-in Wellhead Pressure Sensitivity Plot - Absolute Pressure Difference

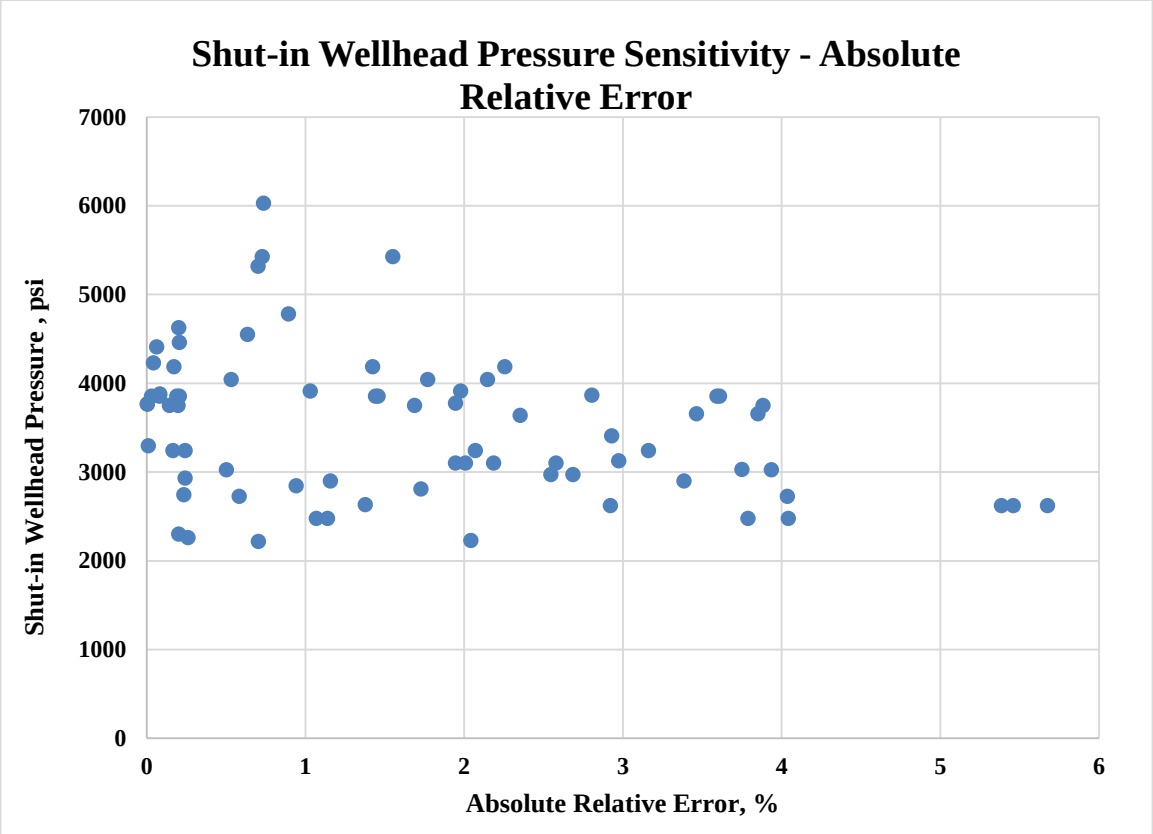

Figure 14: Shut-in Wellhead Pressure Sensitivity Plot - Absolute Relative Error

7.2 Effect of Shut-in Wellhead Temperature

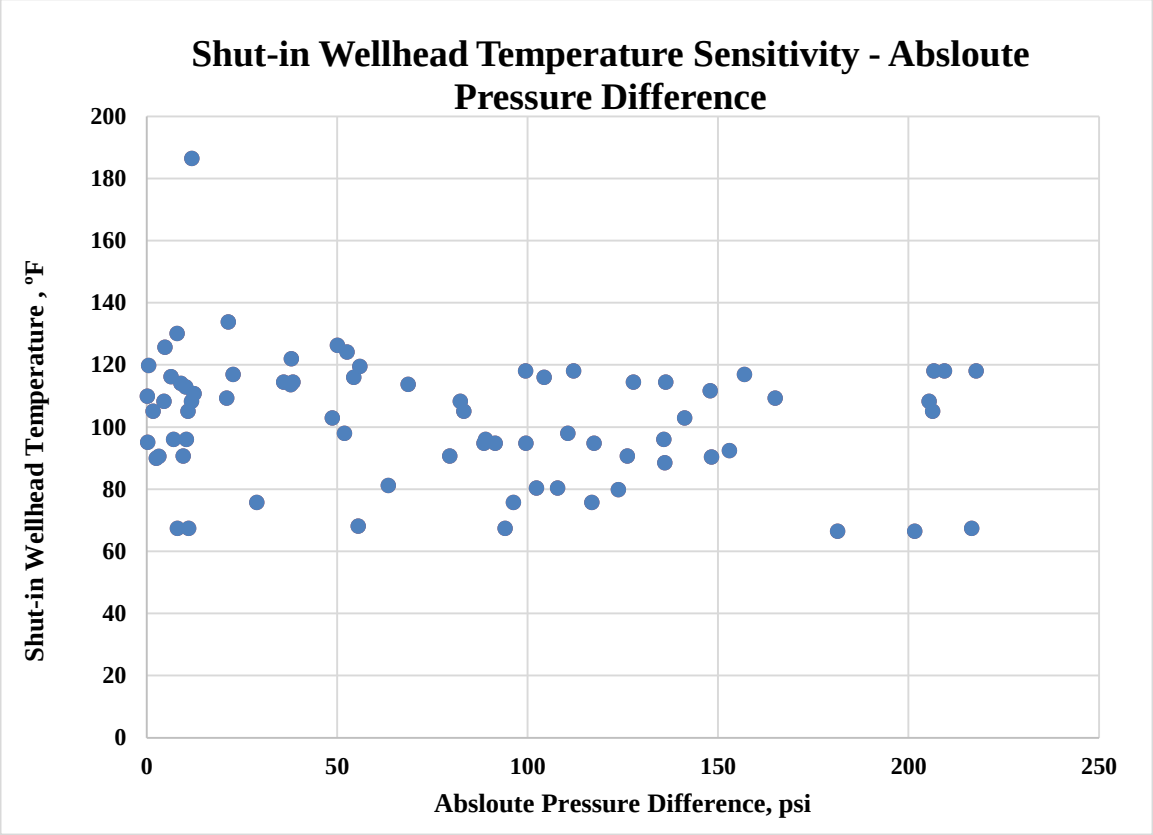

Figure 15: Shut-in Wellhead Temperature Sensitivity Plot - Absolute Pressure Difference

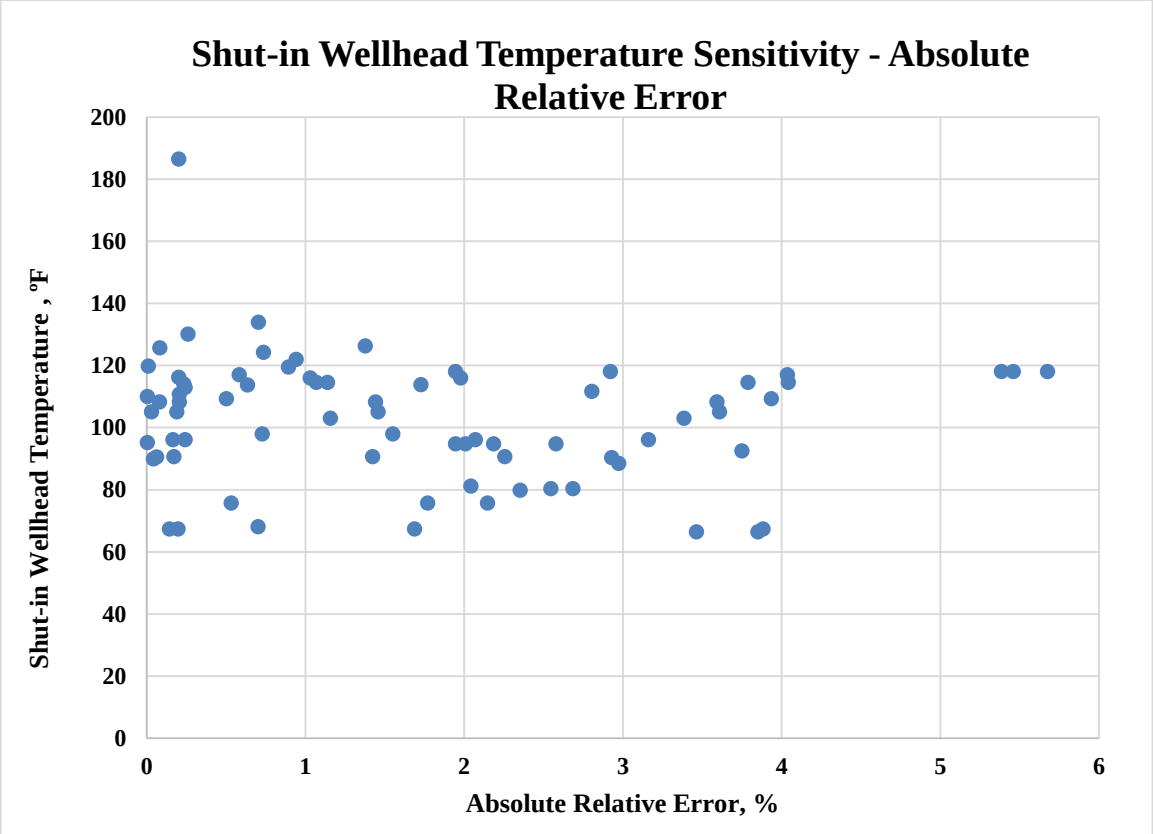

Figure 16: Shut-in Wellhead Temperature Sensitivity Plot - Absolute Relative Error

7.3 Effect of Well Depth

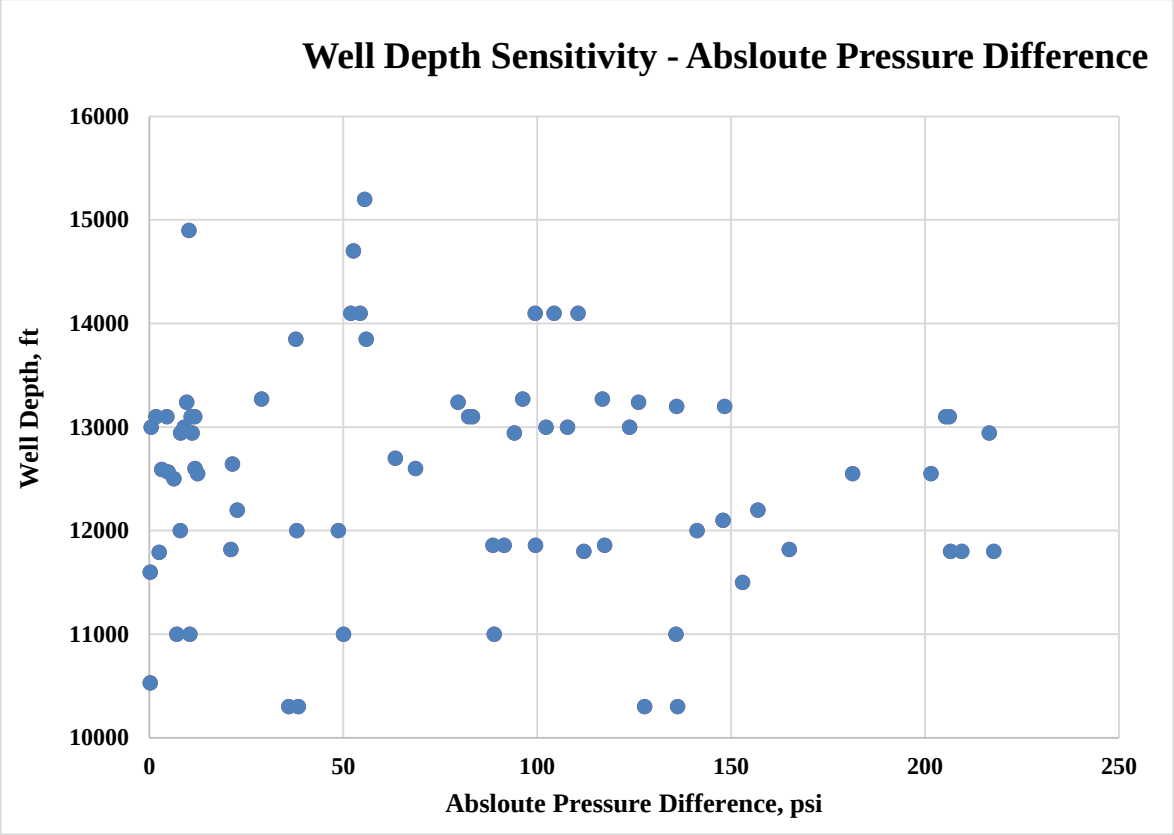

Figure 17: Well Depth Sensitivity Plot - Absolute Pressure Difference

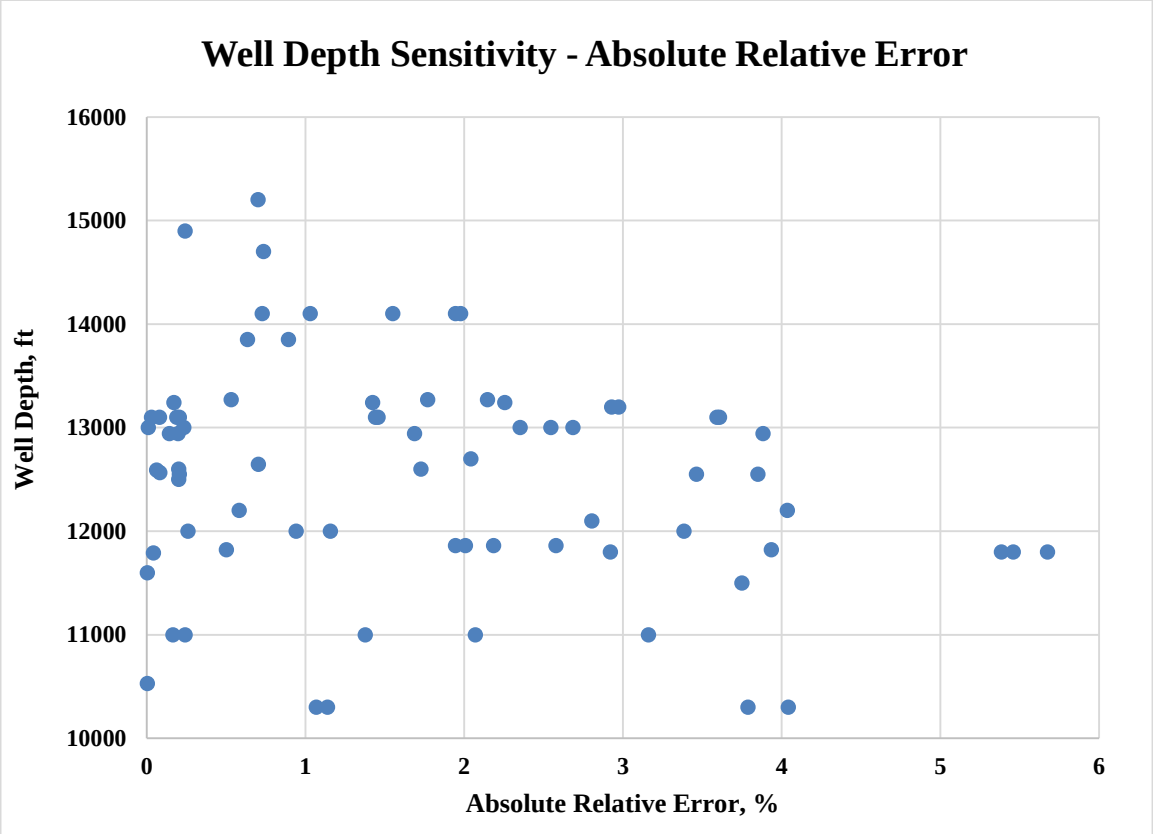

Figure 18: Well Depth Sensitivity Plot - Absolute Relative Error

7.4 Effect of Bottomhole Pressure

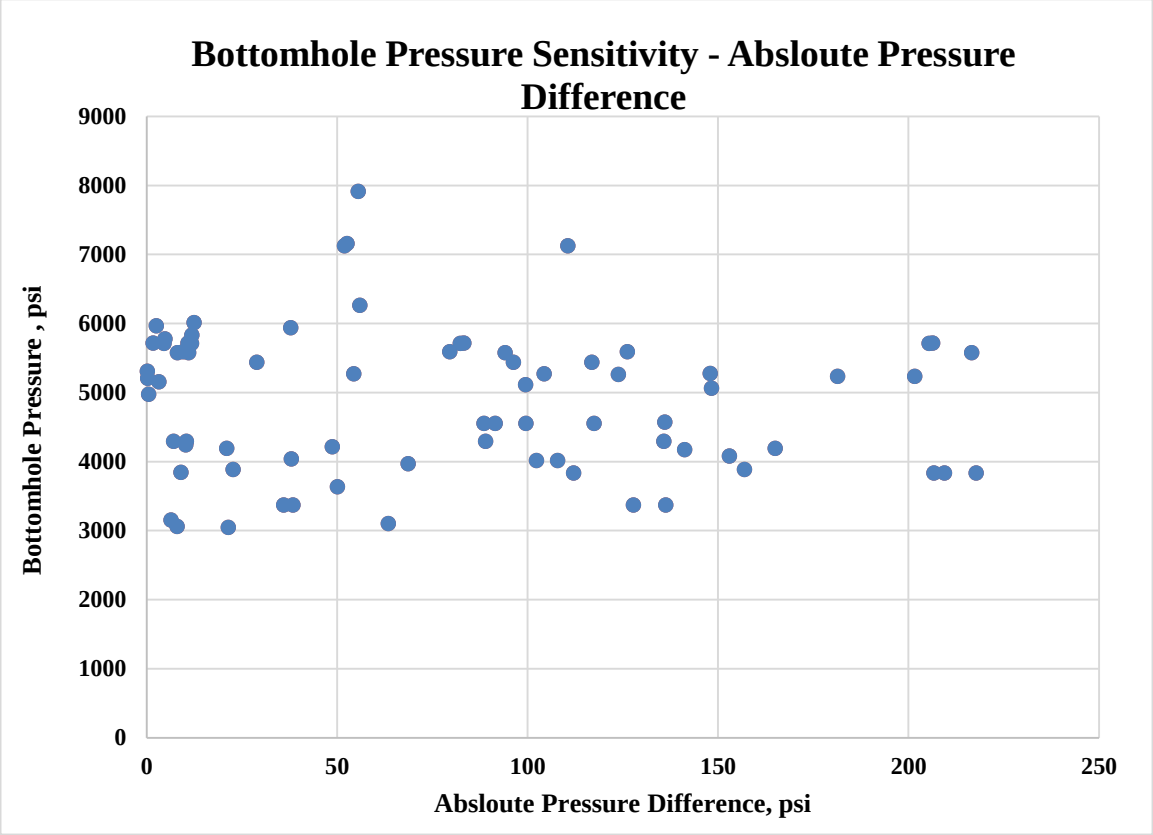

Figure 19: Bottomhole Pressure Sensitivity Plot - Absolute Pressure Difference

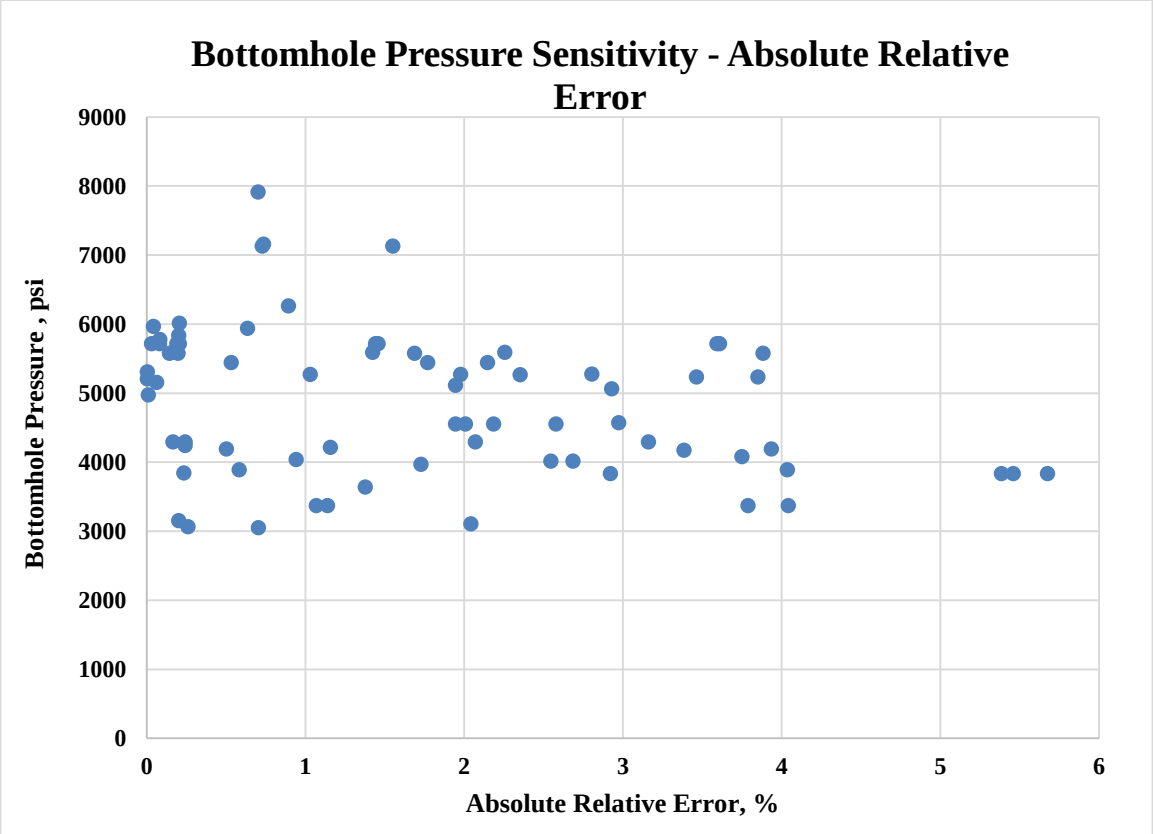

Figure 20: Bottomhole Pressure Sensitivity Plot - Absolute Relative Error

7.5 Effect of Bottomhole Temperature

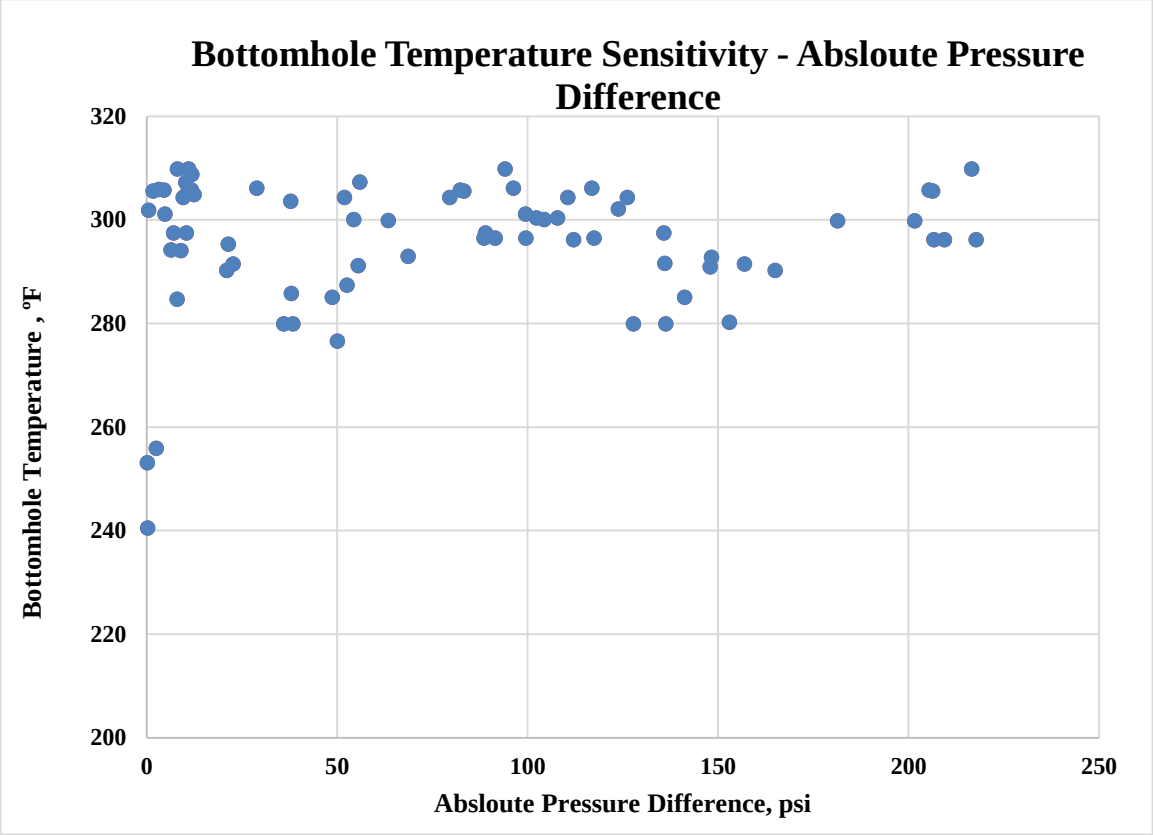

Figure 21: Bottomhole Temperature Sensitivity Plot - Absolute Pressure Difference

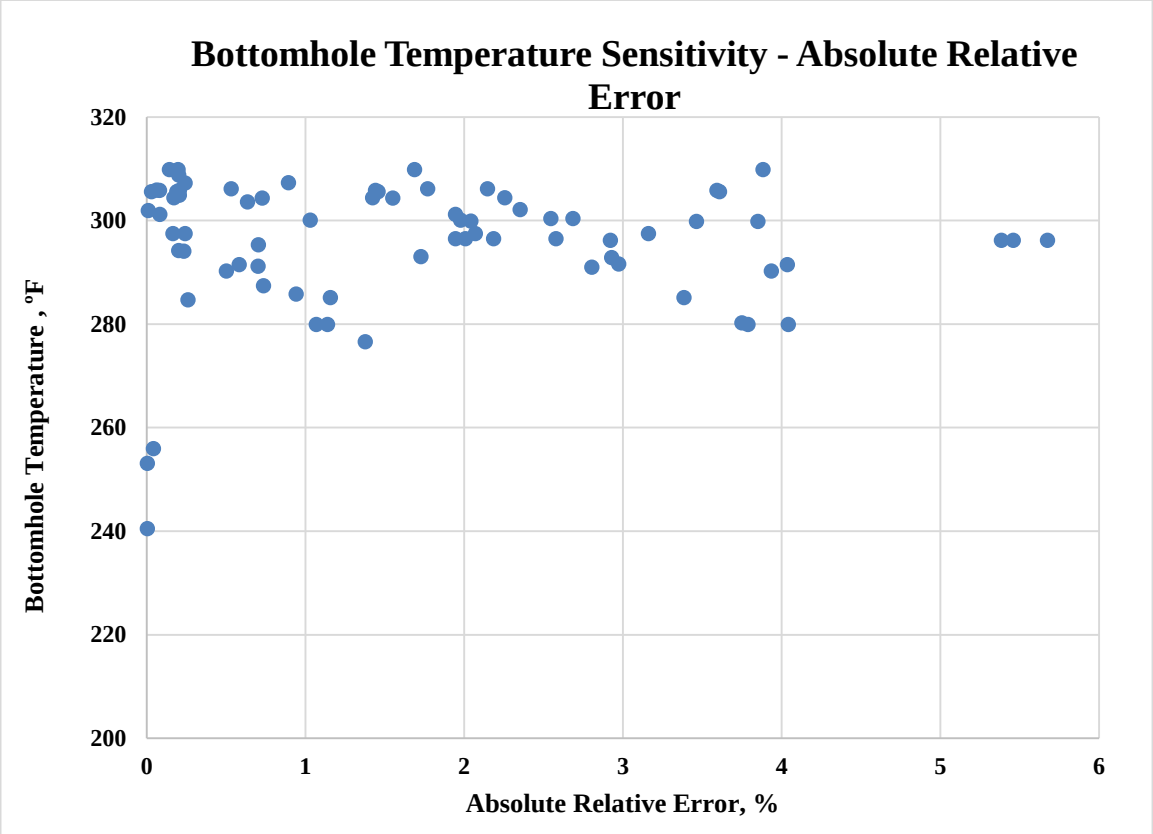

Figure 22: Bottomhole Temperature Sensitivity Plot - Absolute Relative Error

7.6 Effect of Well Gradient

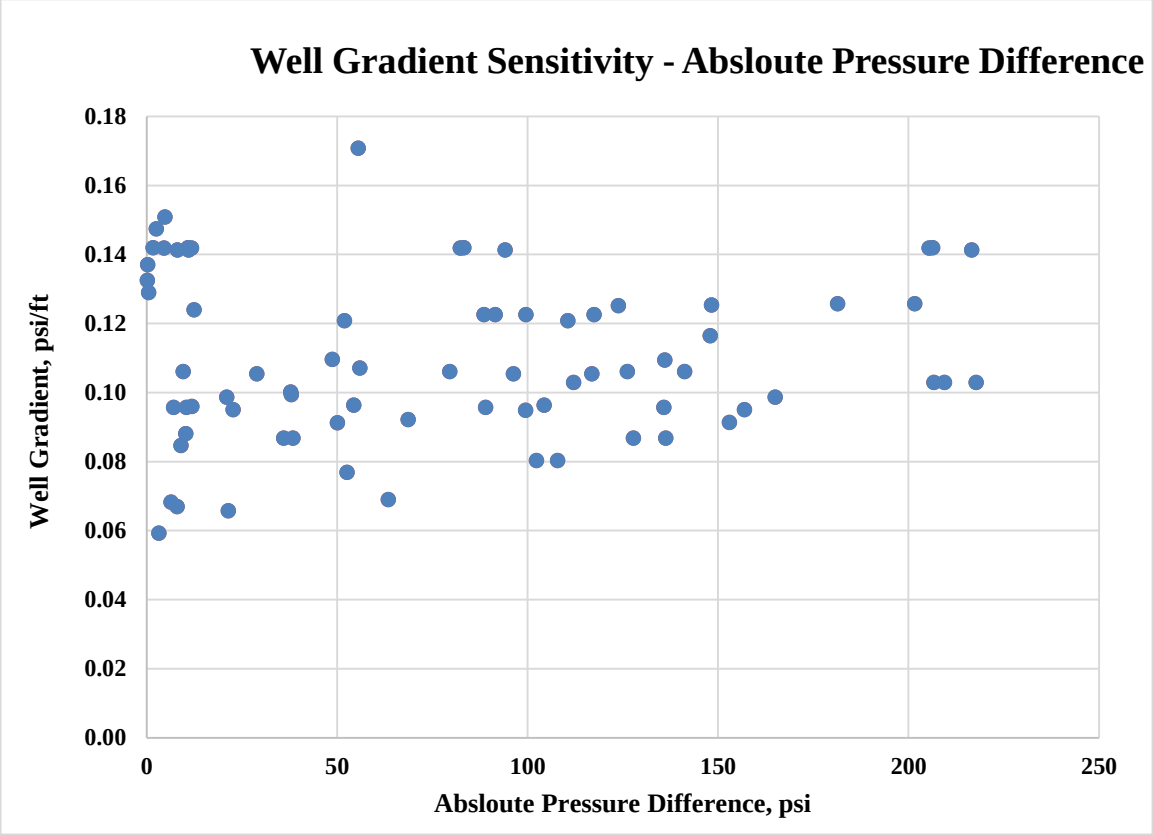

Figure 23: Well Gradient Sensitivity Plot - Absolute Pressure Difference

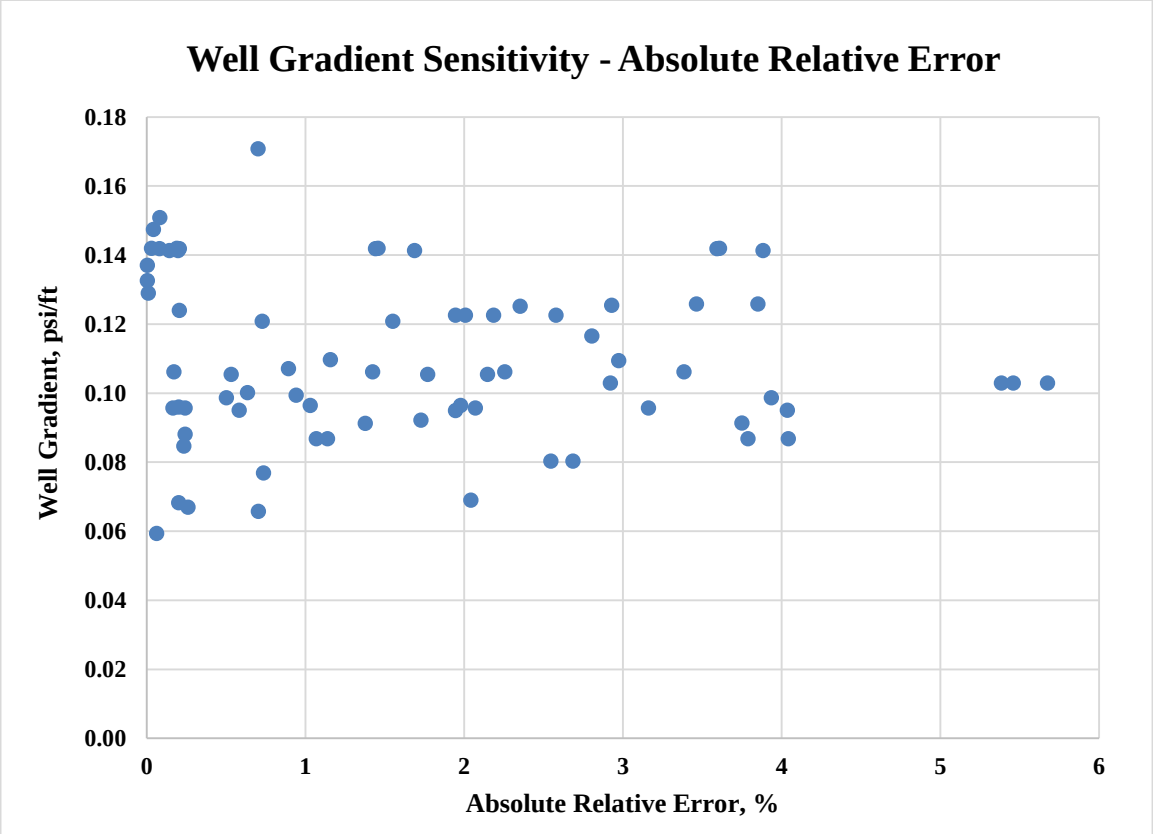

Figure 24: Well Gradient Sensitivity Plot - Absolute Relative Error

7.7 Effect of Well Average Z-Factor

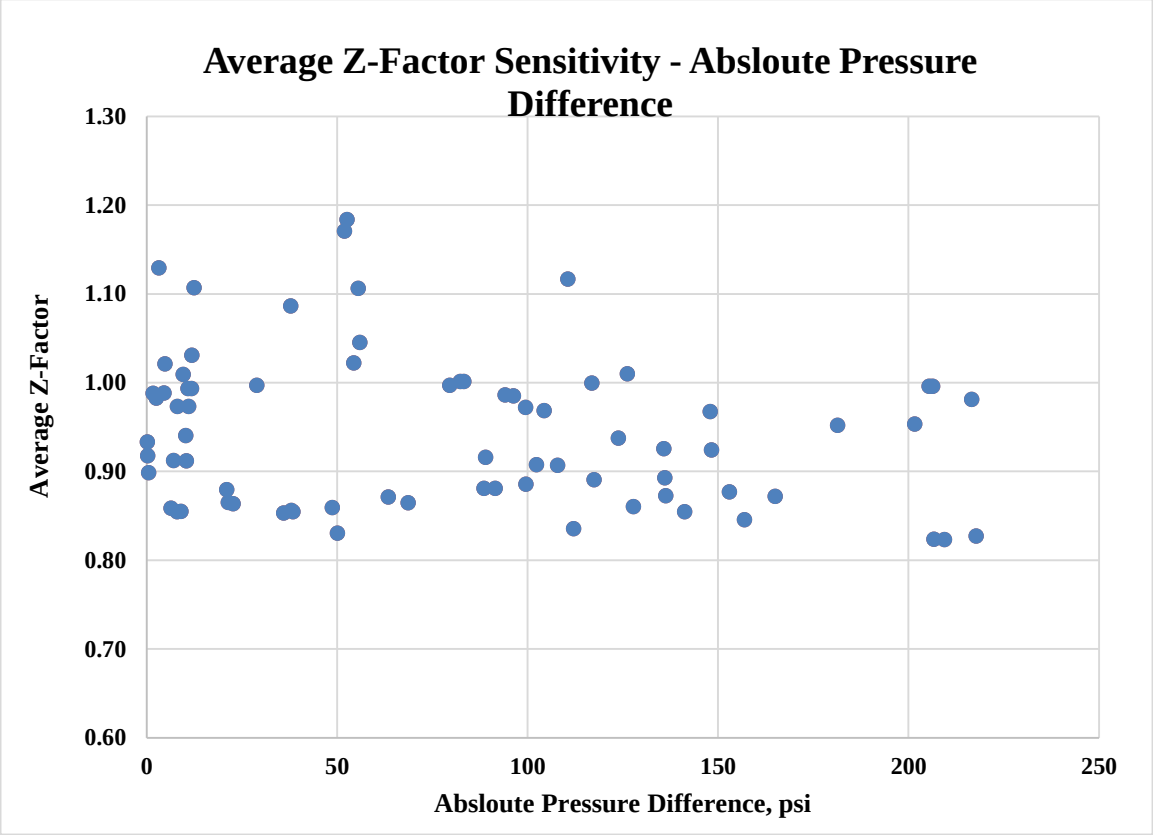

Figure 25: Well Average Z-Factor Sensitivity Plot - Absolute Pressure Difference

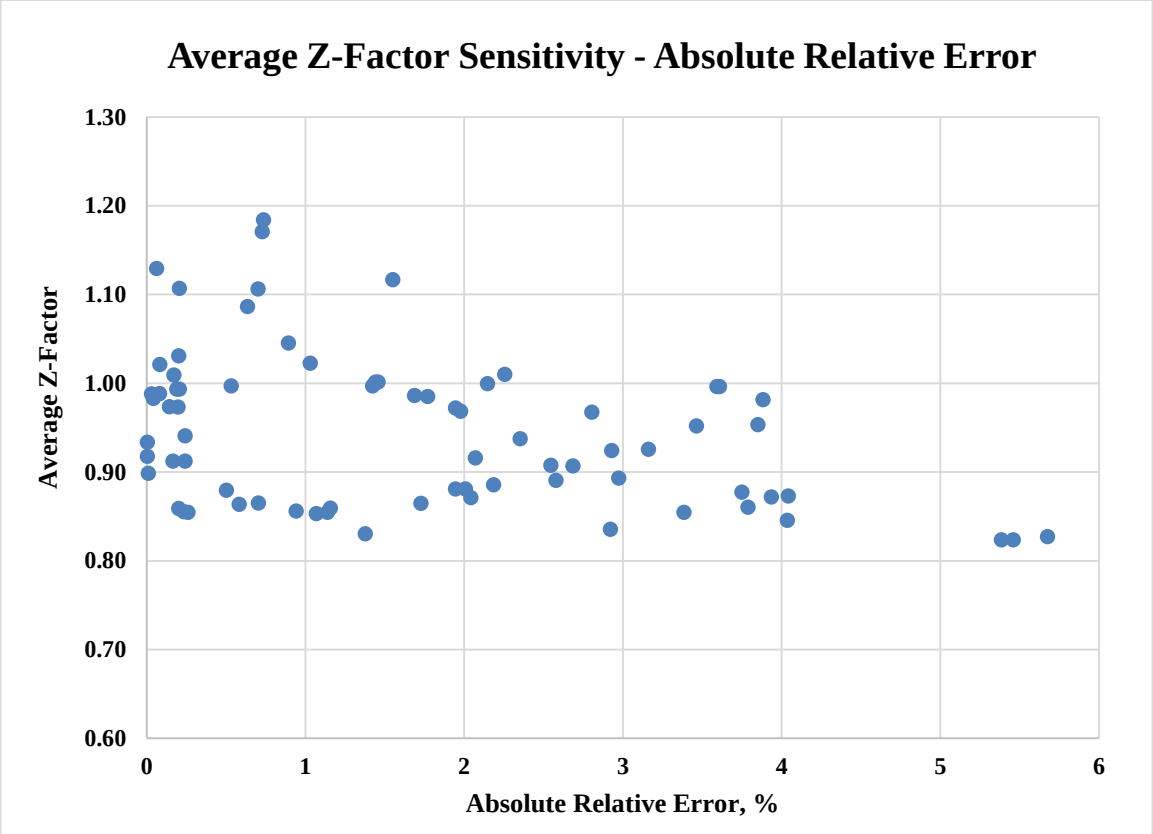

Figure 26: Well Average Z-Factor Sensitivity Plot - Absolute Relative Error

7.8 Effect of Well Average Molecular Weight

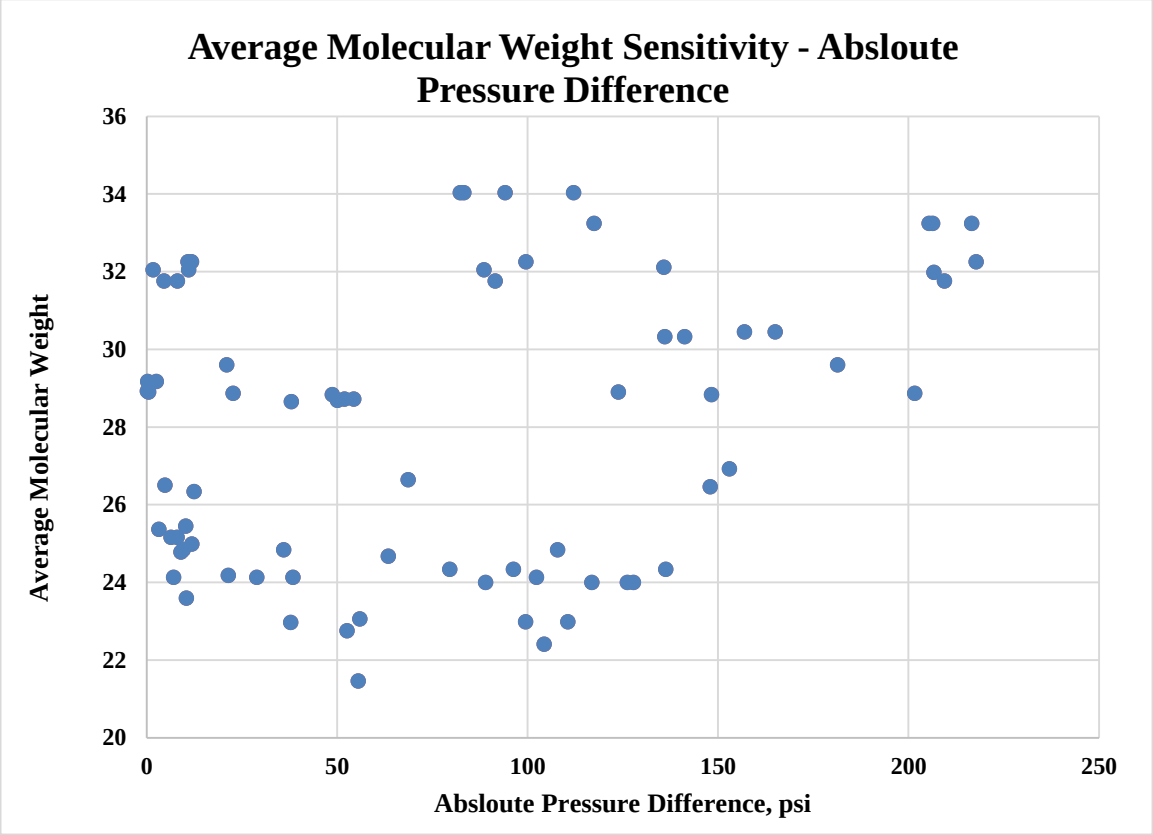

Figure 27: Well Average Molecular Weight Sensitivity Plot - Absolute Pressure Difference

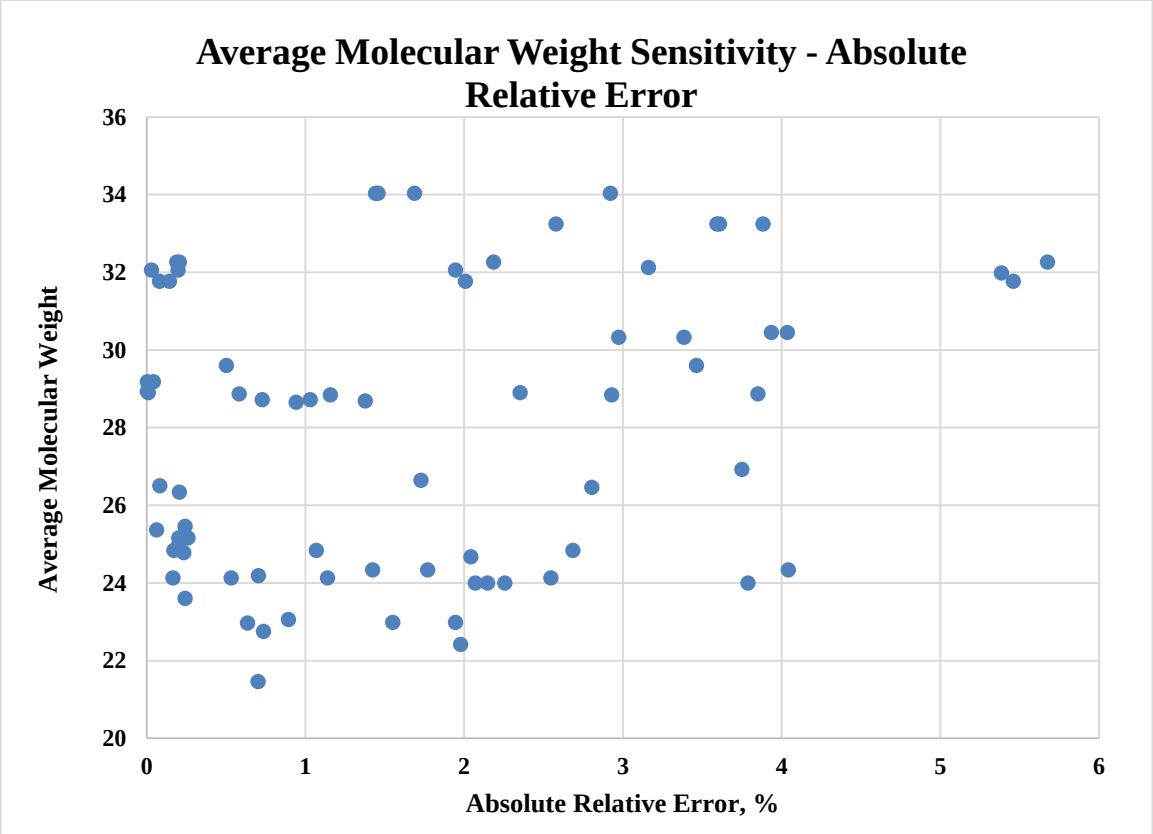

Figure 28: Well Average Molecular Weight Sensitivity Plot - Absolute Relative Error

7.9 Effect of Well Average Specific Gravity

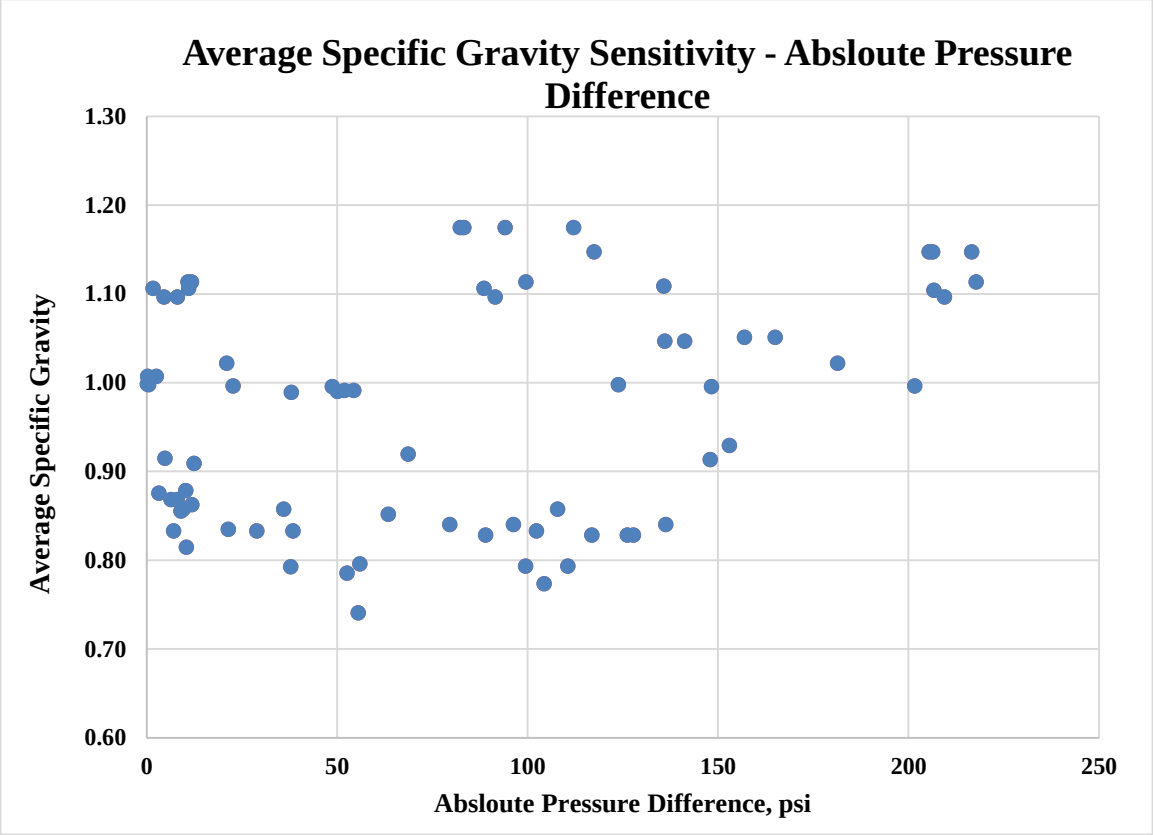

Figure 29: Well Average Specific Gravity Sensitivity Plot - Absolute Pressure Difference

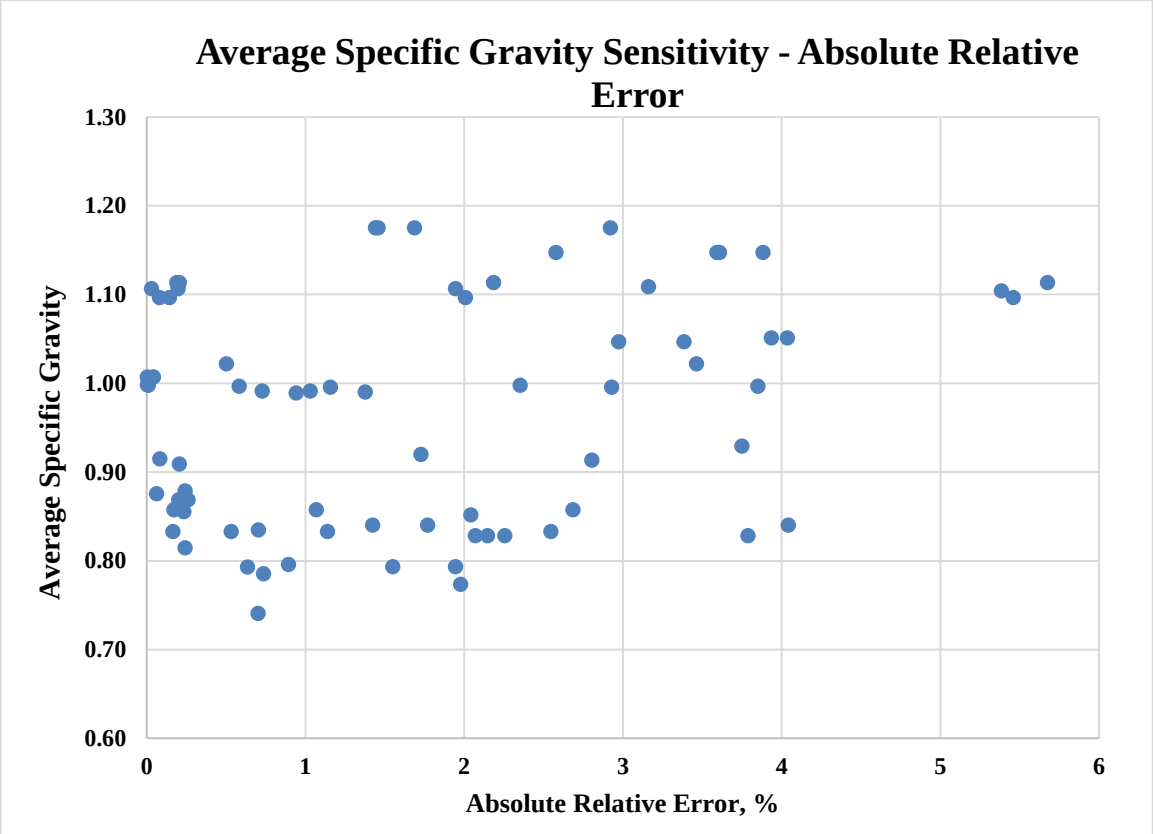

Figure 30: Well Average Specific Gravity Sensitivity Plot - Absolute Relative Error

7.10 Effect of Elapsed Time

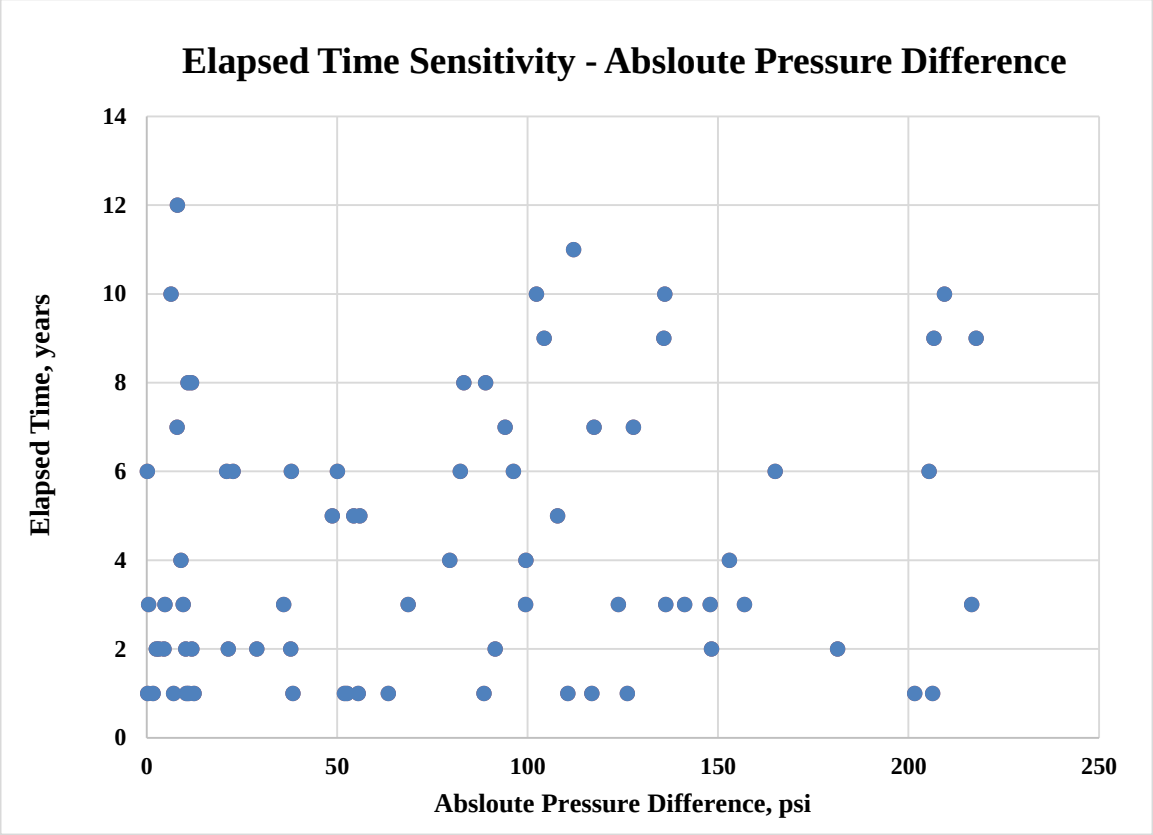

Figure 31: Elapsed Time Sensitivity Plot - Absolute Pressure Difference

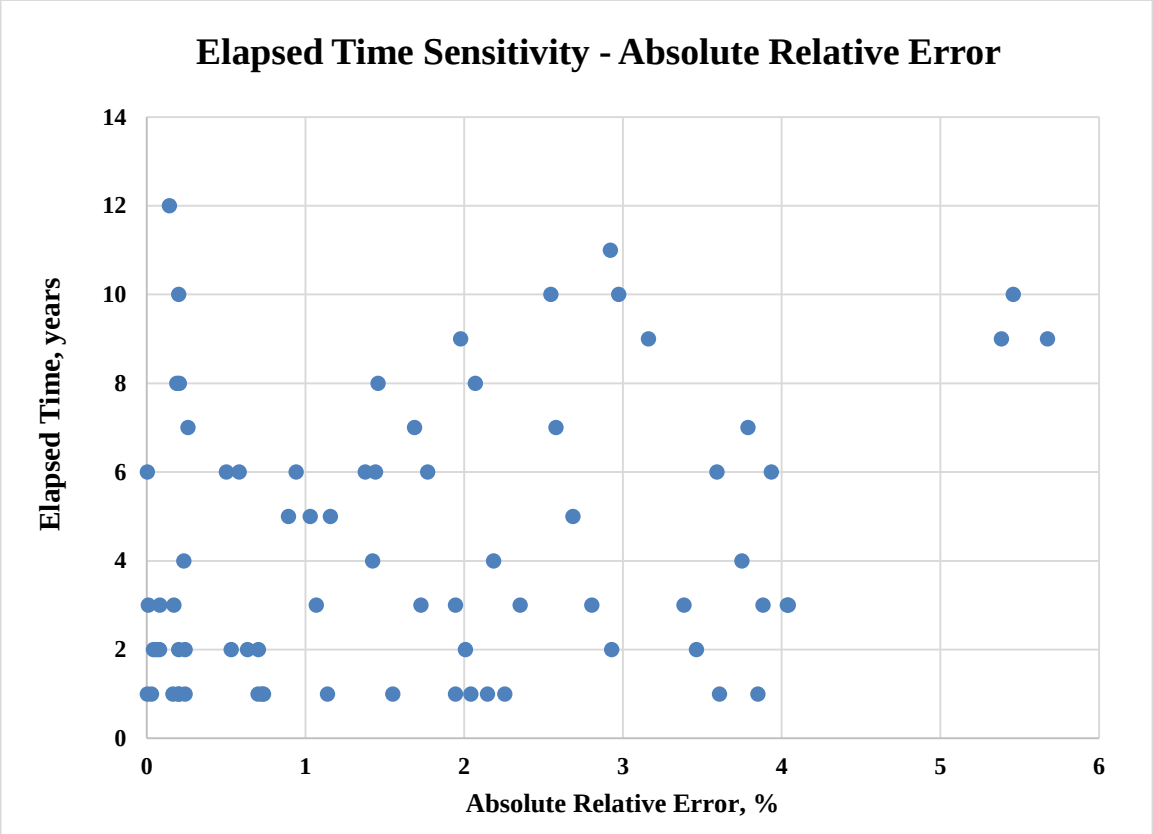

Figure 32: Elapsed Time Sensitivity Plot - Absolute Relative Error

7.11 Effect of Non-hydrocarbon Components

As stated in the methodology section, the effect of non-hydrocarbon components which are Hydrogen Sulfide, Carbon Dioxide, and Nitrogen are not factored into the top node calculations. These components are typically obtained by laboratory analysis narrowing the applicability of the top node method on the gas well intended for SBHP calculations.

In this section, we will factor in the effect of impurities on the top node calculation results. Six gas wells were selected to run the sensitives. All six wells have been analyzed in the laboratory for impurities. Table 18 below shows the impurities concentrations in % Mole.

Well #	H_2S, % Mole	CO_2, % Mole	N_2, % Mole
A	0	0.45	6.83
E	0.44	2.75	12.61
F	2.34	3.88	13.4
H	0	1.07	7.88
I	5.22	3.31	11.52
J	0	3.79	14.69

Table 18: Impurties Concentrations in % Mole

The concentrations of the impurities were factored into the pseudo critical pressure and temperatures and were assumed constant throughout the top node calculation intervals. It is important to note that well stream samples were collected to perform the compositional analysis and obtain the respective non-hydrocarbon component concentrations. Table 19 below shows the results of the top node calculations of the six selected wells when the impurities corrections were taken into account.

Well	Top Node without Correction, psi	Top Node with Correction, psi	Actual Pressure, psi	Top Node Error, %	Top Node Pressure Difference, psi	Corrected Top Node Error, %	Corrected Top Node Pressure Difference, psi
A	5307.8	5307.84	5307.45	0.007%	0.35	0.007%	0.39
D	5160.14	5156.65	5156.07	0.079%	4.07	0.011%	0.58
F	3151.58	3151.77	3152.8	0.039%	1.22	0.033%	1.03
H	4971.22	4971.23	4972	0.016%	0.78	0.015%	0.77
I	3836.21	3836.92	3841.2	0.130%	4.99	0.111%	4.28
J	7071.12	7090.97	7128	0.798%	56.88	0.520%	37.03

Table 19: The Results of the Corrected Top Node Calculations

From the above results, we notice marginal improvement of the error for all wells except for Well-A.

7.12 Effect of Water Vapor Content

The water vapor pressure correction as proposed by Bukacek was applied on the top node calculations to study its effect on the error. A sample of five wells exhibiting the highest

error was selected to run the calculations. Table 20 below shows the results of the water vapor content sensitivity.

Well	Top Node without Correction, psi	Top Node with Correction, psi	Actual Pressure, psi	Top Node Error, %	Top Node Pressure Difference, psi	Corrected Top Node Error, %	Corrected Top Node Pressure Difference, psi
C1	4846.21	4869.14	5122.80	5.399	276.59	4.952	253.66
C2	4062.86	4065.00	3836.71	5.894	226.15	5.950	228.29
C3	4358.60	4360.53	4191.91	3.976	166.69	4.023	168.62
C4	4048.15	4051.51	3888.00	4.119	160.15	4.206	163.51
C5	4054.33	4057.13	3836.71	5.672	217.62	5.745	220.42

Table 20: The Results of the Water Vapor Content Sensitivity

The above results show that error has in fact increase in all wells except Well-C1.

7.13 Discussion on the Sensitivity Studies

All ten parameters correlated poorly with results of the top node calculations in terms of the absolute pressure difference and absolute relative error. The coefficient of determination for all the generated sensitivities did not exceed 0.2 in all the plots. Accordingly, no discernable trends can be generated from these sensitivity studies based on the obtained results.

It is believed that because the time-lapse prediction model results error (based on the Brill & Beggs-Standing combination of correlations) is already very low, no further enhancement or correction factors can be applied to the top node SBHP calculation methodology to reduce the error.

The effect of non-hydrocarbon components correction has shown that slight improvement in error are obtained in most cases. However, accounting for these correction will limit the applicability of the top node method from all wells with gradient surveys to wells with

gradient surveys and compositional analysis. On the other hand, the water vapor content correction did not improve the error in most case studies. Rather, increase of the error was obtained. The effect of the water vapor content remains an area of further research.

CHAPTER 8

CONCLUSIONS

The following constitutes the main conclusions for this research work:

1- A new method to calculate the static bottomhole pressures of wet gas wells was developed. The method deploys the apparent molecular weight profiling concept to capture changes in gas molecular weights for wet gas wells. Top node calculations using a modified form of the equation of state are used to predict the bottomhole pressure. The method requires the presence of a gradient pressure and temperature survey as inputs for the computations.

2- Out of six correlation combinations, the Brill and Beggs-Standing combination generated the best error in the time-lapse computation category. An average overall error of 1.71 % (78.78 psi) was obtained using this combination.

3- The method was found to be widely applicable across a variety of fields and reservoirs. A data set of 138 case studies was used in this research.

4- The top node method was compared with four other calculation methods existing in the literature. The comparison results revealed that the top node method has outperformed all four other methods to calculate the SBHP in terms of absolute pressure difference in psi and absolute relative error in %.

5- Error analysis of the results indicate a strong correlation between predicted and actual bottomhole values.

6- Error breakdown by reservoir and field revealed no noticeable error trends; hence, reservoir and field properties do not influence the top node method's performance.

7- The effects of ten parameters (Shut-in Wellhead Pressure, Shut-in Wellhead Temperature, Well Depth, Bottomhole Pressure, Bottomhole Temperature, Well Gradient, Average Well Z-Factor, Average Well Molecular Weight, Average Well Specific Gravity, and Elapsed Time) were studied and no discernable trends could be observed from these sensitivity studies.

Appendix A: Predicted Downhole Pressures – Calibration Models

Well No	Actual Pressure, psi	DAK-Sutton, psi	DAK-Standing, psi	Brill & Beggs-Sutton, psi	Brill & Beggs-Standing, psi	Mahmoud-Sutton, psi	Mahmoud-Standing, psi
1	5938.32	5907.77	5977.98	5937.17	5937.00	5937.63	5937.53
2	5265.30	5264.49	5316.38	5264.35	5264.22	5264.31	5264.11
3	6948.10	6947.00	6969.39	6948.48	6948.33	6920.03	6949.24
4	6838.79	6841.65	6859.38	6847.65	6847.07	6783.02	6845.31
5	7051.80	7055.88	7071.28	7064.79	7064.25	7008.35	7049.07
6	6950.32	6955.65	6973.84	6954.69	6954.20	6958.10	6957.57
7	5866.50	5871.92	5924.68	5865.58	5865.40	5856.58	5865.76
8	7209.88	7201.29	7220.14	7210.10	7209.93	7131.14	7211.51
9	5277.70	5284.68	5446.11	5278.07	5277.77	5278.34	5277.46
10	6866.38	6851.66	6884.08	6866.50	6866.38	6806.63	6867.23
11	7912.76	7882.67	7900.31	7913.35	7913.22	7578.98	7913.10
12	3104.90	3118.95	3117.95	3025.15	3024.95	3025.07	3024.76
13	5999.99	5969.92	6051.03	6000.17	6000.01	6000.36	6000.24
14	4972.00	4945.09	5057.05	4971.22	4971.05	4970.96	4970.52
15	5112.80	5082.60	5027.66	4846.21	4955.16	4904.21	5082.76
16	6274.39	6234.90	6314.48	6275.52	6275.38	6275.88	6275.82
17	3740.92	3769.33	3890.12	3740.94	3740.71	3740.82	3740.30
18	4590.77	4626.16	4810.99	4541.71	4541.41	4542.73	4542.07
19	4673.30	4717.51	4779.64	4673.59	4673.44	4673.66	4673.23
20	3299.00	3337.50	3457.06	3298.34	3298.09	3298.10	3297.62
21	5293.30	5358.86	5365.81	5270.86	5270.55	5271.51	5270.43
22	3501.47	3457.32	3651.14	3501.53	3501.29	3501.31	3500.82
23	5853.40	5936.60	5911.71	5857.87	5857.72	5858.09	5857.99
24	5147.00	5229.88	5233.69	5147.48	5147.30	5147.83	5147.47
25	5132.60	5221.63	5232.57	5100.05	5099.82	5100.37	5099.89
26	4802.99	4887.22	4902.84	4803.36	4803.20	4803.49	4803.13
27	3184.06	3247.93	3243.38	3125.61	3125.40	3125.35	3124.99
28	3645.20	3723.62	3804.48	3645.35	3645.11	3645.21	3644.71
29	3143.72	3215.32	3236.16	3143.36	3143.15	3143.15	3142.81
30	3720.32	3780.16	3794.37	3721.25	3720.99	3721.42	3720.79
31	3844.71	3935.23	3982.07	3845.06	3844.81	3845.08	3844.61
32	4300.00	4402.41	4465.84	4309.80	4309.56	4309.88	4309.32
33	4829.40	4947.95	4952.71	4822.25	4821.96	4818.78	4817.95
34	5965.00	5818.46	6029.22	5958.09	5957.87	5884.88	5958.51

35	**3706.58**	**3799.53**	**3816.45**	**3667.13**	**3666.82**	**3665.10**	**3664.49**
36	**3454.00**	**3363.02**	**3609.84**	**3454.45**	**3454.22**	**3454.65**	**3454.17**
37	**2989.00**	**3144.76**	**3126.11**	**2947.86**	**2947.54**	**2945.05**	**2944.35**
38	**4446.61**	**4577.24**	**4712.52**	**4439.80**	**4439.50**	**4440.99**	**4440.34**
39	**4220.26**	**4355.69**	**4365.32**	**4216.69**	**4216.47**	**4216.30**	**4215.82**
40	**3152.80**	**3261.51**	**3257.61**	**3151.58**	**3151.36**	**3151.12**	**3150.77**
41	**3841.20**	**3976.52**	**3968.54**	**3836.21**	**3835.98**	**3834.68**	**3834.16**
42	**2641.00**	**2738.74**	**2746.74**	**2626.56**	**2626.34**	**2626.23**	**2625.89**
43	**3479.51**	**3608.79**	**3602.73**	**3479.50**	**3479.28**	**3479.42**	**3479.03**
44	**4097.00**	**4136.48**	**4220.80**	**4096.59**	**4096.39**	**4096.16**	**4095.66**
45	**4307.60**	**4478.95**	**4475.51**	**4308.14**	**4307.88**	**4308.22**	**4307.60**
46	**3944.30**	**4101.41**	**4091.97**	**3934.06**	**3933.76**	**3930.40**	**3929.58**
47	**3918.90**	**4081.25**	**4071.78**	**3918.88**	**3918.65**	**3919.49**	**3918.99**
48	**2948.50**	**3071.75**	**3056.37**	**2923.93**	**2923.69**	**2923.63**	**2923.23**
49	**3160.80**	**3025.28**	**3306.92**	**3129.36**	**3129.10**	**3128.80**	**3128.29**
50	**3192.90**	**3330.39**	**3313.45**	**3173.31**	**3173.08**	**3172.57**	**3172.13**
51	**3815.07**	**3985.79**	**3987.20**	**3814.56**	**3814.31**	**3814.20**	**3813.68**
52	**3510.14**	**3671.38**	**3662.72**	**3509.63**	**3509.38**	**3509.29**	**3508.78**
53	**2991.97**	**3132.16**	**3114.65**	**2979.81**	**2979.56**	**2977.28**	**2976.77**
54	**2671.50**	**2801.52**	**2786.13**	**2674.20**	**2674.03**	**2675.63**	**2675.40**
55	**3283.60**	**3443.49**	**3428.55**	**3283.57**	**3283.34**	**3283.42**	**3282.98**
56	**3781.48**	**3968.21**	**4097.19**	**3775.54**	**3775.14**	**3775.56**	**3774.67**
57	**3322.00**	**3489.23**	**3472.67**	**3321.53**	**3321.28**	**3321.14**	**3320.67**
58	**3126.19**	**3288.71**	**3282.52**	**3126.04**	**3125.80**	**3125.80**	**3125.39**
59	**3165.59**	**3330.86**	**3324.45**	**3165.69**	**3165.47**	**3165.53**	**3165.07**
60	**3596.42**	**3790.24**	**3908.82**	**3599.02**	**3598.65**	**3597.88**	**3597.12**
61	**2763.06**	**2920.09**	**2875.55**	**2762.31**	**2762.12**	**2761.93**	**2761.60**
62	**3108.00**	**3290.34**	**3271.97**	**3117.25**	**3116.93**	**3121.80**	**3121.46**
63	**3933.44**	**4167.98**	**4174.98**	**3933.57**	**3933.27**	**3933.55**	**3932.87**

Appendix B: Predicted Downhole Pressures – Time-lapse Prediction Models

Well No	Actual Pressure, psi	DAK-Sutton, psi	DAK-Standing, psi	Brill & Beggs-Sutton, psi	Brill & Beggs-Standing, psi	Mahmoud-Sutton, psi	Mahmoud-Standing, psi
1	5938.32	5934.47	5927.77	5900.53	5900.54	5904.17	5905.63
2	5775.40	5860.00	5868.34	5770.69	5770.57	5763.42	5764.13
3	7912.76	7870.87	7979.30	7968.72	7968.29	7684.60	7806.79
4	7128.65	7116.84	7122.05	7019.87	7018.13	6991.38	6980.83
5	5274.84	5287.08	5296.60	5127.30	5126.85	5160.94	5162.81
6	5156.67	5180.00	5202.62	5160.14	5159.88	5169.10	5167.50
7	5235.22	5214.10	5231.22	5033.15	5033.60	5054.67	5059.73
8	5967.19	5938.05	6035.15	5969.94	5969.70	5899.46	5970.66
9	7159.79	7104.57	7089.75	7106.86	7107.16	7042.18	7330.86
10	4295.30	4322.62	4324.51	4206.84	4206.34	4224.62	4224.53
11	5591.17	5630.20	5636.35	5466.61	5465.01	5526.17	5525.17
12	5062.15	5098.25	5116.64	4913.70	4913.82	4922.60	4924.82
13	4295.30	4326.06	4333.19	4302.67	4302.40	4288.45	4285.23
14	5264.90	5225.62	5599.89	5387.23	5388.75	5360.37	5372.39
15	5441.30	5487.07	5492.68	5326.04	5324.43	5385.81	5384.88
16	6265.10	6203.06	6369.38	6321.35	6321.02	6306.67	6311.57
17	5235.22	5287.63	5307.66	5053.17	5053.84	5096.18	5104.74
18	5207.58	5154.00	5317.48	5208.02	5207.80	5207.79	5207.87
19	4295.30	4340.09	4347.03	4306.06	4305.73	4289.54	4286.70
20	7128.65	7206.23	7188.41	7071.12	7076.71	7000.38	7003.87
21	6015.10	6001.24	6085.88	6027.65	6027.51	6019.11	6019.51
22	5115.19	5174.96	5189.96	5213.67	5214.68	5388.76	5363.36
23	3370.93	3329.24	3330.77	3335.36	3334.93	3262.75	3257.87
24	5579.22	5652.20	5697.29	5358.57	5362.60	5379.24	5403.71
25	5591.17	5664.48	5677.67	5600.94	5600.77	5593.09	5597.45
26	5273.53	5342.94	5358.03	5377.00	5377.89	5546.62	5524.07
27	3104.90	3063.45	3136.23	3041.71	3041.49	3042.81	3042.51
28	5579.22	5654.26	5700.26	5569.14	5568.19	5588.81	5581.68
29	5579.22	5657.11	5703.44	5572.13	5571.19	5591.65	5584.65
30	5441.30	5520.40	5533.31	5470.50	5470.23	5472.87	5471.73
31	5715.15	5801.25	5848.98	5504.35	5508.85	5516.65	5543.78
32	5714.57	5801.27	5849.32	5504.68	5509.18	5516.96	5544.09
33	5835.44	5802.15	5869.71	5823.88	5823.63	5831.34	5830.32
34	5715.15	5802.15	5850.39	5717.11	5716.84	5716.26	5716.80

35	**5714.57**	**5804.44**	**5852.87**	**5719.39**	**5719.13**	**5719.10**	**5718.91**
36	**3370.93**	**3316.01**	**3317.94**	**3332.82**	**3332.51**	**3263.27**	**3258.02**
37	**3049.74**	**3100.69**	**3099.09**	**3027.41**	**3028.31**	**3014.18**	**3015.09**
38	**3970.00**	**4051.79**	**4070.69**	**3901.88**	**3901.39**	**3920.01**	**3919.89**
39	**5715.15**	**5822.76**	**5875.03**	**5725.50**	**5725.97**	**5707.80**	**5713.20**
40	**3370.93**	**3307.01**	**3303.79**	**3243.00**	**3243.18**	**3202.80**	**3201.86**
41	**5714.57**	**5823.09**	**5875.37**	**5725.83**	**5726.31**	**5708.08**	**5713.50**
42	**5579.22**	**5693.21**	**5745.94**	**5481.55**	**5485.11**	**5449.69**	**5471.15**
43	**4243.20**	**4331.96**	**4429.43**	**4253.99**	**4253.43**	**4275.51**	**4275.29**
44	**5715.15**	**5840.75**	**5896.17**	**5627.65**	**5631.86**	**5584.18**	**5609.31**
45	**5714.57**	**5841.08**	**5896.51**	**5627.99**	**5632.19**	**5584.48**	**5609.62**
46	**4215.00**	**4322.20**	**4331.82**	**4166.78**	**4166.24**	**4151.42**	**4148.91**
47	**4037.30**	**4142.07**	**4209.22**	**3999.48**	**3999.29**	**4023.23**	**4024.27**
48	**3888.30**	**3992.43**	**3996.33**	**3866.15**	**3865.61**	**3840.92**	**3838.29**
49	**4016.30**	**4125.36**	**4131.58**	**4118.71**	**4118.59**	**4077.41**	**4074.11**
50	**5273.53**	**5419.90**	**5401.98**	**5322.18**	**5327.92**	**5308.53**	**5320.77**
51	**4554.85**	**4697.90**	**4724.57**	**4436.08**	**4437.41**	**4469.98**	**4478.38**
52	**4016.30**	**4143.14**	**4149.07**	**4124.36**	**4124.14**	**4081.47**	**4078.42**
53	**3370.93**	**3263.94**	**3261.83**	**3234.35**	**3234.66**	**3177.13**	**3175.96**
54	**3063.51**	**3174.35**	**3170.19**	**3071.63**	**3071.49**	**3066.72**	**3066.32**
55	**4974.00**	**5157.08**	**5178.97**	**4974.78**	**4974.48**	**4974.96**	**4974.31**
56	**4554.85**	**4725.50**	**4757.53**	**4648.37**	**4643.44**	**4735.20**	**4689.49**
57	**3152.80**	**3271.19**	**3270.38**	**3158.91**	**3159.16**	**3152.31**	**3153.05**
58	**4554.85**	**4728.52**	**4760.86**	**4651.34**	**4646.36**	**4738.87**	**4692.94**
59	**4554.85**	**4748.44**	**4783.84**	**4659.26**	**4654.44**	**4721.72**	**4685.68**
60	**3844.71**	**4012.56**	**3967.59**	**3853.69**	**3853.73**	**3834.90**	**3834.33**
61	**5591.17**	**5842.83**	**5858.31**	**5670.95**	**5670.76**	**5737.52**	**5743.47**
62	**5441.30**	**5699.60**	**5714.98**	**5540.88**	**5537.62**	**5609.50**	**5616.01**
63	**3638.09**	**3818.08**	**3848.94**	**3688.54**	**3688.20**	**3667.86**	**3666.05**
64	**4079.03**	**4284.92**	**4295.16**	**4233.16**	**4232.00**	**4227.49**	**4217.49**
65	**5307.45**	**5038.15**	**5426.09**	**5307.88**	**5307.65**	**5305.71**	**5307.68**
66	**4191.91**	**4411.94**	**4421.76**	**4212.96**	**4212.93**	**4236.51**	**4238.53**
67	**3888.30**	**4116.36**	**4128.83**	**4048.15**	**4045.26**	**4048.03**	**4013.84**
68	**4191.91**	**4442.44**	**4457.60**	**4358.67**	**4356.92**	**4363.83**	**4346.92**
69	**4172.80**	**4457.56**	**4469.41**	**4316.17**	**4314.05**	**4307.82**	**4296.44**
70	**4571.98**	**4878.89**	**4880.79**	**4709.37**	**4707.99**	**4711.67**	**4704.47**
71	**3836.71**	**4110.86**	**4132.09**	**4051.42**	**4043.36**	**4127.18**	**4054.84**
72	**3836.71**	**4114.02**	**4135.48**	**4054.33**	**4046.18**	**4131.44**	**4058.39**
73	**3836.71**	**4124.23**	**4143.40**	**3951.84**	**3948.79**	**3924.06**	**3910.00**
74	**3836.71**	**4136.31**	**4160.30**	**4062.86**	**4054.49**	**4108.55**	**4048.71**
75	**4295.30**	**4641.54**	**4622.71**	**4417.87**	**4431.11**	**4455.93**	**4484.45**

Appendix C: Downhole Pressure Difference – Calibration Models

Well No	Actual Pressure, psi	DAK-Sutton, psi	DAK-Standing, psi	Brill & Beggs-Sutton, psi	Brill & Beggs-Standing, psi	Mahmoud-Sutton, psi	Mahmoud-Standing, psi
1	5938.32	-30.55	39.66	-1.15	-1.32	-0.69	-0.79
2	5265.30	-0.81	51.08	-0.95	-1.08	-0.99	-1.19
3	6948.10	-1.10	21.29	0.38	0.23	-28.07	1.14
4	6838.79	2.86	20.59	8.86	8.28	-55.77	6.52
5	7051.80	4.08	19.48	12.99	12.45	-43.45	-2.73
6	6950.32	5.33	23.53	4.38	3.88	7.78	7.26
7	5866.50	5.42	58.18	-0.92	-1.10	-9.92	-0.74
8	7209.88	-8.59	10.26	0.22	0.05	-78.74	1.63
9	5277.70	6.98	168.41	0.37	0.07	0.64	-0.24
10	6866.38	-14.72	17.70	0.12	0.00	-59.75	0.85
11	7912.76	-30.09	-12.45	0.59	0.46	-333.78	0.34
12	3104.90	14.05	13.05	-79.75	-79.95	-79.83	-80.14
13	5999.99	-30.07	51.04	0.18	0.02	0.37	0.25
14	4972.00	-26.91	85.05	-0.78	-0.95	-1.04	-1.48
15	5112.80	-30.20	-85.14	-266.59	-157.64	-208.59	-30.04
16	6274.39	-39.49	40.09	1.13	0.99	1.49	1.43
17	3740.92	28.41	149.20	0.02	-0.21	-0.10	-0.62
18	4590.77	35.39	220.22	-49.06	-49.36	-48.04	-48.70
19	4673.30	44.21	106.34	0.29	0.14	0.36	-0.07
20	3299.00	38.50	158.06	-0.66	-0.91	-0.90	-1.38
21	5293.30	65.56	72.51	-22.44	-22.75	-21.79	-22.87
22	3501.47	-44.15	149.67	0.06	-0.18	-0.16	-0.65
23	5853.40	83.20	58.31	4.47	4.32	4.69	4.59
24	5147.00	82.88	86.69	0.48	0.30	0.83	0.47
25	5132.60	89.03	99.97	-32.55	-32.78	-32.23	-32.71
26	4802.99	84.23	99.85	0.37	0.21	0.50	0.14
27	3184.06	63.87	59.32	-58.45	-58.66	-58.71	-59.07
28	3645.20	78.42	159.28	0.15	-0.09	0.01	-0.49
29	3143.72	71.60	92.44	-0.36	-0.57	-0.57	-0.91
30	3720.32	59.84	74.05	0.93	0.67	1.10	0.47
31	3844.71	90.52	137.36	0.35	0.10	0.37	-0.10
32	4300.00	102.41	165.84	9.80	9.56	9.88	9.32
33	4829.40	118.55	123.31	-7.15	-7.44	-10.62	-11.45
34	5965.00	-146.54	64.22	-6.91	-7.13	-80.12	-6.49

35	**3706.58**	**92.95**	**109.87**	**-39.45**	**-39.76**	**-41.48**	**-42.09**
36	**3454.00**	**-90.98**	**155.84**	**0.45**	**0.22**	**0.65**	**0.17**
37	**2989.00**	**155.76**	**137.11**	**-41.14**	**-41.46**	**-43.95**	**-44.65**
38	**4446.61**	**130.63**	**265.91**	**-6.81**	**-7.11**	**-5.62**	**-6.27**
39	**4220.26**	**135.43**	**145.06**	**-3.57**	**-3.79**	**-3.96**	**-4.44**
40	**3152.80**	**108.71**	**104.81**	**-1.22**	**-1.44**	**-1.68**	**-2.03**
41	**3841.20**	**135.32**	**127.34**	**-4.99**	**-5.22**	**-6.52**	**-7.04**
42	**2641.00**	**97.74**	**105.74**	**-14.44**	**-14.66**	**-14.77**	**-15.11**
43	**3479.51**	**129.28**	**123.22**	**-0.01**	**-0.23**	**-0.09**	**-0.48**
44	**4097.00**	**39.48**	**123.80**	**-0.41**	**-0.61**	**-0.84**	**-1.34**
45	**4307.60**	**171.35**	**167.91**	**0.54**	**0.28**	**0.62**	**0.00**
46	**3944.30**	**157.11**	**147.67**	**-10.24**	**-10.54**	**-13.90**	**-14.72**
47	**3918.90**	**162.35**	**152.88**	**-0.02**	**-0.25**	**0.59**	**0.09**
48	**2948.50**	**123.25**	**107.87**	**-24.57**	**-24.81**	**-24.87**	**-25.27**
49	**3160.80**	**-135.52**	**146.12**	**-31.44**	**-31.70**	**-32.00**	**-32.51**
50	**3192.90**	**137.49**	**120.55**	**-19.59**	**-19.82**	**-20.33**	**-20.77**
51	**3815.07**	**170.72**	**172.13**	**-0.51**	**-0.76**	**-0.87**	**-1.39**
52	**3510.14**	**161.24**	**152.58**	**-0.51**	**-0.76**	**-0.85**	**-1.36**
53	**2991.97**	**140.19**	**122.68**	**-12.16**	**-12.41**	**-14.69**	**-15.20**
54	**2671.50**	**130.02**	**114.63**	**2.70**	**2.53**	**4.13**	**3.90**
55	**3283.60**	**159.89**	**144.95**	**-0.03**	**-0.26**	**-0.18**	**-0.62**
56	**3781.48**	**186.73**	**315.71**	**-5.94**	**-6.34**	**-5.92**	**-6.81**
57	**3322.00**	**167.23**	**150.67**	**-0.47**	**-0.72**	**-0.86**	**-1.33**
58	**3126.19**	**162.52**	**156.33**	**-0.15**	**-0.39**	**-0.39**	**-0.80**
59	**3165.59**	**165.27**	**158.86**	**0.10**	**-0.12**	**-0.06**	**-0.52**
60	**3596.42**	**193.82**	**312.40**	**2.60**	**2.23**	**1.46**	**0.70**
61	**2763.06**	**157.03**	**112.49**	**-0.75**	**-0.94**	**-1.13**	**-1.46**
62	**3108.00**	**182.34**	**163.97**	**9.25**	**8.93**	**13.80**	**13.46**
63	**3933.44**	**234.54**	**241.54**	**0.13**	**-0.17**	**0.11**	**-0.57**

Appendix D: Downhole Pressure Difference – Time-lapse Prediction Models

Well No	Actual Pressure, psi	DAK-Sutton, psi	DAK-Standing, psi	Brill & Beggs-Sutton, psi	Brill & Beggs-Standing, psi	Mahmoud-Sutton, psi	Mahmoud-Standing, psi
1	5938.32	-3.85	-10.55	-37.79	-37.78	-34.15	-32.69
2	5775.40	84.60	92.94	-4.71	-4.83	-11.98	-11.27
3	7912.76	-41.89	66.54	55.96	55.53	-228.16	-105.97
4	7128.65	-11.81	-6.60	-108.78	-110.53	-137.27	-147.82
5	5274.84	12.24	21.76	-147.54	-147.99	-113.90	-112.03
6	5156.67	23.33	45.95	3.47	3.21	12.43	10.83
7	5235.22	-21.12	-4.00	-202.07	-201.62	-180.56	-175.49
8	5967.19	-29.14	67.96	2.75	2.51	-67.73	3.47
9	7159.79	-55.22	-70.04	-52.93	-52.63	-117.61	171.07
10	4295.30	27.32	29.21	-88.46	-88.96	-70.68	-70.77
11	5591.17	39.03	45.18	-124.56	-126.16	-65.00	-66.00
12	5062.15	36.10	54.50	-148.45	-148.32	-139.54	-137.32
13	4295.30	30.76	37.89	7.37	7.10	-6.85	-10.07
14	5264.90	-39.28	334.99	122.33	123.85	95.47	107.49
15	5441.30	45.77	51.38	-115.26	-116.87	-55.49	-56.42
16	6265.10	-62.04	104.28	56.25	55.92	41.57	46.47
17	5235.22	52.41	72.44	-182.05	-181.39	-139.04	-130.48
18	5207.58	-53.58	109.90	0.44	0.22	0.21	0.29
19	4295.30	44.79	51.73	10.76	10.43	-5.76	-8.60
20	7128.65	77.58	59.75	-57.53	-51.94	-128.27	-124.78
21	6015.10	-13.86	70.78	12.55	12.41	4.01	4.41
22	5115.19	59.77	74.77	98.48	99.49	273.57	248.17
23	3370.93	-41.69	-40.16	-35.57	-36.00	-108.18	-113.06
24	5579.22	72.97	118.07	-220.66	-216.63	-199.98	-175.51
25	5591.17	73.31	86.50	9.77	9.60	1.92	6.28
26	5273.53	69.41	84.50	103.47	104.36	273.09	250.54
27	3104.90	-41.45	31.33	-63.19	-63.41	-62.09	-62.39
28	5579.22	75.04	121.04	-10.09	-11.03	9.58	2.45
29	5579.22	77.89	124.21	-7.09	-8.04	12.43	5.42
30	5441.30	79.10	92.01	29.20	28.93	31.57	30.43
31	5715.15	86.10	133.83	-210.80	-206.30	-198.50	-171.37
32	5714.57	86.70	134.75	-209.89	-205.39	-197.61	-170.48
33	5835.44	-33.29	34.27	-11.56	-11.81	-4.10	-5.12
34	5715.15	87.00	135.24	1.96	1.69	1.11	1.65

35	**5714.57**	**89.87**	**138.30**	**4.82**	**4.56**	**4.53**	**4.34**
36	**3370.93**	**-54.92**	**-52.99**	**-38.11**	**-38.42**	**-107.66**	**-112.91**
37	**3049.74**	**50.95**	**49.35**	**-22.33**	**-21.43**	**-35.56**	**-34.65**
38	**3970.00**	**81.79**	**100.69**	**-68.12**	**-68.61**	**-49.99**	**-50.11**
39	**5715.15**	**107.61**	**159.88**	**10.35**	**10.82**	**-7.35**	**-1.95**
40	**3370.93**	**-63.92**	**-67.14**	**-127.93**	**-127.75**	**-168.13**	**-169.07**
41	**5714.57**	**108.52**	**160.80**	**11.26**	**11.74**	**-6.49**	**-1.07**
42	**5579.22**	**113.99**	**166.72**	**-97.67**	**-94.12**	**-129.53**	**-108.07**
43	**4243.20**	**88.76**	**186.23**	**10.79**	**10.23**	**32.31**	**32.09**
44	**5715.15**	**125.60**	**181.02**	**-87.50**	**-83.29**	**-130.97**	**-105.84**
45	**5714.57**	**126.51**	**181.94**	**-86.58**	**-82.38**	**-130.09**	**-104.95**
46	**4215.00**	**107.20**	**116.82**	**-48.22**	**-48.76**	**-63.58**	**-66.09**
47	**4037.30**	**104.77**	**171.92**	**-37.82**	**-38.01**	**-14.07**	**-13.03**
48	**3888.30**	**104.13**	**108.03**	**-22.15**	**-22.69**	**-47.38**	**-50.01**
49	**4016.30**	**109.06**	**115.28**	**102.41**	**102.29**	**61.11**	**57.81**
50	**5273.53**	**146.37**	**128.45**	**48.65**	**54.39**	**35.00**	**47.24**
51	**4554.85**	**143.05**	**169.72**	**-118.77**	**-117.44**	**-84.87**	**-76.47**
52	**4016.30**	**126.84**	**132.77**	**108.06**	**107.84**	**65.17**	**62.12**
53	**3370.93**	**-106.99**	**-109.10**	**-136.58**	**-136.27**	**-193.80**	**-194.97**
54	**3063.51**	**110.84**	**106.68**	**8.12**	**7.98**	**3.21**	**2.81**
55	**4974.00**	**183.08**	**204.97**	**0.78**	**0.48**	**0.96**	**0.31**
56	**4554.85**	**170.65**	**202.68**	**93.52**	**88.59**	**180.35**	**134.64**
57	**3152.80**	**118.39**	**117.58**	**6.11**	**6.36**	**-0.49**	**0.25**
58	**4554.85**	**173.67**	**206.01**	**96.49**	**91.51**	**184.02**	**138.09**
59	**4554.85**	**193.59**	**228.99**	**104.41**	**99.59**	**166.87**	**130.83**
60	**3844.71**	**167.85**	**122.88**	**8.98**	**9.02**	**-9.81**	**-10.38**
61	**5591.17**	**251.66**	**267.14**	**79.78**	**79.59**	**146.35**	**152.30**
62	**5441.30**	**258.30**	**273.68**	**99.58**	**96.32**	**168.20**	**174.71**
63	**3638.09**	**179.99**	**210.85**	**50.45**	**50.11**	**29.77**	**27.96**
64	**4079.03**	**205.89**	**216.13**	**154.13**	**152.97**	**148.46**	**138.46**
65	**5307.45**	**-269.30**	**118.64**	**0.43**	**0.20**	**-1.74**	**0.23**
66	**4191.91**	**220.03**	**229.86**	**21.05**	**21.03**	**44.61**	**46.62**
67	**3888.30**	**228.06**	**240.53**	**159.85**	**156.96**	**159.73**	**125.54**
68	**4191.91**	**250.53**	**265.70**	**166.77**	**165.02**	**171.92**	**155.02**
69	**4172.80**	**284.76**	**296.61**	**143.37**	**141.25**	**135.02**	**123.64**
70	**4571.98**	**306.91**	**308.81**	**137.39**	**136.01**	**139.69**	**132.49**
71	**3836.71**	**274.15**	**295.38**	**214.71**	**206.65**	**290.47**	**218.13**
72	**3836.71**	**277.31**	**298.77**	**217.62**	**209.47**	**294.73**	**221.68**
73	**3836.71**	**287.52**	**306.69**	**115.13**	**112.08**	**87.35**	**73.29**
74	**3836.71**	**299.60**	**323.59**	**226.15**	**217.78**	**271.84**	**212.00**
75	**4295.30**	**346.24**	**327.41**	**122.57**	**135.81**	**160.63**	**189.15**

Appendix E: Downhole Pressure Difference Absolute Relative Error – Calibration Models

Well No	Actual Pressure, psi	DAK-Sutton, %	DAK-Standing, %	Brill & Beggs-Sutton, %	Brill & Beggs-Standing, %	Mahmoud-Sutton, %	Mahmoud-Standing, %
1	5938.32	-0.51	0.67	-0.02	-0.02	-0.01	-0.01
2	5265.30	-0.02	0.97	-0.02	-0.02	-0.02	-0.02
3	6948.10	-0.02	0.31	0.01	0.00	-0.40	0.02
4	6838.79	0.04	0.30	0.13	0.12	-0.82	0.10
5	7051.80	0.06	0.28	0.18	0.18	-0.62	-0.04
6	6950.32	0.08	0.34	0.06	0.06	0.11	0.10
7	5866.50	0.09	0.99	-0.02	-0.02	-0.17	-0.01
8	7209.88	-0.12	0.14	0.00	0.00	-1.09	0.02
9	5277.70	0.13	3.19	0.01	0.00	0.01	0.00
10	6866.38	-0.21	0.26	0.00	0.00	-0.87	0.01
11	7912.76	-0.38	-0.16	0.01	0.01	-4.22	0.00
12	3104.90	0.45	0.42	-2.57	-2.57	-2.57	-2.58
13	5999.99	-0.50	0.85	0.00	0.00	0.01	0.00
14	4972.00	-0.54	1.71	-0.02	-0.02	-0.02	-0.03
15	5112.80	-0.59	-1.67	-5.21	-3.08	-4.08	-0.59
16	6274.39	-0.63	0.64	0.02	0.02	0.02	0.02
17	3740.92	0.76	3.99	0.00	-0.01	0.00	-0.02
18	4590.77	0.77	4.80	-1.07	-1.08	-1.05	-1.06
19	4673.30	0.95	2.28	0.01	0.00	0.01	0.00
20	3299.00	1.17	4.79	-0.02	-0.03	-0.03	-0.04
21	5293.30	1.24	1.37	-0.42	-0.43	-0.41	-0.43
22	3501.47	-1.26	4.27	0.00	-0.01	0.00	-0.02
23	5853.40	1.42	1.00	0.08	0.07	0.08	0.08
24	5147.00	1.61	1.68	0.01	0.01	0.02	0.01
25	5132.60	1.73	1.95	-0.63	-0.64	-0.63	-0.64
26	4802.99	1.75	2.08	0.01	0.00	0.01	0.00
27	3184.06	2.01	1.86	-1.84	-1.84	-1.84	-1.86
28	3645.20	2.15	4.37	0.00	0.00	0.00	-0.01
29	3143.72	2.28	2.94	-0.01	-0.02	-0.02	-0.03
30	3720.32	1.61	1.99	0.02	0.02	0.03	0.01
31	3844.71	2.35	3.57	0.01	0.00	0.01	0.00
32	4300.00	2.38	3.86	0.23	0.22	0.23	0.22
33	4829.40	2.45	2.55	-0.15	-0.15	-0.22	-0.24
34	5965.00	-2.46	1.08	-0.12	-0.12	-1.34	-0.11

35	**3706.58**	**2.51**	**2.96**	**-1.06**	**-1.07**	**-1.12**	**-1.14**
36	**3454.00**	**-2.63**	**4.51**	**0.01**	**0.01**	**0.02**	**0.01**
37	**2989.00**	**5.21**	**4.59**	**-1.38**	**-1.39**	**-1.47**	**-1.49**
38	**4446.61**	**2.94**	**5.98**	**-0.15**	**-0.16**	**-0.13**	**-0.14**
39	**4220.26**	**3.21**	**3.44**	**-0.08**	**-0.09**	**-0.09**	**-0.11**
40	**3152.80**	**3.45**	**3.32**	**-0.04**	**-0.05**	**-0.05**	**-0.06**
41	**3841.20**	**3.52**	**3.32**	**-0.13**	**-0.14**	**-0.17**	**-0.18**
42	**2641.00**	**3.70**	**4.00**	**-0.55**	**-0.56**	**-0.56**	**-0.57**
43	**3479.51**	**3.72**	**3.54**	**0.00**	**-0.01**	**0.00**	**-0.01**
44	**4097.00**	**0.96**	**3.02**	**-0.01**	**-0.01**	**-0.02**	**-0.03**
45	**4307.60**	**3.98**	**3.90**	**0.01**	**0.01**	**0.01**	**0.00**
46	**3944.30**	**3.98**	**3.74**	**-0.26**	**-0.27**	**-0.35**	**-0.37**
47	**3918.90**	**4.14**	**3.90**	**0.00**	**-0.01**	**0.02**	**0.00**
48	**2948.50**	**4.18**	**3.66**	**-0.83**	**-0.84**	**-0.84**	**-0.86**
49	**3160.80**	**-4.29**	**4.62**	**-0.99**	**-1.00**	**-1.01**	**-1.03**
50	**3192.90**	**4.31**	**3.78**	**-0.61**	**-0.62**	**-0.64**	**-0.65**
51	**3815.07**	**4.47**	**4.51**	**-0.01**	**-0.02**	**-0.02**	**-0.04**
52	**3510.14**	**4.59**	**4.35**	**-0.01**	**-0.02**	**-0.02**	**-0.04**
53	**2991.97**	**4.69**	**4.10**	**-0.41**	**-0.41**	**-0.49**	**-0.51**
54	**2671.50**	**4.87**	**4.29**	**0.10**	**0.09**	**0.15**	**0.15**
55	**3283.60**	**4.87**	**4.41**	**0.00**	**-0.01**	**-0.01**	**-0.02**
56	**3781.48**	**4.94**	**8.35**	**-0.16**	**-0.17**	**-0.16**	**-0.18**
57	**3322.00**	**5.03**	**4.54**	**-0.01**	**-0.02**	**-0.03**	**-0.04**
58	**3126.19**	**5.20**	**5.00**	**0.00**	**-0.01**	**-0.01**	**-0.03**
59	**3165.59**	**5.22**	**5.02**	**0.00**	**0.00**	**0.00**	**-0.02**
60	**3596.42**	**5.39**	**8.69**	**0.07**	**0.06**	**0.04**	**0.02**
61	**2763.06**	**5.68**	**4.07**	**-0.03**	**-0.03**	**-0.04**	**-0.05**
62	**3108.00**	**5.87**	**5.28**	**0.30**	**0.29**	**0.44**	**0.43**
63	**3933.44**	**5.96**	**6.14**	**0.00**	**0.00**	**0.00**	**-0.01**

Appendix F: Downhole Pressure Difference Absolute Relative Error – Time-lapse Prediction Models

Well No	Actual Pressure, psi	DAK-Sutton, %	DAK-Standing, %	Brill & Beggs-Sutton, %	Brill & Beggs-Standing, %	Mahmoud-Sutton, %	Mahmoud-Standing, %
1	5938.32	-0.06	-0.18	-0.64	-0.64	-0.58	-0.55
2	5775.40	1.46	1.61	-0.08	-0.08	-0.21	-0.20
3	7912.76	-0.53	0.84	0.71	0.70	-2.88	-1.34
4	7128.65	-0.17	-0.09	-1.53	-1.55	-1.93	-2.07
5	5274.84	0.23	0.41	-2.80	-2.81	-2.16	-2.12
6	5156.67	0.45	0.89	0.07	0.06	0.24	0.21
7	5235.22	-0.40	-0.08	-3.86	-3.85	-3.45	-3.35
8	5967.19	-0.49	1.14	0.05	0.04	-1.14	0.06
9	7159.79	-0.77	-0.98	-0.74	-0.74	-1.64	2.39
10	4295.30	0.64	0.68	-2.06	-2.07	-1.65	-1.65
11	5591.17	0.70	0.81	-2.23	-2.26	-1.16	-1.18
12	5062.15	0.71	1.08	-2.93	-2.93	-2.76	-2.71
13	4295.30	0.72	0.88	0.17	0.17	-0.16	-0.23
14	5264.90	-0.75	6.36	2.32	2.35	1.81	2.04
15	5441.30	0.84	0.94	-2.12	-2.15	-1.02	-1.04
16	6265.10	-0.99	1.66	0.90	0.89	0.66	0.74
17	5235.22	1.00	1.38	-3.48	-3.46	-2.66	-2.49
18	5207.58	-1.03	2.11	0.01	0.00	0.00	0.01
19	4295.30	1.04	1.20	0.25	0.24	-0.13	-0.20
20	7128.65	1.09	0.84	-0.81	-0.73	-1.80	-1.75
21	6015.10	-0.23	1.18	0.21	0.21	0.07	0.07
22	5115.19	1.17	1.46	1.93	1.95	5.35	4.85
23	3370.93	-1.24	-1.19	-1.06	-1.07	-3.21	-3.35
24	5579.22	1.31	2.12	-3.95	-3.88	-3.58	-3.15
25	5591.17	1.31	1.55	0.17	0.17	0.03	0.11
26	5273.53	1.32	1.60	1.96	1.98	5.18	4.75
27	3104.90	-1.34	1.01	-2.04	-2.04	-2.00	-2.01
28	5579.22	1.34	2.17	-0.18	-0.20	0.17	0.04
29	5579.22	1.40	2.23	-0.13	-0.14	0.22	0.10
30	5441.30	1.45	1.69	0.54	0.53	0.58	0.56
31	5715.15	1.51	2.34	-3.69	-3.61	-3.47	-3.00
32	5714.57	1.52	2.36	-3.67	-3.59	-3.46	-2.98
33	5835.44	-0.57	0.59	-0.20	-0.20	-0.07	-0.09
34	5715.15	1.52	2.37	0.03	0.03	0.02	0.03

35	**5714.57**	**1.57**	**2.42**	**0.08**	**0.08**	**0.08**	**0.08**
36	**3370.93**	**-1.63**	**-1.57**	**-1.13**	**-1.14**	**-3.19**	**-3.35**
37	**3049.74**	**1.67**	**1.62**	**-0.73**	**-0.70**	**-1.17**	**-1.14**
38	**3970.00**	**2.06**	**2.54**	**-1.72**	**-1.73**	**-1.26**	**-1.26**
39	**5715.15**	**1.88**	**2.80**	**0.18**	**0.19**	**-0.13**	**-0.03**
40	**3370.93**	**-1.90**	**-1.99**	**-3.80**	**-3.79**	**-4.99**	**-5.02**
41	**5714.57**	**1.90**	**2.81**	**0.20**	**0.21**	**-0.11**	**-0.02**
42	**5579.22**	**2.04**	**2.99**	**-1.75**	**-1.69**	**-2.32**	**-1.94**
43	**4243.20**	**2.09**	**4.39**	**0.25**	**0.24**	**0.76**	**0.76**
44	**5715.15**	**2.20**	**3.17**	**-1.53**	**-1.46**	**-2.29**	**-1.85**
45	**5714.57**	**2.21**	**3.18**	**-1.52**	**-1.44**	**-2.28**	**-1.84**
46	**4215.00**	**2.54**	**2.77**	**-1.14**	**-1.16**	**-1.51**	**-1.57**
47	**4037.30**	**2.60**	**4.26**	**-0.94**	**-0.94**	**-0.35**	**-0.32**
48	**3888.30**	**2.68**	**2.78**	**-0.57**	**-0.58**	**-1.22**	**-1.29**
49	**4016.30**	**2.72**	**2.87**	**2.55**	**2.55**	**1.52**	**1.44**
50	**5273.53**	**2.78**	**2.44**	**0.92**	**1.03**	**0.66**	**0.90**
51	**4554.85**	**3.14**	**3.73**	**-2.61**	**-2.58**	**-1.86**	**-1.68**
52	**4016.30**	**3.16**	**3.31**	**2.69**	**2.69**	**1.62**	**1.55**
53	**3370.93**	**-3.17**	**-3.24**	**-4.05**	**-4.04**	**-5.75**	**-5.78**
54	**3063.51**	**3.62**	**3.48**	**0.27**	**0.26**	**0.10**	**0.09**
55	**4974.00**	**3.68**	**4.12**	**0.02**	**0.01**	**0.02**	**0.01**
56	**4554.85**	**3.75**	**4.45**	**2.05**	**1.94**	**3.96**	**2.96**
57	**3152.80**	**3.75**	**3.73**	**0.19**	**0.20**	**-0.02**	**0.01**
58	**4554.85**	**3.81**	**4.52**	**2.12**	**2.01**	**4.04**	**3.03**
59	**4554.85**	**4.25**	**5.03**	**2.29**	**2.19**	**3.66**	**2.87**
60	**3844.71**	**4.37**	**3.20**	**0.23**	**0.23**	**-0.26**	**-0.27**
61	**5591.17**	**4.50**	**4.78**	**1.43**	**1.42**	**2.62**	**2.72**
62	**5441.30**	**4.75**	**5.03**	**1.83**	**1.77**	**3.09**	**3.21**
63	**3638.09**	**4.95**	**5.80**	**1.39**	**1.38**	**0.82**	**0.77**
64	**4079.03**	**5.05**	**5.30**	**3.78**	**3.75**	**3.64**	**3.39**
65	**5307.45**	**-5.07**	**2.24**	**0.01**	**0.00**	**-0.03**	**0.00**
66	**4191.91**	**5.25**	**5.48**	**0.50**	**0.50**	**1.06**	**1.11**
67	**3888.30**	**5.87**	**6.19**	**4.11**	**4.04**	**4.11**	**3.23**
68	**4191.91**	**5.98**	**6.34**	**3.98**	**3.94**	**4.10**	**3.70**
69	**4172.80**	**6.82**	**7.11**	**3.44**	**3.39**	**3.24**	**2.96**
70	**4571.98**	**6.71**	**6.75**	**3.00**	**2.97**	**3.06**	**2.90**
71	**3836.71**	**7.15**	**7.70**	**5.60**	**5.39**	**7.57**	**5.69**
72	**3836.71**	**7.23**	**7.79**	**5.67**	**5.46**	**7.68**	**5.78**
73	**3836.71**	**7.49**	**7.99**	**3.00**	**2.92**	**2.28**	**1.91**
74	**3836.71**	**7.81**	**8.43**	**5.89**	**5.68**	**7.09**	**5.53**
75	**4295.30**	**8.06**	**7.62**	**2.85**	**3.16**	**3.74**	**4.40**

Appendix G: Changes in Molecular Weight & Specific Gravity with Depth

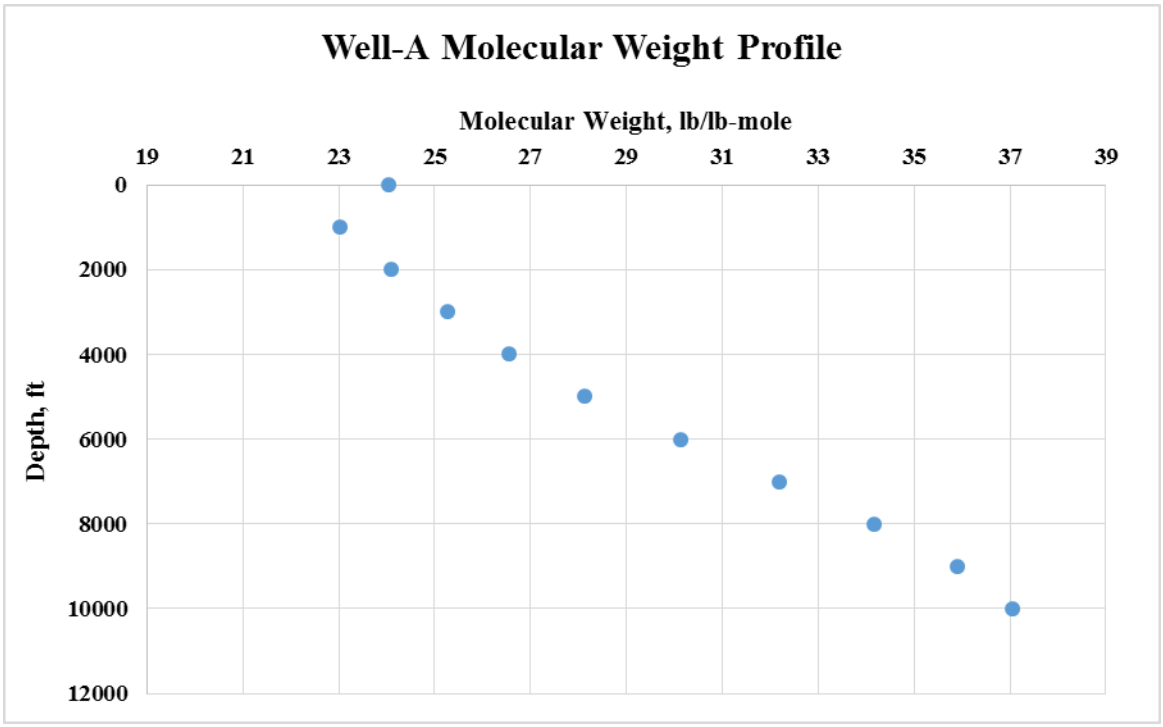

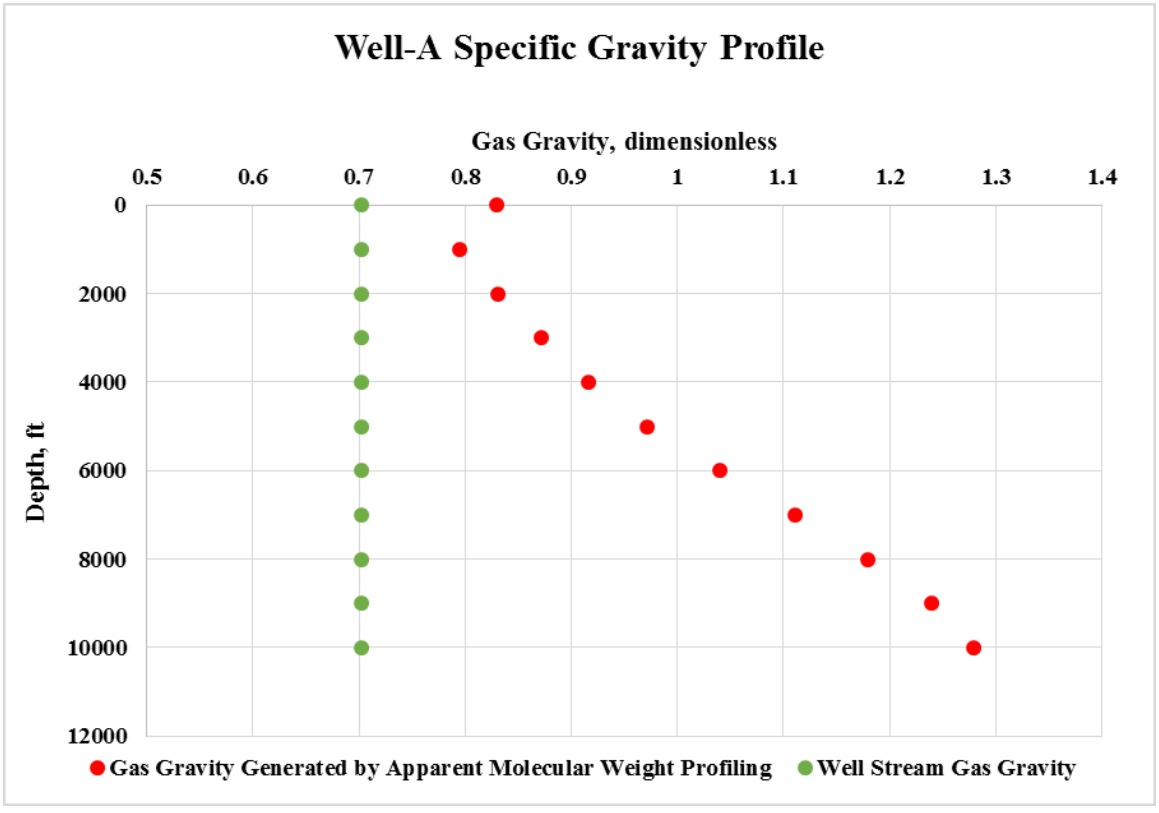

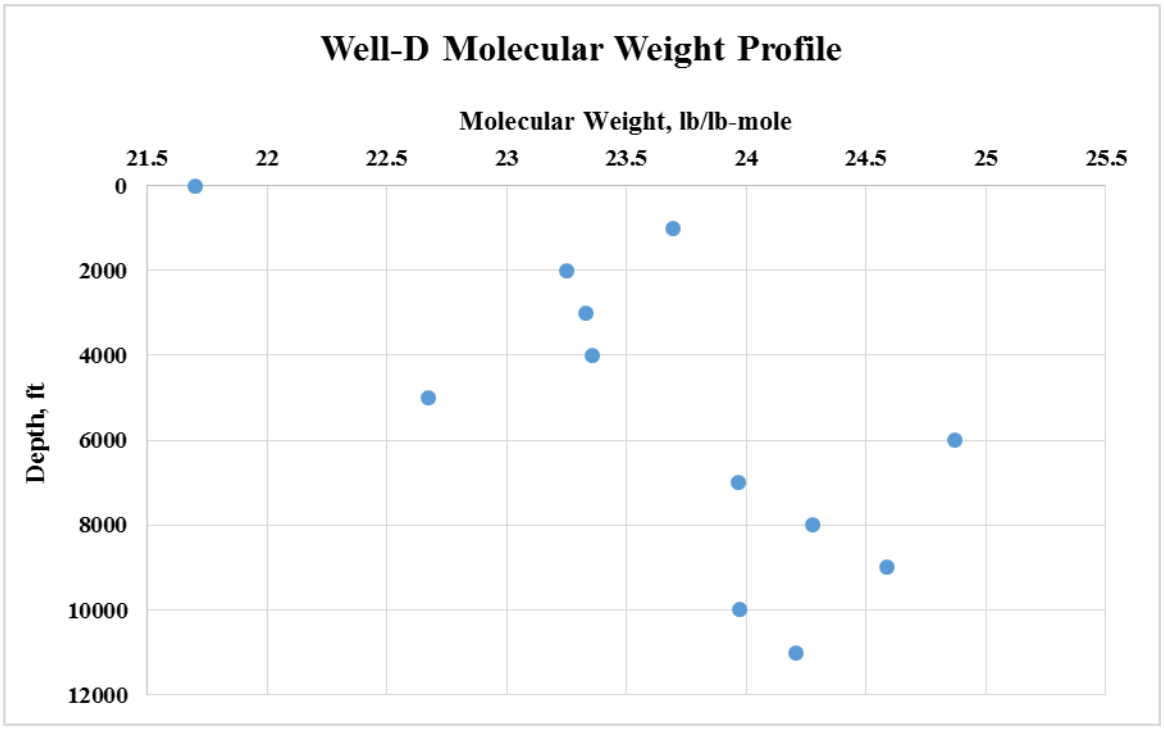
Well-D Molecular Weight Profile
Molecular Weight, lb/lb-mole
21.5
22
22.5
23
23.5
24
24.5
25
25.5
Depth, ft
0
2000
4000
6000
8000
10000
12000

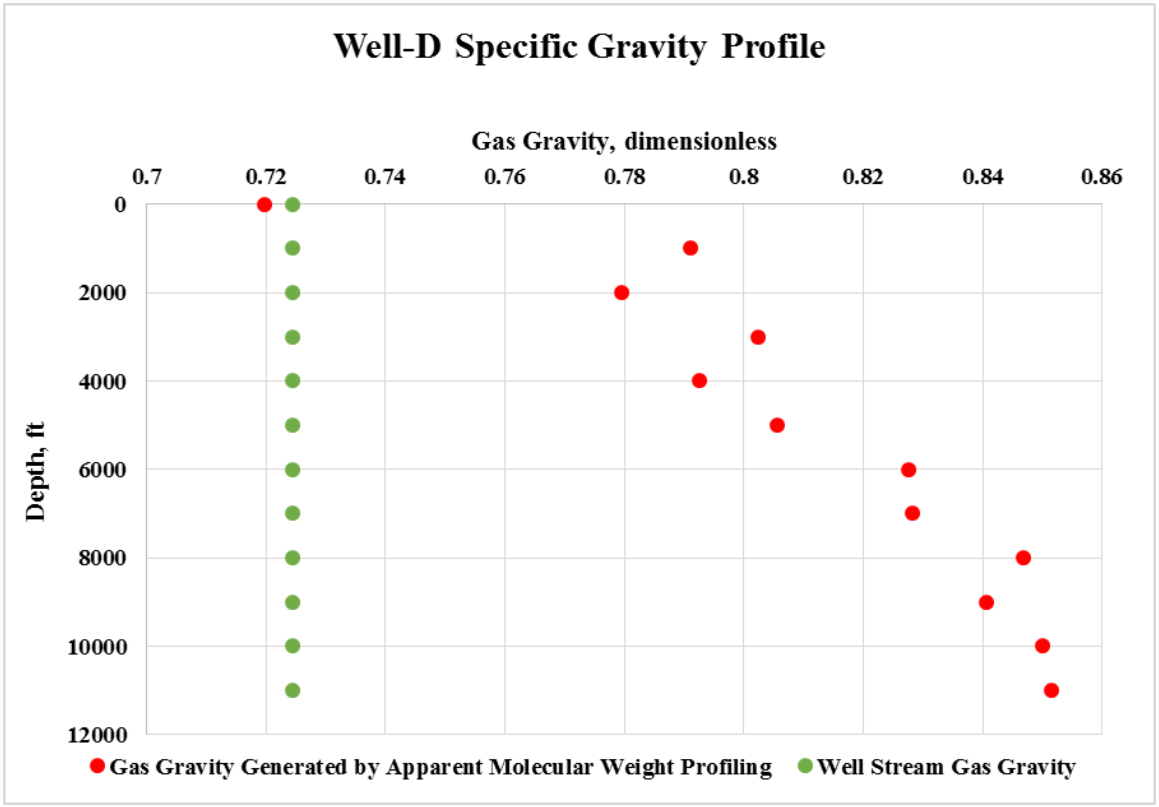
Well-D Specific Gravity Profile
Gas Gravity, dimensionless
0.7
0.72
0.74
0.76
0.78
0.8
0.82
0.84
0.86
Depth, ft
0
2000
4000
6000
8000
10000
12000
Gas Gravity Generated by Apparent Molecular Weight Profiling
Well Stream Gas Gravity

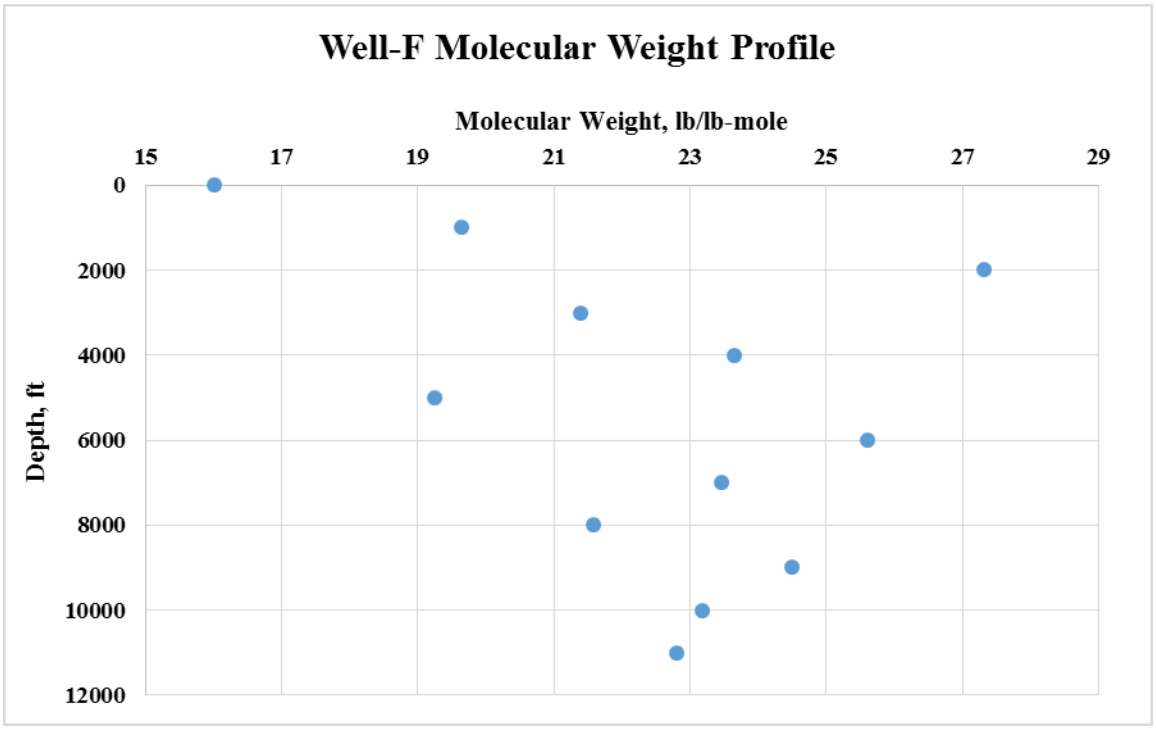
Well-F Molecular Weight Profile
Molecular Weight, lb/lb-mole
15
17
19
21
23
25
27
29
Depth, ft
0
2000
4000
6000
8000
10000
12000

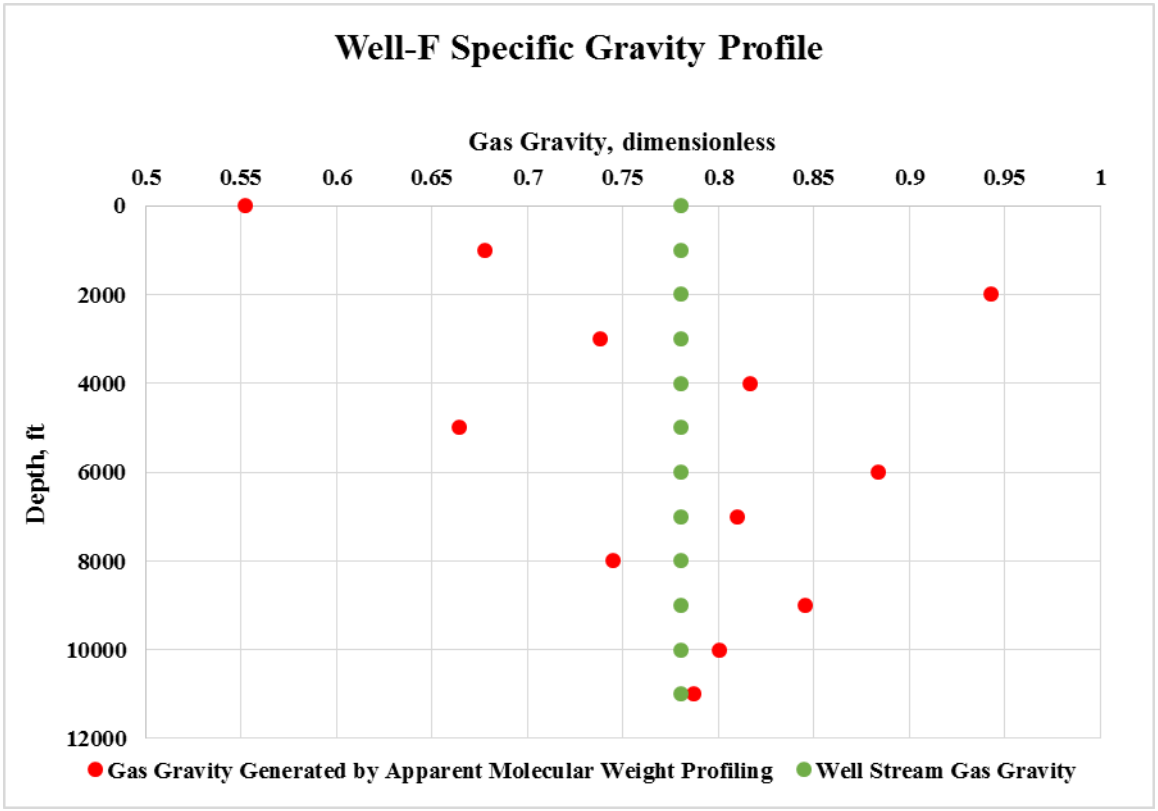
Well-F Specific Gravity Profile
Gas Gravity, dimensionless
0.5
0.55
0.6
0.65
0.7
0.75
0.8
0.85
0.9
0.95
1
Depth, ft
0
2000
4000
6000
8000
10000
12000
Gas Gravity Generated by Apparent Molecular Weight Profiling
Well Stream Gas Gravity

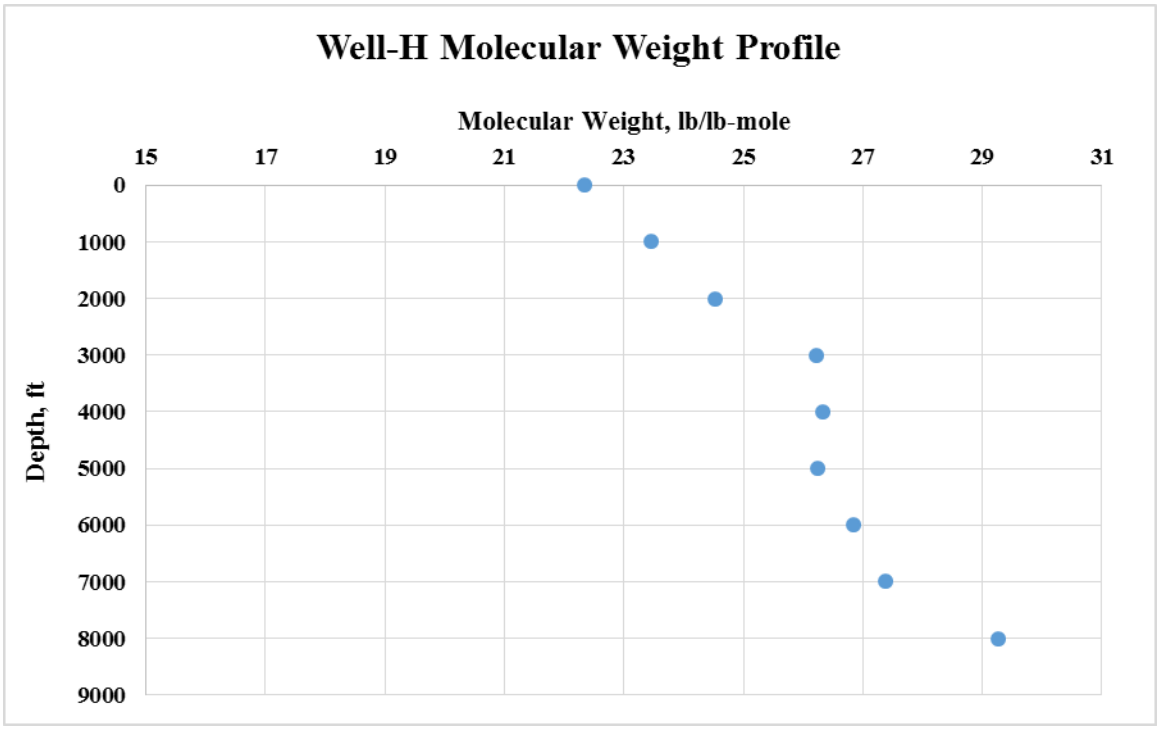
Well-H Molecular Weight Profile
Molecular Weight, lb/lb-mole
15
17
19
21
23
25
27
29
31
Depth, ft
0
1000
2000
3000
4000
5000
6000
7000
8000
9000

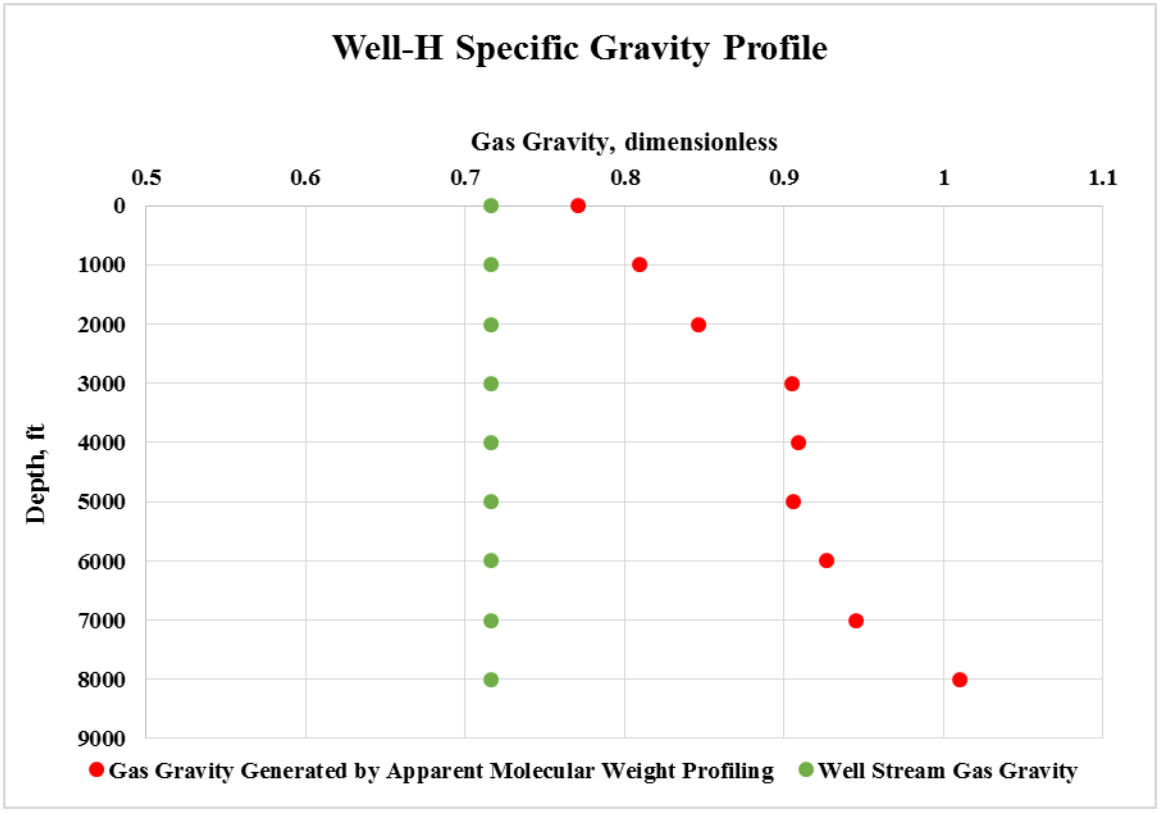
Well-H Specific Gravity Profile
Gas Gravity, dimensionless
0.5
0.6
0.7
0.8
0.9
1
1.1
Depth, ft
0
1000
2000
3000
4000
5000
6000
7000
8000
9000
Gas Gravity Generated by Apparent Molecular Weight Profiling
Well Stream Gas Gravity

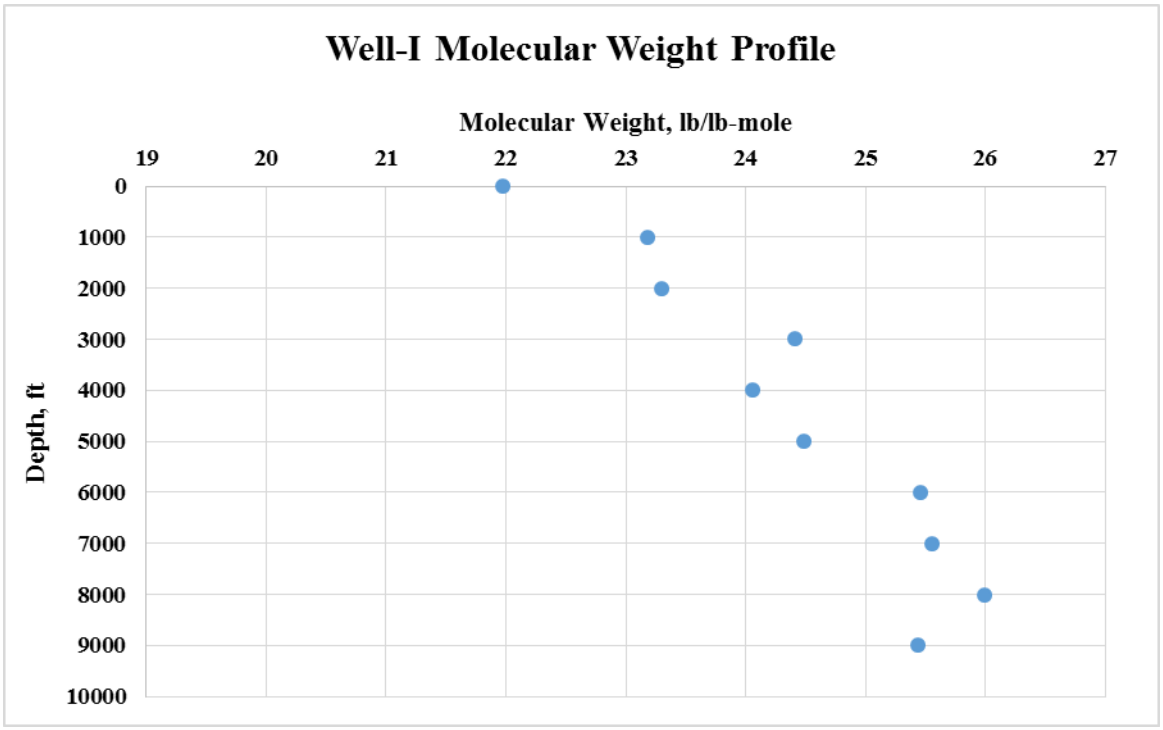
Well-I Molecular Weight Profile
Molecular Weight, lb/lb-mole
19
20
21
22
23
24
25
26
27
Depth, ft
0
1000
2000
3000
4000
5000
6000
7000
8000
9000
10000

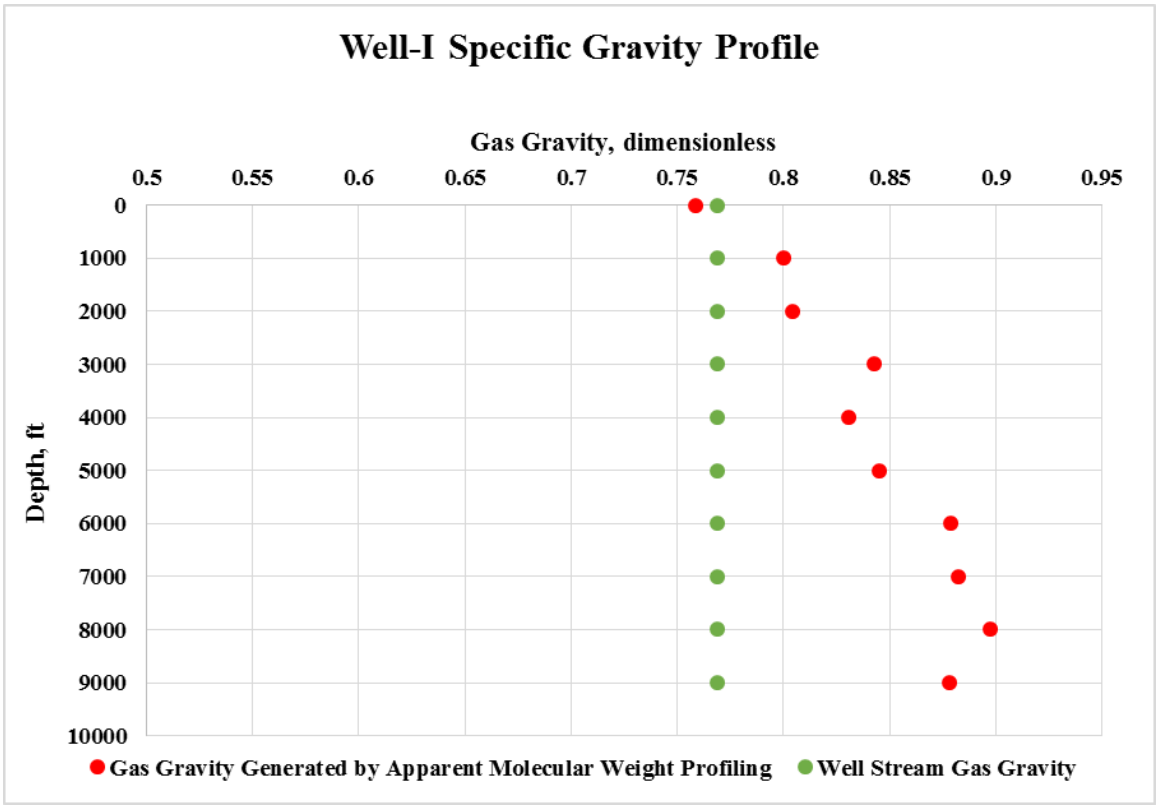
Well-I Specific Gravity Profile
Gas Gravity, dimensionless
0.5
0.55
0.6
0.65
0.7
0.75
0.8
0.85
0.9
0.95
Depth, ft
0
1000
2000
3000
4000
5000
6000
7000
8000
9000
10000
Gas Gravity Generated by Apparent Molecular Weight Profiling
Well Stream Gas Gravity

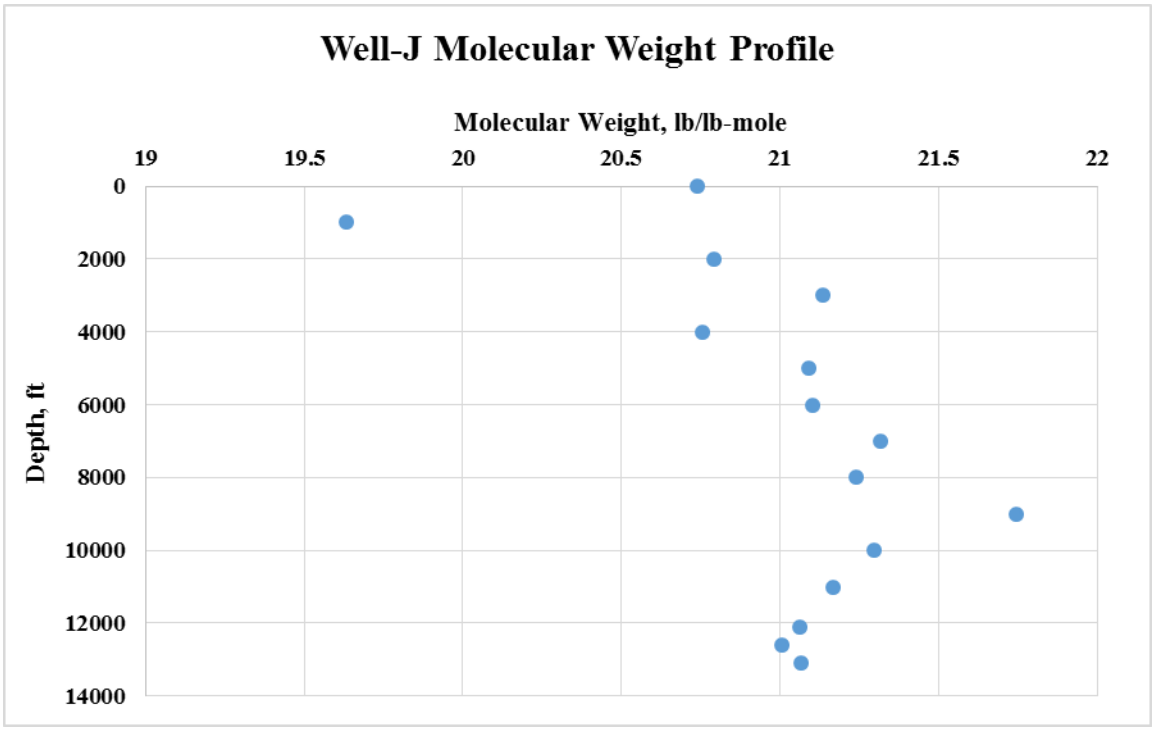
Well-J Molecular Weight Profile
Molecular Weight, lb/lb-mole
19
19.5
20
20.5
21
21.5
22
Depth, ft
0
2000
4000
6000
8000
10000
12000
14000

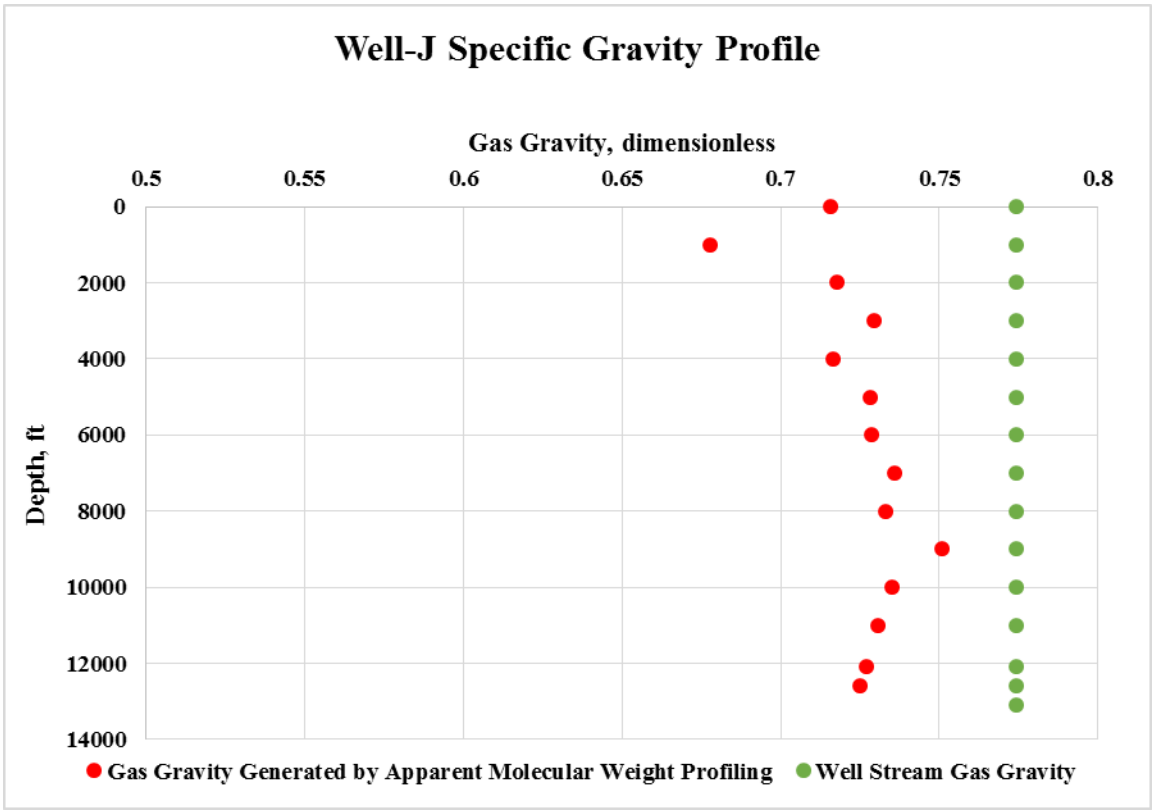
Well-J Specific Gravity Profile
Gas Gravity, dimensionless
0.5
0.55
0.6
0.65
0.7
0.75
0.8
Depth, ft
0
2000
4000
6000
8000
10000
12000
14000
Gas Gravity Generated by Apparent Molecular Weight Profiling
Well Stream Gas Gravity

Nomenclature:

P: Pressure, psia

V: Volume, ft^3

n: Number of moles

R: Universal Gas Constant, 10.732 psia.cu ft/lb mole. R

T: Temperature, R

Z: Compressibility Factor

MM_a: Apparent Molecular Weight, lb/lb-mole

M_i: Molecular Weight of i^{th} gas component, lb/lb-mole

M_{air}: Molecular Weight of air=28.96, lb/lb-mole

y_i: Mole fraction of a particular component in gas mixture

ρ_g: Gas Density, lbm/ft^3

m: Mass, lbm

γ_g: Gas Specific Gravity

ρ_{air}: Dry Air Density, lbm/ft^3

Ppr: Pseudoredused Pressure

Pr: Reduced Pressure

Ppc: Pseudocritical Pressure, psia

Pc: Critical Pressure, psia

Tpr: Pseudoreduced Temperature

Tpc: Pseudocritical Temperature, R

Tr: Reduced Temperature

Tc: Critical Temperature, R

P_{pch}: Pseudocritical Pressure of Hydrocarbon Components, psia

T_{pch}: Pseudocritical Temperature of Hydrocarbon Components, R

γ_h: Specific Gravity of Hydrocarbon Components

y_{H2S}: Mole Fraction of $H2S$

y_{CO2}: Mole Fraction of $CO2$

y_{N2}: Mole Fraction of $N2$

y_{H2O}: Mole Fraction of $H2O$

References:

Agbi, D. 1975. Calculation of Bottom-Hole Pressures in Single Phase Gas Wells From Wellhead Measurements. Presented at the Annual Technical Meeting, June 11 - 13, Banff, American Samoa, 11—13 June. SPE-7509. http://dx.doi.org/10.2118/7509.

Aziz, K. 1967. Calculation of Bottom-Hole Pressure in Gas Wells. *Journal of Petroleum Technology* **19** (7): 897—899. SPE-1676. http://dx.doi.org/10.2118/1676.

Aziz, K. (1963) Ways to Calculate Gas Flow and Static Head, Handbook Reprint from Pet. Eng., Dallas, Tex

Baxendell, P.B. and Thomas, R. 1961. The Calculation of Pressure Gradients in High-Rate Flowing Wells. *Journal of Petroleum Technology* **13** (10): 1023—1028. SPE-2. http://dx.doi.org/10.2118/2.

Bender, C.V. and Holden, W.R. 1984. Static Pressure Gradient Reversals in Gas Wells. Presented at the SPE Annual Technical Conference and Exhibition, Houston, Texas, 16—19 September. SPE-13092. http://dx.doi.org/10.2118/13092

Beggs and Brill, 1973 H.D. Beggs, J.P. Brill A study of two-phase flow in inclined pipes

J. Pet. Technol., 25 (5) (1973), pp. 607–617 http://dx.doi.org/10.2118/4007-PA

Cornell, D. and Katz, D. 1953. Pressure Gradients in Natural Gas Reservoirs. *Journal of Petroleum Technology* **5** (3): 61—70. SPE-233. http://dx.doi.org/10.2118/233.

Cullender, M.H. and Smith, R.V. 1956. Practical Solution of Gas Flow Equations for Wells and Pipelines with Large Temperature Gradients. Transactions AIME, 207, pp. 281&-287

Dranchuk. P. M., and Abou-Kassem, J. H., 1975, "Calculation of Z Factor for Natural Gases Using Equation of State," J. Can. Pet. Technol., **14**(3), pp. 34–36.

Fang, C.S. 1983. Calculations of Bottom-Hole Pressures of Gas Wells Using an Equation of State. , Lafayette, Louisiana. SPE-12559. http://dx.doi.org/10.2118/12559.

Katz, D. L., Cornell, D., Kobayashi, R., Poettmann, F. H., Vary, J. A., and Elenbass, J. R., 1959, Handbook of Natural Gas Engineering, McGraw-Hill Book Company, New York.

Kern, C. P., & Nicholson, F. R. (1965, December 1). Practical Application of Calculated Multiphase Flowing Bottom-Hole Pressures. *Journal of Petroleum Technology*: 1373—1378. doi:10.2118/1218-PA

Lee, W. J., and Wattenbarger, R. A., 1996, "Properties of Natural Gases: Gas Reservoir Engineering," Vol. 5 (SPE Textbook Series), Society of Petroleum Engineering, Richardson, TX.

MacCain, William D., Jr.: The Properties of Petroleum Fluids, 2nd ed., PennWell Books, Tulsa,1990.

Mahmoud, M. 2014. Development of a New Correlation of Gas Compressibility Factor (Z-Factor) for High Pressure Gas Reservoirs. 012903-1, *Journal of Energy Resources Technology*, **136: 1-11**. http://dx.doi.org/10.1115/1.4025019.

Messer P H, Raghavan Ramey H J Jr. Calculation of bottom-hole pressures for deep, hot, sour gas wells [J]. Journal of Petroleum Technology, 1974, 26(1): 85–92. doi:10.2118/3913-PA

Oden, R.D., Jennings, J.W., 1988. Modification of the cullender and smith equation for more accurate bottomhole pressure calculations in gas wells. In: Proceedings of the Paper 17306-MS Presented at the SPE Permian Basin Oil and Gas Recovery Conference Held in Midland, (Texas), 10-1 March. http://dx.doi.org/10.2523/17306-ms

Rawlins, E. L, and Shellhardt, M. A. 1935. 'Back-pressure data on natural-gas wells and their application to production practices,: U.S. Bureau of Mines Monograph 7

Rzasa, M. J., Katz, D. L. Calculation of static pressure gradient in gas wells [J]. Petroleum Transactions, AIME, 1945, 160(1): 100–106.

Standing, M. B., and Katz, D. L., 1942, "Density of Natural Gases," Trans. AIME, 146, pp. 140–149.

Standing, M. B.: Volumetric and Phase Behavior of Oil Field Hydrocarbon Systems, 9th printing, Society of Petroleum Engineers of AIME, Dallas, TX (1981).

Standing, M.B. and Katz, D.L. 1942. Density of Natural Gases. In Transactions of the American Institute of Mining and Metallurgical Engineers, No. 142, SPE-942140-G, 140–149. New York: American Institute of Mining and Metallurgical Engineers Inc.

Sukkar, Y. K., and Cornell, D.: "Direct Calculation of Bottom-Hole Pressures in Natural Gas Wells," Trans., AIME (19S5) 204, 43-48.

Sutton, R. P., 2007, “Fundamentals PVT Calculations for Associated and Gas/Condensate Natural-Gas Systems,” SPE Reservoir Eng. Eval. J., 10(3), pp. 270–284.

Tek, M.R., Katz, D.L., Elanbaas, J.R., Whims, M., Roberts, J.L., 1978. Temperature and pressure gradients in Gas Wells. SPE Paper 7495 Presented at the SPE Fall Meeting held in Houston Texas.

K. L. Young, Effect of assumption used to calculate bottomhole pressure in gas wells, Journal of Petroleum Technology 19 (1967) 94-103.

Vitae

Name	Nasser Mubarak Saeed Al-Hajri
Nationality	Saudi
Email	nasser.hajri.22@aramco.com
Mailing Address	P.O. Box 339 - 31311 Aramco, Abqaiq, Saudi Arabia

Education	B.Sc. in Petroleum Engineering from KFUPM – 2013
Professional Experience	Water Injection Engineer, Saudi Aramco, February, 2013 to June, 2015 Drilling & Workover Engineer, Saudi Aramco, July, 2015 to June, 2016 Oil Production Engineer, Saudi Aramco, July, 2016 to present.

Publications

1. SPE-172546-MS (Setting a New Milestone in Carbonate Matrix Stimulation with Coiled Tubing).
2. SPE-174348-MS (Full System Analysis to Predict the Reliability of a Wastewater Disposal System; a Hydraulic Simulation-Based Approach).
3. SPE-175186-MS (Disposal Wells Stimulation; Unique Challenges and Innovative Solutions (A Success Story)).
4. SPE-177488-MS (Forecasting the Reliability of a Wastewater Disposal System and Predicting Future Corrective Actions using Hydraulic Simulation).
5. SPE-182817-MS (Model assisted examination of disposal system capacity based on injected water quality).
6. SPE-182931-MS (Managing crucial business decisions related to a wastewater disposal system using hydraulic simulation).
7. SPE-182756-MS (Gravity water injectors; highlights from Saudi Aramco's 51 years of experience in a mature field).
8. SPE-181333-MS (Leveraging single phase characteristics of water injectors to optimize reservoir pressure surveillance).
9. SPE-181335-MS (Workover operations optimized in tubingless water injectors through comprehensive analysis of rigless securement practices).
10. SPE-182804-MS (Real time well integrity diagnostics using the latest development in visual logging technology).
11. SPE-182758-MS (Field Application of Electromagnetic Eddy Current Technology enables proactive near surface casing inspection).
12. SPE-182815-MS (Investigation of Tubing Failure Rates in Standalone Water Injectors with Dual Completions).
13. SPE-182818-MS (Field Application of Glass Reinforced Epoxy GRE Coating in Water Injection Wells Resolves Reoccurrence of Tubing Failures).
14. SPE-182798-MS (Feasibility Study of Utilizing Hydraulic Turbines to Recover Excess Power from Water Injection Systems).

15. SPE-182156-MS (Innovative Logging Technique Enables Accurate Detection of Temperature Anomaly Source in a Special Completion).
16. SPE-178984-MS (Comprehensive Field-Scale Injection Performance Analysis Associated with Injected Water Quality Parameters).
17. SPE-182236-MS (Strategies for Early Detection of Downhole Casing Failures Caused by Corrosive Formations).
18. SPE-184124-MS (Wellbore Organic Deposits Dissolution Using an Emulsified Solvent System - Field Treatment).
19. SPE-184083-MS (Laboratory Analysis of Several Solvent Systems to Dissolve Wellbore Organic Deposits).
20. SPE-184776-MS (Electric-Line Milling Operation on Tree Master Valve of a High Surface Pressure Well Enables Well Control).